Analyzing the role of lipid elongases in *Drosophila* development: From barriers to behavior

PRACHI GUPTA

A Thesis

Submitted to the Faculty

of

WORCESTER POLYTECHNIC INSTITUTE

In partial fulfillment of requirements for the degree

Doctor of Philosophy

in

Biology & Biotechnology

December 2013

APPROVED BY:

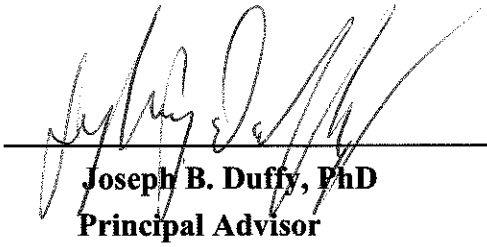

Joseph B. Duffy, PhD
Principal Advisor
WPI

Committee Members

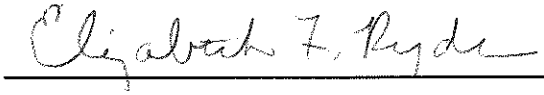

Elizabeth Ryder, PhD
WPI

Reeta P. Rao, PhD
WPI

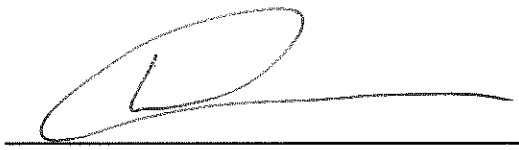

Robert Gegear, PhD
WPI

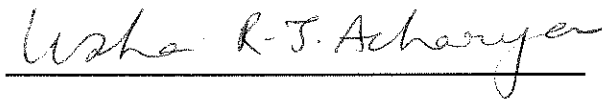

Usha Acharya, PhD
UMass Medical

ABSTRACT

Long chain fatty acids (LCFA) constitute a particular class of lipids whose developmental roles are coming under increasing scrutiny. These LCFAs not only have important cell specific functions but their dysregulation also forms the underlying cause of several lipid based disorders. Fatty acids are elongated *in vivo* by multi-enzymatic machinery in a stepwise manner. The first step of this process is carried out by a family of enzymes, conserved from yeast to humans, known as Elongases (Elos). It has been suggested that Elos work independently to elongate a fatty acid to a distinct length and perform distinct functions. Work in different species has implicated Elos in different biological roles such as barrier function, fertility, behavior and lipid homeostasis, but our understanding of the precise roles of these elongases in fatty acid elongation and how it relates to their physiological roles is not very well understood. To better understand the functions of Elos, I have characterized all *Drosophila* elongases for their developmental roles. In this thesis, I have shown that *Drosophila* elongases that are more conserved across species have more important functions (eg viability) as compared to the less conserved elongases. More specifically, I have discovered an elongases, *sit still* (*sits*), disruption of which in the nervous system results in striking locomotor and behavior defects, as well as decreased lifespan. I have also characterized another elongase, *baldspot*, which is important for imparting the epidermal barrier function in *Drosophila*, a conserved function of elongases across species. By elucidating the *in vivo* functions of these two *Drosophila* elongases, this work provides insight into the developmental roles of Elos and their links to diseases such as psoriasis, icthyosis, macular degeneration, Adrenoleukodystrophy (ALD) and Multiple Sclerosis (MS).

TABLE OF CONTENTS

LIST OF FIGURES AND TABLES

Chapter 1

Chapter 2

Chapter 3

Chapter 4

Chapter 5

Chapter 6

Conclusions and future directions

Appendix

ACKNOWLEDGEMENTS

I would like to thank the following people for their help, support, love and friendship that helped me in achieving my personal and professional goals.

To my advisor, **Joseph Duffy**, for his excellent mentorship and guidance. Thank you for helping me make sense of complex data. You taught me how to do quality science by asking the right questions. I am a better scientist because of you.

To my committee members: **Liz Ryder**, **Reeta Rao**, **Rob Gegear** and **Usha Acharya** for their constant guidance and feedback and adjusting their schedules to make time for committee meetings at short notices. Special thanks to Reeta for always giving me good counseling and advice.

To all Duffy Lab members: **Debora Afezolli**, **Aneliya Rankova**, **Cassie Buck**, **Christina Ernst**, **Michelle Arata**, **Edith Plada**, **Shreelekha Mandal**, **Tran Nguyen**, **Alex Putnam**, **Harita Menon** and **Charu Jain**. You guys made lab a fun place to work. Thank you Harita for all the scientific and non-scientific discussions. Thank you Charu for being a constant companion.

Thanks to **Terri Camesano** and her lab for their support and encouragement during thesis writing. Special thanks to **Kathleen Wang** for being a good friend and helping me in meeting my writing deadlines.

To BBT staff and faculty, especially **Carol Butler** and **Alexandra Riviera** for taking care of all the paper work that would have otherwise driven me crazy.

To the 'Woosta Gang': **Archana**, **Abhishek**, **Varun**, **Ananya**, **Arunabh**, **Sweta**, **Jeffery**, **Raj**, **Garima** and **Rohit** for their friendship and all the wonderful parties and outings that helped me take my mind off work.

Special thanks to my loving parents **D.K.Gupta** and **Asha Gupta** for believing in me and letting me pursue my dream even though it meant sending me thousands of miles away from them. Mummy and Papa, its because of your blessings that I have this degree.

To my husband **CD**, who has always been my pillar of strength. Thank you for your unconditional love and support and being always there for me. This wouldn't have been possible without you. Thanks to my cat, **Elsa**, for being my stress buster over the years.

Thank you almighty for showing me the way and showering me with great opportunities and awesome people.

Chapter 1

Introduction

Fatty acids, Elongases and Drosophila

Fatty Acids and Lipids

Lipids form an important class of macromolecules that perform a variety of structural, metabolic and biological functions. Fatty acids (FAs) are a diverse set of biomolecules that are chemically composed of carboxylic acids with hydrocarbon chains and represent one category of lipids (Figure 1.1A). In addition, fatty acids, generally in the form of Very Long Chain Fatty Acids (VLCFAs), are the building blocks of complex lipids that perform a myriad of cellular (cell membranes in form of phospholipids), metabolic (energy storage as triglycerides) and signaling (lipid rafts and hormones) functions.

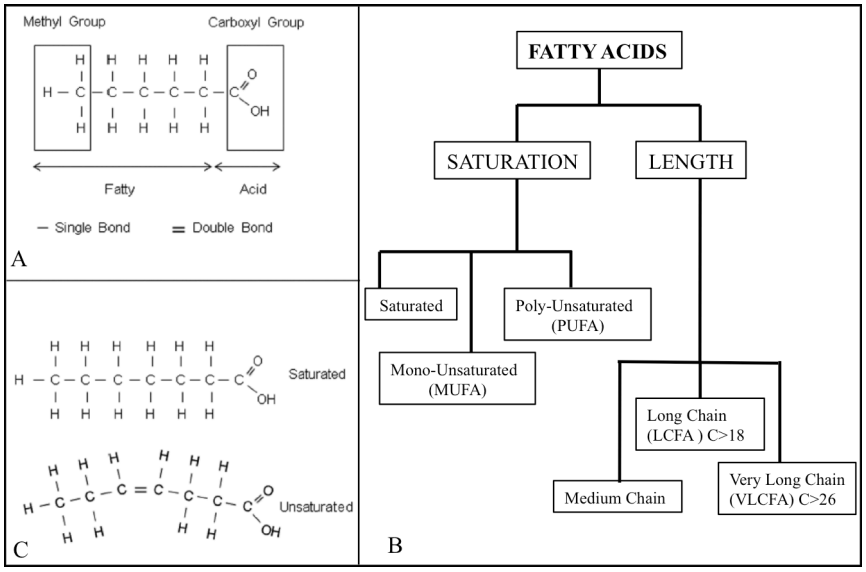

Figure 1.1: Fatty acids are long chain carboxylic acids that are classified into different subcategories. A) Basic structure of a fatty acid. B) Flowchart depicting fatty acid classification. C) Fatty acid structures with and without a double bond.
(Panel A and B have been taken from (Kalish et al., 2012))

Structurally, fatty acids can be broadly classified based on their saturation (presence, absence or number of double bonds) and length (number of Carbon atoms) (Figure 1.1B).

Saturated fatty acids, ie palmitic acid (C16:0), lack double bonds, whereas oleic acid (C18:1) contains one double bond and is thus unsaturated. In the nomenclature, the first number represents the number of carbons in the backbone, while the number following the colon represents the number of double bonds. Furthermore, fatty acids with one

double bond are known as mono-unsaturated (MUFA) fatty acids and those with more than one double bond form poly-unsaturated (PUFA) fatty acids. Most of the fatty acids are synthesized *in vivo* by the fatty acid biosynthetic machinery, but some fatty acids can only be acquired through diet. These latter ones are known as *essential* fatty acids such as ω-3 and ω-6 PUFAs (ω-3 or 6 indicative of the double bond position) and along with endogenous fatty acids, form an integral part of the organism's lipid composition.

Fatty acid Elongases: Sequence conservation and structure

Fatty acid elongases/Elongases (Elos) are a family of enzymes, conserved from yeast to humans, (Table 1.1) that function in the first step of the fatty acid elongation process to synthesize VLCFAs, which typically range in length from 20 to 36 carbons (Nugteren, 1965). Sequence analysis using different prediction algorithms suggests that these enzymes encode for multipass transmembrane proteins (typically 5-7) (Doetsch, 2004). Family members also contain a tripartite signature sequence termed the H-box, MY motif and the Q-tip domain indicative of their related structural and functional properties (Figure 1.2) but nothing is known about individual roles of these domains in VLCFA biosynthesis (Doetsch, 2004).

Table 1.1: Predicted number of elongases in selected species, based on the presence of conserved HY-Q tripartite motifs sequence, identified by BLAST.

Species	***Predicted # of Elongases***	***References***
Homo sapiens	7 (ELOVL1-7)	(Jump, 2009)
Mus musculus	7 (Elov1-7)	(Jump, 2009)
Drosophila melanogaster	20 (Elo 1-20)	(Chertemps et al., 2007)
Caenorhabditis elegans	8 (Elo 1-8)	(Kniazeva et al., 2003)
Saccharomyces cerevisiae	3 (ELO 1-3)	(Oh et al., 1997)
Arapidopsis thaliana	21 (Cer/KCS-21)	(Blacklock and Jaworski, 2006)
Trypanosoma brucei	3 (ELO1-3)	(Lee et al., 2006)

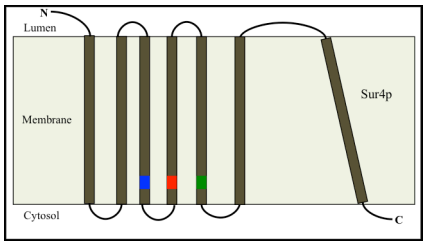

Figure 1.2: Schematic of S. *cerevisiae* fatty acid elongase Sur4p. Blue, red and green boxes denote H-box, MY-motif and the Q tip respectively. Figure adapted from (Denic and Weissman, 2007)

In addition to these conserved motifs, family members also contain a dilysine endoplasmic reticulum (ER) retention signal at their C-terminal end, supporting their localization to the ER, which is the site for long chain fatty acid biosynthesis (Grayson and Molday, 2005).

Biochemical function of Elongases: biosynthesis of VLCFA

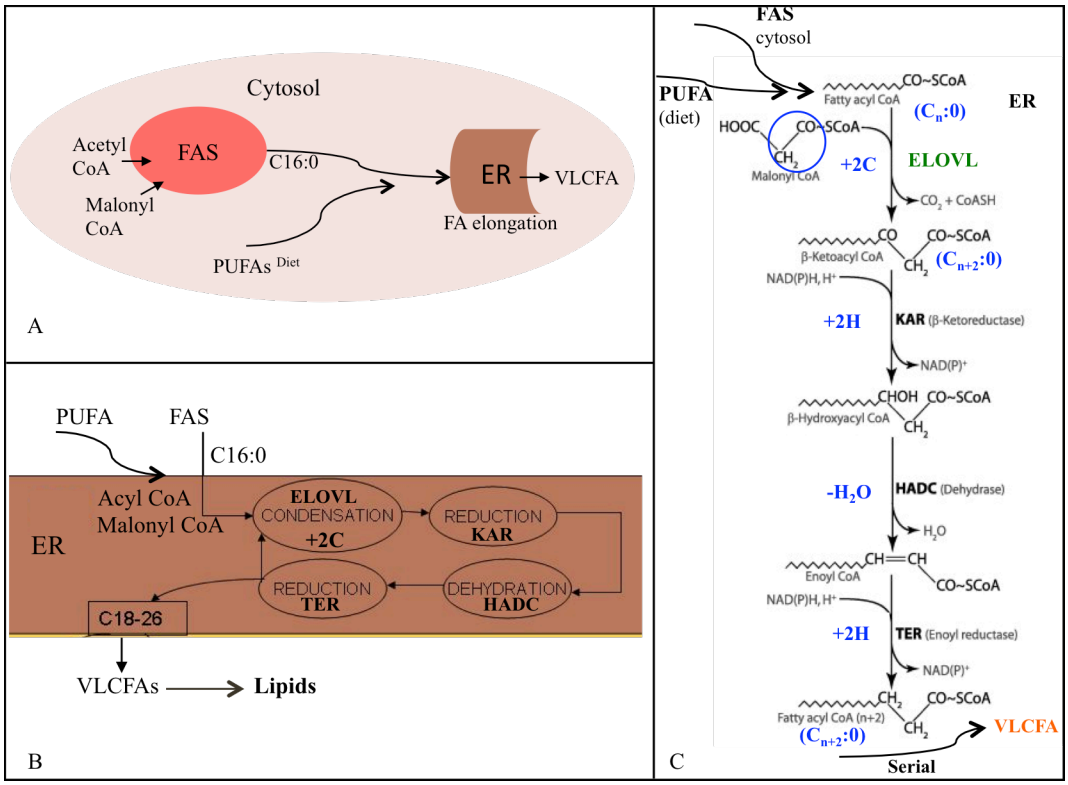

Figure 1.3: VLCFA biosynthesis *in vivo*. A) Fatty Acid Synthase (FAS) in cytosol synthesizes C16:0 which acts as the substrate for elongation machinery present in the ER. B) Schematic of the overall reaction taking place in the ER. C) Specific enzymes and products synthesized suring an elongation reaction. ELOVL (Elongase), KAR (β Keto Acyl Reductase), HADC (Dehydratase) and TER (Tertiary Enoyl Reductase). PUFA are

In vertebrates, VLCFA biosynthesis is a step-wise process that occurs in different compartments of a cell. A fatty acid with 16 carbons (predominantly) is generated in the cytosolic compartment known as fatty acid synthase (FAS)(Jenni et al., 2007; Lomakin et al., 2007), after which it is shuttled to the ER, where elongation takes place (Figure 1.3, B and C). Fatty acids are elongated *in vivo* by multi-enzymatic machinery in a stepwise manner. The overall reaction for fatty acid elongation involves four enzymes, including an Elo, that utilize malonyl CoA, NADPH and fatty acyl CoA (C16:0 or C18:2/C18:3 generated by FAS or unsaturated FAs from diet) as substrates (Figure 1.4). These enzymes carry out a serial set of condensation, reduction, dehydration and reduction reactions to synthesize a long chain fatty acid (LCFAs) or a very long chain fatty acid (VLCFA) (Cinti et al., 1992) (Figure 1.3, B and C). Within this process, biochemically, Elos carry out the condensation reaction, a rate-limiting step, and add two carbon atoms to the cytosolic fatty acid input. The series of these sequential reactions hence elongates the fatty acid substrate to a particular length (Moon et al., 2001). The VLCFA generated in the ER is then released into the cytoplasm, where it combines with different moieties to get incorporated into complex lipids (Jakobsson et al., 2006).

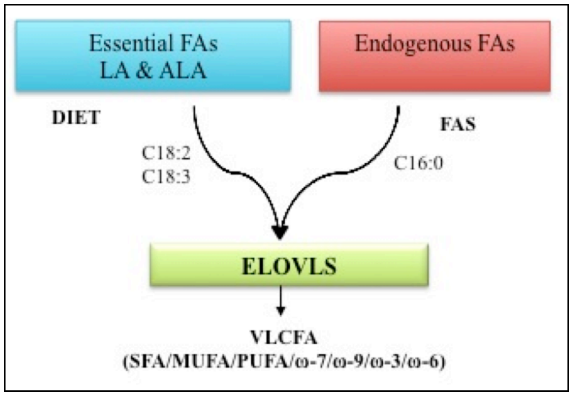

Figure 1.4: Schematic model of Elo function for both endogenous and essential FAs.

Biochemical specificity of Elongases: substrate preference

Different models of VLCFA synthesis by elongases have been proposed in literature, but the exact mechanism by which the *in vivo* fatty acid elongation takes place is not known. The first model suggests a simple sequential mechanism with each elongase acting on a different substrate and producing the substrate for the following elongase. In contrast, the second model suggests they act independently of each other through the extension of a common initial substrate to then produce the required VLCFA. While the first two models represent fairly straightforward mechanisms, the third model indicates they are not mutually exclusive and a combination of these mechanisms may represent the actual mechanism by which VLCFAs are synthesized *in vivo*.

With respect to the production of VLCFAs, the presence of diverse populations of VLCFAs with different chain lengths and degrees of saturation in different tissues suggests that elongases can act on a variety of substrates to yield distinct VLCFAs. Rather than being completely pleiotropic however, there is an increasing pool of evidence that suggests elongases may have some degree of substrate specificity and fatty acid extension length capability. For example, it has been found that ELOVL1, 3, 6 and 7 have a preference for saturated and mono-saturated fatty acids, whereas ELOVL 2, 4 and 5 appear to prefer poly-unsaturated fatty acids as substrates (Guillou et al., 2010; Hashimoto et al., 2008; Zadravec et al., 2011). Moreover, a recent study showed that different elongases have distinct fatty acid length extension capabilities. In this "Caliper" model, elongases act on ~C16:0 substrate via a caliper like mechanism to extend the length of the fatty acid substrate. According to the Caliper model, the distance between the active site of the elongase (facing the cytosol) and a lysine residue (near the luminal

end of the transmembrane helix following the active site) specifies maximal overall chain length (Figure 1.5). For example, ELOVL1 can act on C18:0 to produce C24:0 or C22:0.

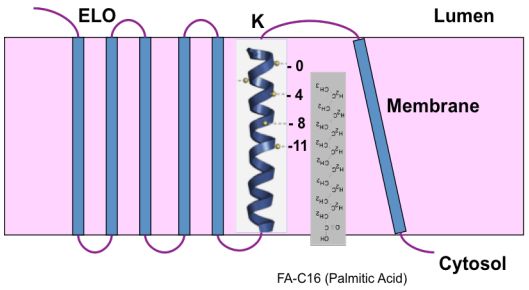

Figure 1.5: Schematic of the caliper model of elongase function. K represents the lysine residue that specifies the final fatty acid length depending upon its position. 0,4,8,11 indicate the potential positions of K. Adapted from (Denic and Weissman, 2007)

However, it is currently unclear if a single elongase is limited to producing fatty acids of only its maximal target length or if it can also produce VLCFA up to and including it's maximal target length. Regardless, this model suggests that each elongase would start from a base cytoplasmic substrate to produce a set of VLCFAs of a given length(s). In this scenario with a common starting substrate, Elos would all work independently to produce different long chain fatty acids (Denic and Weissman, 2007). However, additional data suggests the situation *in vivo* may be more complex. For example, it has been found that ELOVLl, 3, and 7 can each act on a C18:0 fatty acid and elongate it to a C24:0 VLCFA (Guillou et al., 2010). In addition, as shown in Table 1.2, Elos also appear to be able to act on a variety of substrates, suggesting there may in fact be some sequential aspect to VLCFA synthesis. Together, current work, with the fact that elongases have complex expression patterns *in vivo*, suggests a combinatorial mechanism is likely to account for the diversity of VLCFAs present *in vivo*. Nevertheless, the ambiguity associated with the underlying action of these elongases in the production of VLCFAs remains a gap in our knowledge and further study of these Elos will help us eventually uncover their functional relationships.

Table 1.2: Fatty acid substrate specificity for different elongases.

Elongase	*Substrate*	*Product*	*Reference*
Hs ELOVL1	C20, C22 S, MUFA C22	C24 C26	(Ohno et al., 2010) (Ofman et al., 2010)
Mm Elovl1	C20	C28	(Sassa et al., 2013)
Sc Elo1	C14	C16	(Schneiter et al., 2000)
Hs ELOVL2	C20, C22	C24	(Leonard et al., 2000)
Mm Elovl2	C22 PUFA	C28-C30 PUFA	(Zadravec et al., 2011)
Sc Elo2	>C22	C24	(Oh et al., 1997)
Hs ELOVL3	C20	C20, C22	(Westerberg et al., 2006; Westerberg et al., 2004)
Mm Elovl3	C20:1	C22-C24	(Westerberg et al., 2004)
Sc Elo3	C24	C26	(Oh et al., 1997)
Hs ELOVL4	C20:5,6	>C28 C28-38	(Vasireddy et al., 2007) (Yu et al., 2012)
Mm Elovl4	C26	>C28	(Cameron et al., 2007)
Hs ELOVL5	-	-	
Mm Elovl5	C18:1	C20:3, C22:4:	(Tripathy and Jump, 2013; Tripathy et al., 2010)
Hs ELOVL6	-	-	(Matsuzaka et al., 2007)
Mm Elovl6	C18 C16	C22 C18	(Matsuzaka et al., 2007)
Hs ELOVL7	C16, C18, C20	C22, C24	(Naganuma et al., 2011; Tamura et al., 2009)
Mm Elovl7	-	-	

Physiological functions of VLCFA and Elongases: Roles in disease and development

The fatty acid and lipid profile of an organism is indicative of the repertoire of the specialized functions performed by the different classes of these biomolecules. In the brewing yeast, *Saccharomyces cerevisiae,* for example, fatty acid composition consists of palmitic acid (C16:0) and stearic acid (C18:0), with C14:0 and C26:0 being minor species that are incorporated into GPI anchors and sphingolipids (Tehlivets et al., 2007).

In the nematode, *Caenorhabditis elegans*, C20:0 is required for proper neuromuscular development, uniform biological rhythms and normal brood size (Watts et al., 2003). In insects such as *Drosophila melanogaster*, FA content can affect female fecundity (Beaudoin et al., 2000b), as well as courtship behavior by affecting the production of sex pheromones (Ueyama et al., 2005). At the cellular level, long chain PUFAs derived from dietary precursors (LA and ALA), are involved in cell signaling by activating transient receptor potential (TRP) channels in *Drosophila* (Chyb et al., 1999), (Jors et al., 2006). The vertebrate lipidome consists of a vast repertoire of fatty acids whose activities range from supporting the immune system to critical metabolic functions (Gottrand, 2008; Milte et al., 2009). Not surprisingly, dysregulation in their biosynthesis has been directly associated with many diseases. For example, metabolic disorders including atherosclerosis (Ruan et al., 2009), diabetes (Lopez et al., 2009), adrenoleukodystrophy (ALD), adrenomyeloneuropathy (AMN), and Tay-Sachs are related to defects in fatty acid biosynthesis (Friedman, 1971). Even though the metabolic and structural functions of lipids, as well as their involvement in the disorders above, are long known, a broader appreciation and understanding of their underlying roles in development is only beginning to come to light.

Very long chain fatty acids (VLCFA) constitute a particular class of lipids whose developmental roles are coming under increasing scrutiny. As mentioned above, VLCFA are synthesized *in vivo* by fatty acid elongation machinery with addition of two carbon atoms by elongases being the rate-limiting step. Functional studies of elongases were first reported in *S. cerevisiae,*

Elongases and their roles across species:

Based on sequence homology, elongases have been identified in different species with differences in the number of members present in each species. Figure 1.6 summarizes the known functions of the elongases in different organisms.

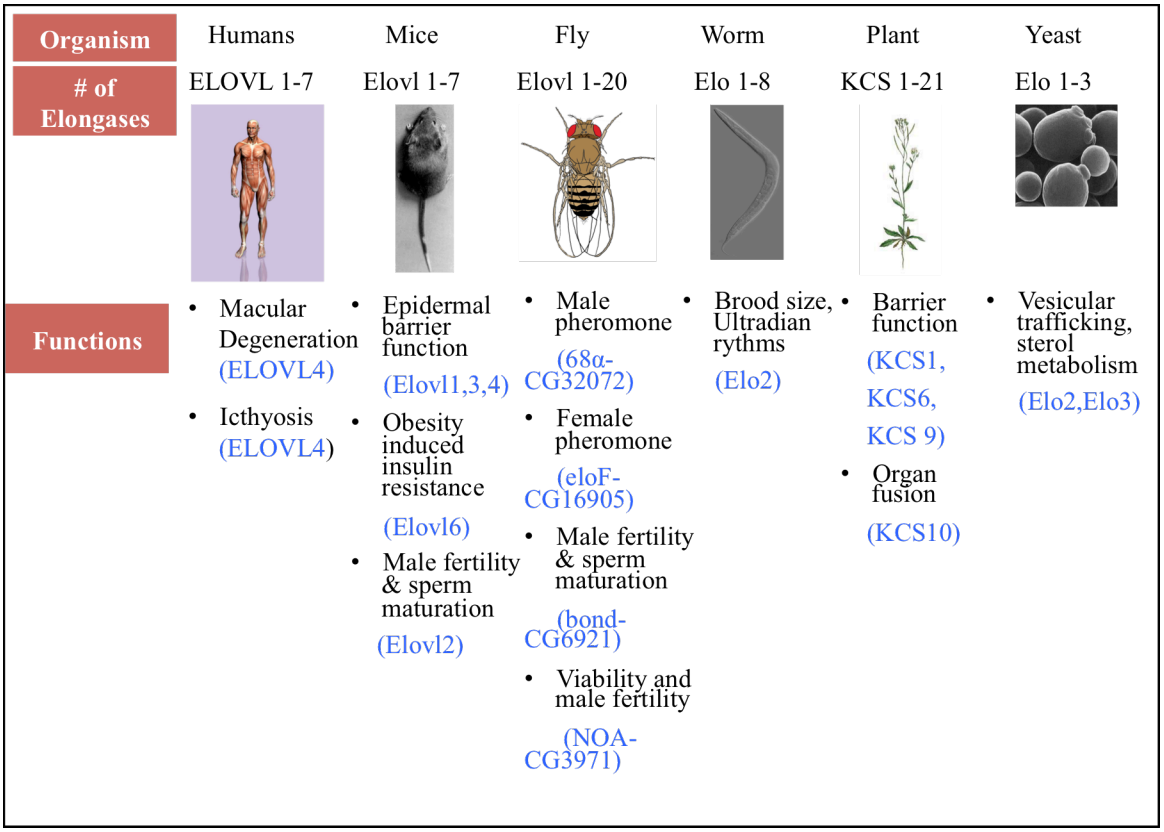

Figure 1.6: Physiological roles of the known elongases in different organisms. The elongase name/number is indicated in blue below its function. KCS = 3, Ketoacyl synthase (plant elos). References for the figure are in text describing these elongases.

Yeast (S. cerevisiae) elongases (Elo1-3)

Elongation of fatty acids in yeast takes place in endoplasmic reticulum by enzymes Elo1, Elo2 and Elo3 (Toke and Martin, 1996). Yeast Elo1 can synthesize small and medium fatty acids whereas Elo2 and Elo3 have specificity to synthesize very long chain fatty

acids (C22 and C26 respectively) (Dittrich et al., 1998; Oh et al., 1997). There seems to be some functional overlap in yeast Elo2 and Elo3 as the single mutants are viable. In contrast, the *elo2 elo3* yeast double mutant is lethal and can be rescued by the heterologous expression of FAE1 *Arabidopsis* enzymes (Oh et al., 1997). In addition, mutations in *elo2* and *elo3* have been implicated in defects in vesicular trafficking and sterol metabolism due to the altered synthesis of sphingolipids (containing VLCFA moiety) (David et al., 1998) (Han et al., 2002; Tvrdik et al., 2000).

Worm (C. elegans) elongase (Elo1-8)

There are eight putative Elos in *C. elegans* with functional conservation evident as heterologous expression of *C. elegans* Elo-1 in yeast resulted in specific elongation of C18 PUFAs substrates to C20 PUFAs (Beaudoin et al., 2000a). Providing further evidence for functional conservation, loss of *elo-1* and *elo-2* results in changes in fatty acid composition (Watts and Browse, 2002). *elo-1* mutants do not display any physiological phenotype except for a decrease in the synthesis of C20 PUFA (Wallis et al., 2002). RNAi mediated suppression of *elo-2* resulted in slow growth, smaller brood size and altered rhythmic behavior as compared to the control worms. Double suppression of both *elo-1* and *elo2* resulted in severe defects in body size and reproduction (Kniazeva et al., 2003).

Plant (A.thaliana) elongases

Arabidopsis utilizes a repertoire of VLCFAs that perform variety of functions, such as energy storage in seeds, building blocks in membranes and barrier function for leaves and

stems in the form of cuticular waxes (Jenks et al., 1995; Li et al., 2006a). An elongation reaction takes place in plastid microsomes to yield VLCFAs utilizing elongases known as 3-ketoacyl-CoA synthases (KCS) (Fehling and Mukherjee, 1991). The first *Arabidopsis* elongase identified was *fae-1*, a seed specific elongase implicated in synthesis of storage lipids (James et al., 1995). Since then twenty-one elongases have been identified in *Arabidopsis* based on sequence homology, but only eight have been found to encode proteins that can mediate VLCFA synthesis when expressed heterogeneously in yeast (Costaglioli et al., 2005; Paul et al., 2006; Trenkamp et al., 2004). Expression analysis of the KCS elongase family using RT-PCR suggests widely distributed expression patterns with different levels in *Arabidopsis* (Joubes et al., 2008). Functional analysis of KCS elongases has suggested functional specificities of these enzymes. Two KCS have been implicated in epicuticular wax synthesis (CER 6/ KCS6 and KCS1), whereas another - KCS10/FDH has been implicated in organ development (Millar et al., 1999; Todd et al., 1999). Loss of function mutations in FDH/KCS10 leads to defective trichome differentiation and increased tissue fusion and ectopic expression of KCS10 leads to delayed growth and development accompanied by the dwarf phenotypes (Yephremov et al., 1999). Suppression of *kcs6* in transgenic *Arabidopsis* led to waxless stems with increased levels of C24 VLCFA wax precursors, whereas *kcs1* mutants exhibit thinner stems and less resistance to low humidity stress with marked decrease in C26 to C30 wax alcohols and aldehydes (Millar et al., 1999; Todd et al., 1999). KCS9 has been recently found to be important for biosynthesis of cuticular waxes and membrane lipids like sphingolipids and phospholipids (Kim et al., 2013). The *kcs9* knockout mutants had a reduced repertoire of C24 VLCFAs with an accumulation of C20 and C22 VLCFAs,

suggesting a role for KCS9 in elongating C20 and C22 saturated fatty acids (Kim et al., 2013).

Fly (D. melanogaster) elongases (Elovl1-20)

In total, *Drosophila* has a repertoire of twenty putative elongases as compared to vertebrates that have only seven (ELOVL1-7). Of the twenty elongases in flies, detailed studies have only been reported for four members of the family. *Drosophila* elongase F (eloF-CG16905) was shown to be important for female pheromone biosynthesis (it can elongate both saturated and unsaturated fatty acids to C30 VLCFAs, specifically 7,11-dienes of 29 carbons) and thus courtship behavior (Chertemps et al., 2007). Elo68alpha (CG32072) is specifically expressed in the male genital system and mutations in this gene lead to the reduction the male pheromone cis-vaccenyl acetate (Chertemps et al., 2005). Another male specific elongase CG6921 (*bond*) is specifically expressed in spermatocytes and loss of function of this elongase leads to cytokinesis defects in dividing spermatocytes (Szafer-Glusman et al., 2008). CG3971 or NOA or Baldspot has been shown to function in sperm development/male fertility and viability (Jung et al., 2007).

Mice (M.musculus) elongases

There are seven elongases (Elovl1-7) in mice of which the most thoroughly studied is Elovl4. Two studies have shown that *elovl4* mutant (homozygous knockin and knockout) mice die shortly after birth (neonatal lethal) due to defective epidermal barrier function (Cameron et al., 2007; Li et al., 2007). In these mice, production of free fatty acids >C26

was found dramatically reduced as compared to the wild type pups, suggesting a role of Elovl4 in synthesizing VLCFA >C26, which form a part of epidermal ceramides (Li et al., 2007; McMahon et al., 2007; Vasireddy et al., 2007). Knockout of another elongase, *elovl3,* using homologous recombination results in mice with sparse fur coat and irritated and eczematous skin (Westerberg et al., 2004). The mutant mice have trouble drying their fur after becoming wet. Thin layer chromatography (TLC) of epidermal lipids suggests reduction in neutral lipids such as triglycerides and wax and sterol esters (Westerberg et al., 2004). Recently it has been found that mice deficient of *elovl1* have severe defects in their epidermal barrier and die shortly after birth similar to *elovl4* mutant mice (Sassa et al., 2013). Lipid analysis of the epidermal tissue of *elovl1* null pups revealed the decreased levels of the ceramides (>C26) and ω-O-acyl-Cers (VLCFA moiety with C30-C36 in which the ω carbon (opposite to the carboxyl group) is hydroxylated and esterified), suggesting the role of Elovl1 in conversion of C24 VLCFAs to C26 VLCFAs and epidermal ceramides (Ohno et al., 2010; Sassa et al., 2013). Another elongase, Elovl6, has been associated in regulating metabolic function. *elovl6* mutant mice are obesity induced insulin resistant because of the continuous signaling through the hepatic insulin receptor substrate-2 resulting in Akt phosphorylation facilitated by the increased availability of C16 (Matsuzaka et al., 2007). Hepatic fatty acid composition of *elovl6* null mice showed the role of Elovl6 in elongation of C16 to C18 fatty acids (Matsuzaka et al., 2007).

elovl5 knockout mouse exhibit reduced levels of arachidonic acid (C20:4, n-6) and docosahexaenoic acid (DHA, C22:6, n-3) (Qin et al., 2009). These PUFAs leads to the activation of sterol regulatory element-binding protein (SREBP)-1c and its target genes

involved in fatty acid and triglyceride synthesis, which leads to hepatic steatosis or fatty liver in *elovl5* mutant mice (Moon et al., 2009). Similar to Elovl5, Elovl2 is implicated in synthesis and elongation of PUFAs as exhibited by *elovl2* mutants that lack C24-C30 PUFAs of ω-6 family. *elovl2* mutant mice have defective male fertility because of the requirement of C24:5n-6 to C30:5n-6 PUFAs in testis, absence of which leads to arrest of spermatogenesis (Zadravec et al., 2011)

Human (H. sapiens) elongases (ELOVL1-7)

Not much is known functionally for human elongases. Mutations in *elovl4* have been characterized in detail and have been associated with Stargardt disease-3 (STGD-3) and autosomal dominant Stargardt like macular dystrophy (adSTD-like MD), dominant forms of macular degeneration characterized by decreased central vision, flecks on the retina and atrophy of the macula or photoreceptor degeneration (Ayyagari et al., 2001; Zhang et al., 2001). Three independent mutations (5-bp deletion, two 1-base deletion and a nonsense mutation) in the last exon (Exon 6) have been identified in *Elovl4* that can lead to the premature truncation of the ELOVL4 protein and thus cause macular degeneration (Vasireddy et al., 2006; Zhang et al., 2001). Mouse models mimicking the phenotypes associated with macular degeneration by creating deletions in the *Elovl4* have been generated to understand the mechanism underlying the photoreceptor degeneration. Using those it has been found that the mutations in *Elovl4* exerts a dominant negative effect where the mutant protein appeared mislocalized as compared to wild-type ELOVL4, which preferentially localizes to the ER (Karan et al., 2005b; Maugeri et al., 2004; Vasireddy et al., 2009; Vasireddy et al., 2005). The mutant ELOVL4 protein misfolds

and sequesters the wild type protein leading to the macular degeneration pathologies (Grayson and Molday, 2005). Fatty acid profile from the retinas of the mutant mice shows the deficiency of C32-C36 acyl phosphatidylcholine, suggesting ELOVL4 causes macular degeneration via polyunsaturated VLCFAs (McMahon et al., 2007). In another study, recessive mutation in *Elovl4* has been associated with clinical conditions of ichthyosis, seizures, mental retardation, and spasticity, further emphasizing the importance of ELOVL4 and VLCFAs in brain development and epidermal barrier integrity (Aldahmesh et al., 2011).

Apart from ELOVL4, only two more human elongases, ELOVL1 and ELOVL7, have been briefly studied using *in vitro* assays. ELOVL1 has been biochemically linked to X-linked Adrenoleukodystrophy as knockdown of *Elovl1* in X-linked adrenoleukodystrophy fibroblasts results in the decrease of C26 VLCFAs, which are otherwise found elevated in plasma and tissue of affected patients (Ofman et al., 2010). ELOVL7 on the other hand has been implicated in prostrate cancer growth via saturated VLCFA (C20, C22, C24) metabolism (Tamura et al., 2009). ELOVL7 has been found overexpressed in prostrate cancer cells, whereas its knockdown in cell culture leads to attenuated growth of the cancerous cells possibly due to reduced VLCFA derivatives (Tamura et al., 2009).

Information on the functions of elongases in different organisms suggests that these elongases are performing important functions, some of which are conserved across species. In short, work in mice reveals different roles for these elongases, hinting at functional distinctions (Cameron et al., 2007; Denic and Weissman, 2007; Wang et al., 2005). Studies on both mouse (Elovl4, Elovl3 and Elovl1) and plant Elos (KCS1/6/9)

have implicated these Elos in barrier function, epithelial and cuticular, respectively (Cameron et al., 2007; Sassa et al., 2013; Westerberg et al., 2004). Metabolic functions have also been tied to Elos, as a knockout of mouse Elovl6 leads to obesity induced insulin resistance and Elovl5 is important for lipid homeostasis in liver (Matsuzaka et al., 2007; Moon et al., 2009). While such results indicate progress is beginning to be made in elucidating the developmental roles of elongases, a large gap in our understanding still remains (Table1.3).

Drosophila as a model system

Drosophila has long proved itself to be an excellent model system to study the molecular bases of vertebrate development. More recently however, (given the conservation of the genes and the pathways involved and the availability of various tools and reagents) it is increasingly becoming a model of choice to also study metabolic pathways and their associated diseases. *Drosophila* has a large repertoire of lipid species that are structurally and functionally similar to vertebrates (Parisi et al., 2011). Studies have shown that a variety of human metabolically related disorders can be recapitulated in *Drosophila* ranging from obesity and diabetes to rare diseases such as Niemann-Pick (Huang et al., 2005) and Adrenoleukodystrophy. Such work and the conservation of these metabolic pathways, including the production of VLCFAs, suggests that insight gained on the function of VLCFA biosynthetic enzymes, such as elongases, in a model organism like *Drosophila,* will lead to an increased understanding of their role in vertebrates as well.

Table 1.3: Different functions performed by Elos in different species.

Organism	***Elongase***	***Function***	***Reference***
S.cereviseae	Elo1, Elo2, Elo3	Vesicular trafficking, Sterol metabolism	(Han et al., 2002; Tvrdik et al., 2000).
C.elegans	Elo2	Fecundity, Growth rate, Ultradian rhythms	(Kniazeva et al., 2003)
D. melanogaster	EloF	Courtship behavior	(Chertemps et al., 2007),
	Baldspot/ NOA	Spermatogenesis	(Jung et al., 2007)
	68 α	Male reproductive system	(Chertemps et al., 2005)
	bond	Male fertility and cytokinesis	(Szafer-Glusman et al., 2008)
M. musculus	Elovl 4	Barrier function, Viability, Stargardt-like macular dystrophy (STGD3)	(Cameron et al., 2007), (Karan et al., 2005a), (Zhang et al., 2001)
	Elovl 3	Barrier function	Westerberg et al., 2004)
	Elovl 6	Obesity induced insulin resistence	(Matsuzaka et al., 2007),
	Elovl 5	Fatty liver, Hepatic lipid and carbohydrate composition	(Moon et al., 2009), (Wang et al., 2008)
	Elovl 2	Sperm maturation, Triacylglycerol synthesis	(Zadravec et al., 2011), (Kobayashi et al., 2007)
	Elovl 1	Barrier function	(Sassa et al., 2013)
H. sapiens	ELOVL 1	Adrenoleukodystrophy	(Ofman et al., 2010)
	ELOVL 7	Prostrate Cancer	(Tamura et al., 2009)
	ELOVL 4	Macular degeneration	(Okuda et al., 2010)
A. thaliana	KCS9	Barrier function	(Kim et al., 2013)

Drosophila Elongases

Based on sequence analysis, twenty putative elongases have been identified in *Drosophila.* These elongases share the tripartite signature sequence consisting of H-box, MY motif and Q-tip along with the ER retention signal (Doetsch, 2004). They also share a strong sequence homology to vertebrate elongases.

Two key questions arise with respect to our overall understanding of elongases.

1) What are the roles of these elongases in vivo (and are these conserved across species)?

2) What are the functional relationships between different elongases - are they performing unique or redundant functions?

To answer these questions it will be important to delve more broadly into functional studies on this family of conserved biosynthetic enzymes. *My hypothesis is that some elongases have conserved functions across species, while others have unique and possibly species-specific functions.* In order to test this hypothesis, I have performed a loss of function screen of all the *Drosophila* elongases and analyzed their functions broadly. Based on the results, I have further analyzed the functions of selected elongases in detail in *Drosophila* development. I have identified a novel role for an elongase, Sit Still, in behavior and locomotion. This is the first evidence linking an elongase, and thereby VLCFAs, to locomotor behavior in any species. I have also continued the characterization of another elongase, Baldspot, implicated in viability and barrier function, similar to the vertebrate elongases Elovl1, Elovl3, and Elovl4 (Cameron et al., 2007; Li et al., 2007; Sassa et al., 2013; Westerberg et al., 2004) confirming conserved functions for some family members. Thus my work provides an initial indication of the

importance of elongases to *Drosophila* development. Beyond the conservation of barrier functions, the conservation of a behavioral role like Sit still would lead to new insights regarding the function of VLCFAs in vertebrates.

Chapter 2

Developmental analyses of a family of conserved fatty acid elongases

ABSTRACT

Elongases are a conserved family of enzymes that have been implicated in elongation of a fatty acid moiety to generate very long chain fatty acids. In doing so, they help generate several classes of more complex lipids that perform a myriad of important cellular and physiological functions. There is growing evidence supporting distinct functions for these elongases based on their spatial and temporal expression and substrate specificity. This chapter illustrates the functional specificities of the family of twenty *Drosophila* elongases during development using RNAi mediated knockdown. Using this approach, the role of family members was tested in viability, fertility, wing and nervous system development. Supporting a model for distinct developmental contributions, different phenotypic effects were observed among family members upon their knockdown. Thus, elongases have specific roles in *Drosophila* development and it is likely that such specificity is likely to be conserved across species.

INTRODUCTION

As mentioned in chapter one, twenty elongases have been identified so far in *Drosophila*. There is very limited work on four of the *Drosophila* elongases that suggests their roles in fertility and behavior, but comprehensive developmental studies have not been undertaken for a large set of the Elo members so far. (Chertemps et al., 2007; Chertemps et al., 2005; Jung et al., 2007; Szafer-Glusman et al., 2008). In this chapter, I have utilized RNA interference (RNAi) as a method to carry out a loss of function screen of all twenty elongases. RNAi induces targeted silencing of gene expression using double stranded RNA (dsRNA) (Grishok and Mello, 2002). It is increasingly being used as a tool to study gene regulation (Castel and Martienssen, 2013), signal transduction (Sansores-Garcia et al., 2013) and disease mechanisms (Miller et al., 2012). RNAi has also shown promise in therapeutic applications and several RNA molecules have made it to clinical trials (Keaney et al., 2011). The basic principle of RNAi is that a double stranded RNA (dsRNA) is recognized by a ribonuclease, known as Dicer, that processes the dsRNA into smaller molecules (21-25 nt) known as small interfering RNAs (siRNAs). These siRNAs are then bound to a ribonucleoprotein complex called RISC (RNA-induced silencing complex), that unwinds the siRNA,

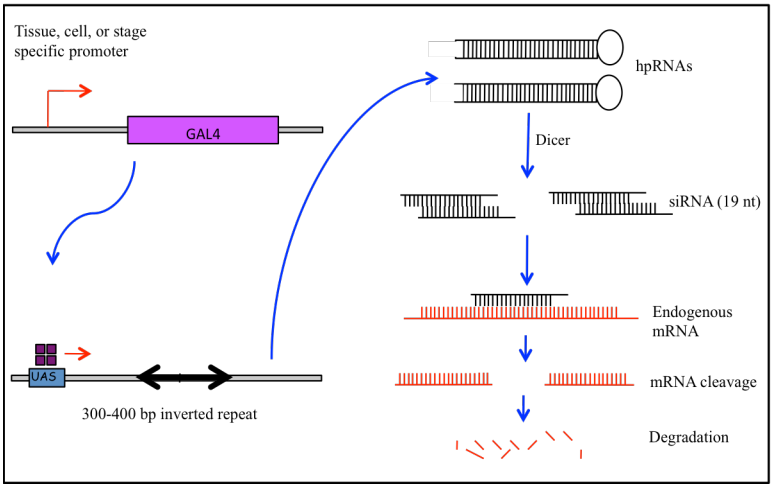

Figure 2.1: siRNA mediated gene silencing method. Figure adapted from VDRC website.

thereby allowing the antisense strand to identify the target mRNA by base complementarity. Once the siRNA binds the target mRNA, the target mRNA is degraded by the endonuclease and exonuclease components of the RISC complex, thus bringing about gene silencing (Figure 2.1). Many genome wide RNAi screens have been done in *C. elegans* and *Drosophila*, the latter both in whole organisms and cell lines, as well as mammalian cell lines, to characterize a diversity of cellular processes (Berns et al., 2004; Fortier and Belote, 2000). Moreover, in *Drosophila* a number of genome-wide transgenic collections exist that contain RNAi triggers for each individual gene under the control of the GAL4/UAS system (Dietzl et al., 2007). I have utilized the same approach to test the tissue specific functions of all *Drosophila* elongases. Since there are twenty elongases in *Drosophila*, the question arises about the functional specificity of these elongases during development. The goal of this chapter is to gain an understanding of the developmental roles of *Drosophila* elongases and hence to determine their functional specificity.

RESULTS

Sequence conservation among elongase members suggests similar yet specific functions.

Sequence analysis of Baldspot revealed that it is a member of evolutionary conserved family of enzymes that function as fatty acid elongases (Doetsch, 2004). Comprehensive phylogenetic analysis with 56 eukaryotic genomes has corroborated that and it was found that elongases could be divided into functional subfamilies based on distinct motifs (Hashimoto et al., 2008). It was also suggested that additional functional divergence may exist even within a subfamily and that's what accounts for fatty acid diversity among organisms (Hashimoto et al., 2008).

In order to understand *Drosophila* elongases better, I performed a more restricted phylogenetic analysis using all twenty *Drosophila* elongases along with vertebrate and fungal elongases. From this analysis, specific clades indicated likely orthologous relationships between fly and vertebrate Elos. For example, and as observed previously, Baldspot is more closely related to Human ELOVL6 and ELOVL3 than to any other fly elongase (Doetsch, 2004; Figure 2.2 clade D). Likewise, clades A and B also revealed likely examples of fly/veretbrate orthology, while clade C represents solely fly elongases arguing for a more restricted function that may be unique to insects (Figure 2.2).

Figure 2.3 shows the Clustal-W alignment of all the Drosophila elongases (CG) along with the known yeast (Sc), Mouse (Mm) and Human (Hs) elongases. The alignment has been truncated to focus on the putative functional domains of the protein family. The alignment revealed unique differences within clades that are potentially important for imparting functional specificity. For example, there are several amino acids that are

unique to the D, or Bals, clade, including W148 that likely impacts activity due to its internal location within the H-box, which has been implicated in catalytic activity of elongases (Shanklin et al., 1994).

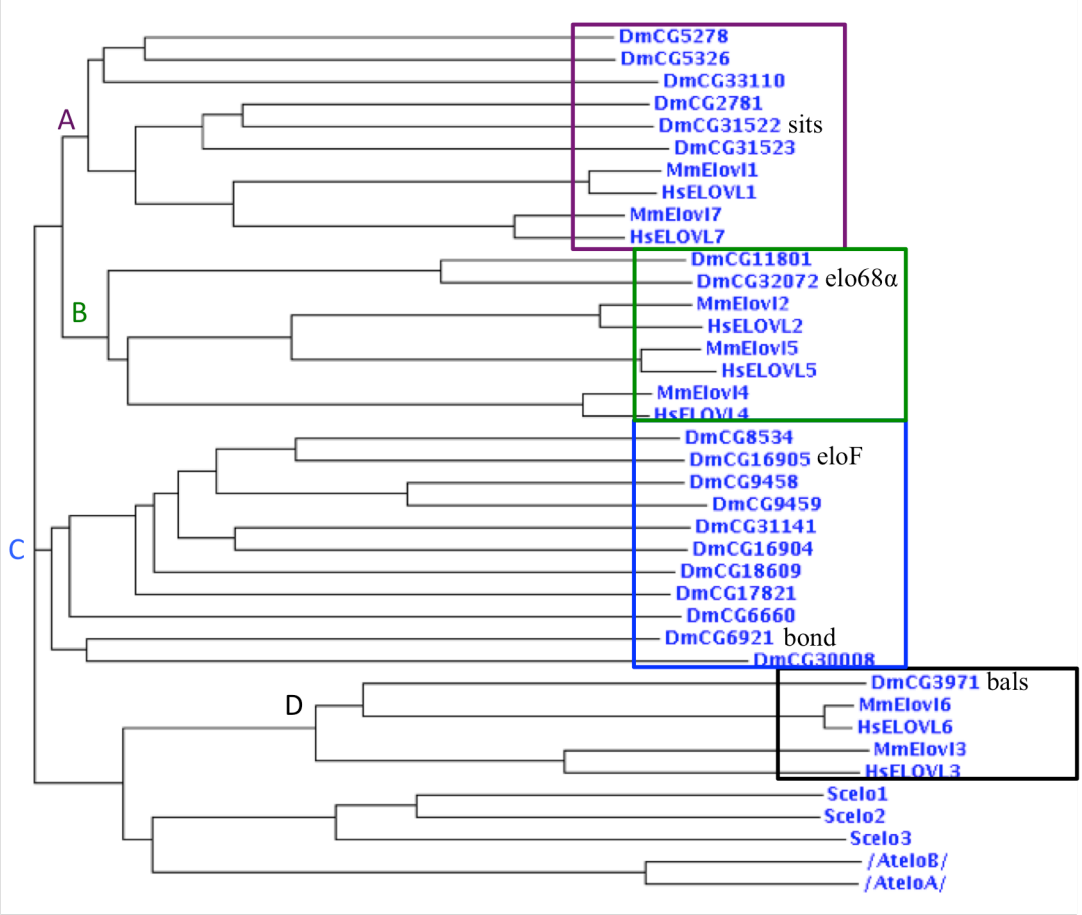

Figure 2.2: Phylogenetic analysis of specific elongases. All known *Saccharomyces cerevisiae* (Scelo), *Mus musculus* (MmElovl), *Homo sapiens* (HsELOVL), *Drosophila melanogaster* (DmCG) and *Arabidopsis thaliana* (Atelo) elongases were included and sequences can be found in Appendix C. The colored boxes represent clustering among/between different elongase species. Neighbor joining method and complete protein sequences have been used to make this tree.

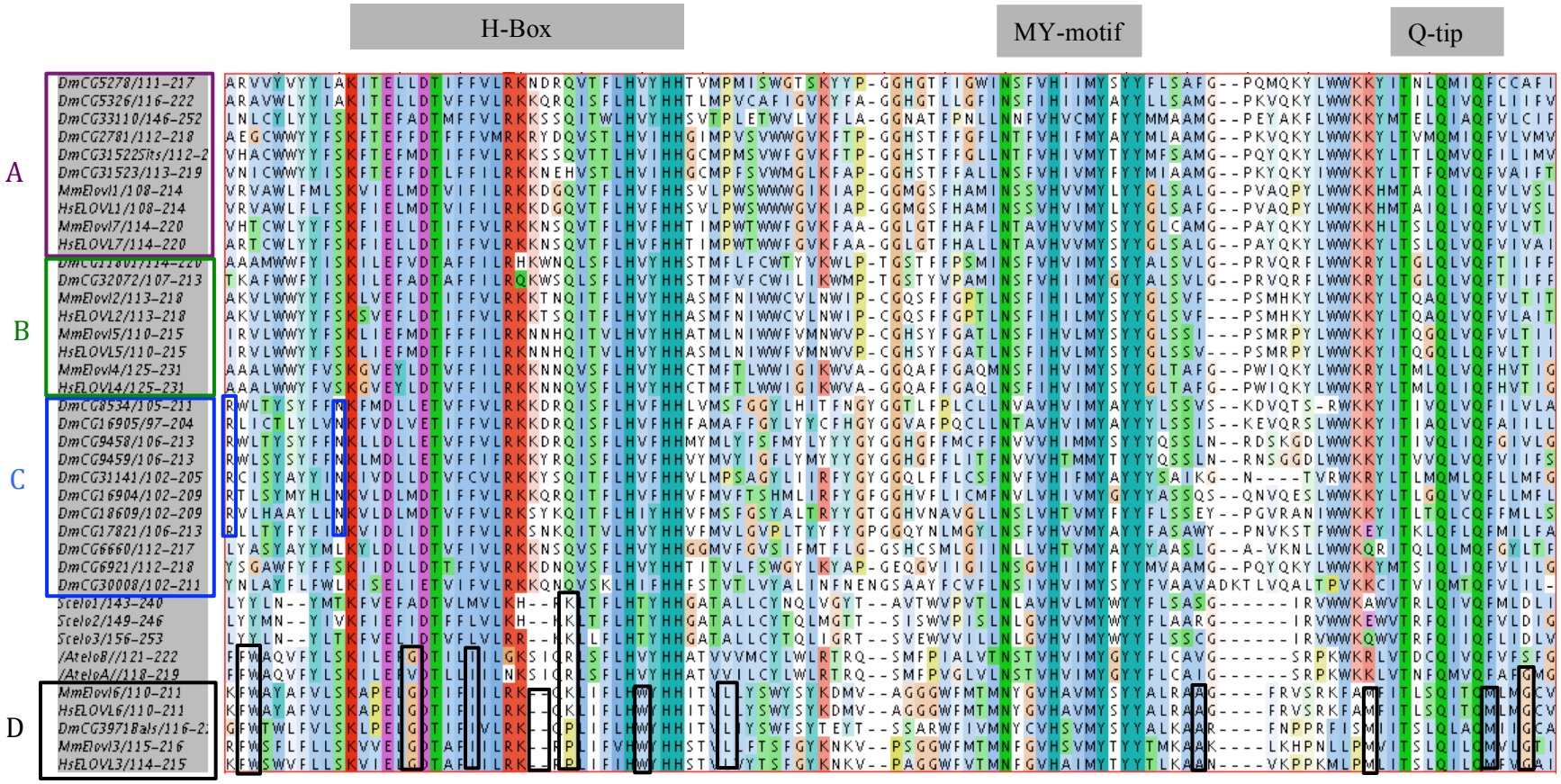

Figure 2.3: Clustal W alignment of selected elongases shows strong conservation of motifs as well as specific residue differences. Grey boxes on top depict the conserved domains H-box, MY- motif and Q-tip. Certain amino acid residues seem to be different/unique for certain elongase groups as pointed out by boxed blue and black amino acids for correspondingly colored elongase group.

Drosophila Elongases exhibit distinct expression patterns during development

Work in vertebrates has started to reveal distinct expression patterns among elongases (Jakobsson et al., 2006). Genome wide expression studies in *Drosophila* also suggest differences in expression patterns among elongases (Tomancak et al., 2002; Tomancak et al., 2007). Table 2.1 compiles the expression patterns of all twenty *Drosophila* elongases from the genome wide RNA expression studies by *Drosophila* community (Tweedie et al., 2009). The available RNA seq data was filtered for each elongase for its expression in different stages of development. A '+' signifies high expression whereas the absence of expression is denoted by '-'. Furthermore, specific tissues of larval and adult stages are listed if expression was detected, but for embryonic and pupal development, only the stage is listed as specific tissues were not tested. Some of the elongases (CG31522, CG2781, CG3971) are expressed throughout development, whereas others (CG16905, CG9458, CG31141) are more highly expressed at particular stages. There is also some overlap in the expression patterns for members within a clade again supporting similar functionality (purple and blue rectangles in Table 2.1). Taken together though, differences in expression patterns argue for distinct developmental rather than more general metabolic roles for family members. To directly test this I set out to broadly assess the function of the collection of *Drosophila* elongases.

Table 2.1: *Drosophila* elongases have different expression patterns during development. The boxes represent the clade specific grouping mentioned earlier.

	Elongase (CG)	Temporal Expression Profile			
		Embryonic	**Larval**	**Pupal**	**Adult**
A	**CG31522**	+ Stage:12-18	+ hindgut, fat body, trachea	+ early pupal stages	+ head, midgut, hindgut
	CG31523	+ Stage:12-18	+ midgut, hindgut, trachea	-	+ head, midgut, hindgut, heart , fat body, spermatheca
	CG2781	+ Stage:12-18	+ carcass	+ early pupal stages	+ head, hindgut, fat body,
	CG5278	+ Stage:18-24	+ early larval stages, carcass	-	+ male accessory gland
	CG5326	+ Stages:12-24	-	+ early pupal stages	+ male accessory gland,
	CG33110 / 6926	-	+ Late larval stages	+ late pupal stages	+ head, carcass
B	**CG11801**	+ Stages:18-24	+ larval trachea	-	-
	CG6261/ 32072	-	+ larval trachea	-	+ adult male
C	**CG6921**	+ Stage:18-24	+ Early larval stages, trachea	-	+ male testis, salivary gland
	CG30008 / 12138	-	-	-	+ male and female, heart, fat body, carcass
	CG6660	-	+ carcass	+ early pupal stages	+ heart, fat body, carcass
	CG17821	-	-	+ late pupal stages	-
	CG8534	-	+ carcass	+ late pupal stages	-
	CG18609	-	-	+ late pupal stages	+ heart, fat body, carcass
	CG16904	-	-	-	+ heart, fat body, carcass
	CG9458	-	-	-	+ heart, fat body, carcass
	CG9459	-	-	-	+ heart, fat body, carcass
	CG16905	-	-	-	+ (female) heart, fat body, carcass
	CG31141	-	-	-	+ testis
D	**CG3971**	+ Stages:12-24	+ CNS, hindgut	+ late pupal stages	+ CNS, midgut, , malphigian tubes, salivary gland, eye

Drosophila elongases play different developmental roles

Some of the *Drosophila* elongases have already been found to be important in reproduction and behavior (Chertemps et al., 2007; Szafer-Glusman et al., 2008). Bals has been shown to be important viability and male fertility (Jung et al., 2007). In order to determine the developmental roles of all elongases in *Drosophila*, an efficient tool was needed that would allow me to induce and rapidly screen loss-of-function (LOF) phenotypes for each elongase. RNAi provides such a tool and UAS lines containing ds-RNA of all the elongases were acquired from Vienna *Drosophila* resource center (Dietzl et al., 2007). Tissue specific knockdown was mediated using GAL4 lines targeting general knockdown, follicle cell knockdown, nervous system and segmental knockdown.

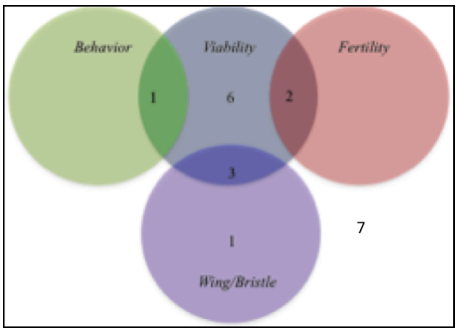

Figure 2.4: Venn diagram representing functional grouping of elongases

Figure 2.4, Figure 2.5, and Table 2.2 represent the compiled results for the screen. It can be concluded from figure 2.4 that elongases can have different roles *in vivo*. Twelve of the twenty elongases seem to be important for viability, two are important for fertility, one for behavior and four for wing/bristle development. Seven of the twenty elongases tested did not show any overt phenotypes in my screen. I also noted that elongases conserved across species were more likely to be functionally important based on their requirement for viability. Specifically, eight of nine of the *Drosophila* elongases that fell in clades including vertebrate elongases (A, B, D) were essential for viability. In contrast, only four of eleven elongases in the *Drosophila* only clade (C) were essential for viability (Figure 2.5). With respect to neural specific knockdown, only three

elongases had effects (viability), with one also exhibiting a unique behavioral phenotype, involving reduced movement. Other than *bals* only one other elongase was important for female fertility, while knockdown phenotypes using the segmental driver Ptc-GAL4 ranged from lethality, to defects in cross veins, wing size and missing bristles, suggesting that some elongases are required for proper wing/bristle development (4/20). Interestingly, I also observed sexual dimorphism in elongase function as knockdown of CG16905 (*eloF*), which is highly expressed in adult females, leads to female specific lethality, whereas CG32072 (elo68α), an elongase implicated in male reproduction, causes lethality in males (Table 2.2). In sum, the screen provides further evidence for developmentally specific roles for elongases, with vital functions being more closely associated with elongases conserved across species (Figure 2.5).

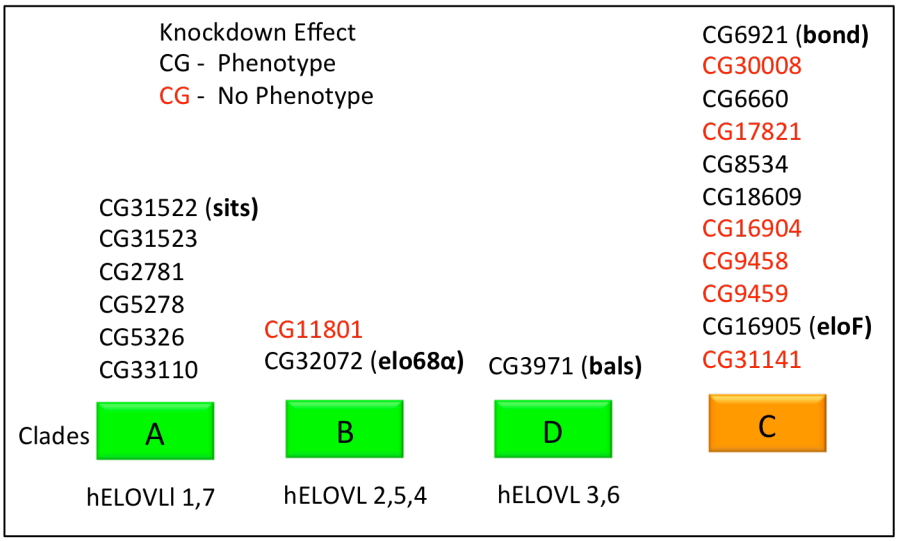

Figure 2.5: Sequence homology/groupings of human and fly elongases in different clades and its functional relevance. CG numbers are the fly elongases. hELOVL are the human elongases. A, B, C and D are different clades based on phylogenetic analysis. Clades A, B and C contains both the fly and human elongases. Clade C does not contain any human elongase. Elongases colored in red did not show any phenotype in the functional screen performed in this chapter.

Table 2.2: Developmental effects of *Drosophila* elongase knockdown. RNAi screen with twenty *Drosophila* elongases in specific tissues was done using Actin-GAL4, CY2-GAL4, C155-GAL4 and Ptc-GAL4.
The elongases that showed an effect in a particular tissue/process along with their phenotypes are highlighted. The boxes represent the clade specific grouping described above.

	Elongase (CG)	RNAi Mediated Elo Knockdown							
		Act GAL4[1] General expression		**C155 GAL4[1,2] Neuronal expression**		**CY2 GAL4[1,3] Follicle cells expression**		**Ptc GAL4[1,4] Segmantal expression (Viability/wing/bristle)**	
		Mutant Ph.	Observation	Mutant Ph.	Observation	Mutant Ph.	Observation	Mutant Ph.	Observation
A	**CG31522**	+	***Lethal*** (0%)$_{N=137}$	+	***Lethargy, Reduced locomotion Pharate lethality***$_{(N>100)}$	-	WT (N>100)	+	***Low Viability*** Reduced mobility (N=75)
	CG31523	+	***Low Viability*** (34%)$_{N=91}$	-	WT (N=25)	+	***CC*** (N>100)	-	WT$_{(N=39)}$
	CG2781	+	***Low Viability*** (1.8%)$_{N=111}$ (some pharate lethality)	-	WT (N=221)	-	WT (N>100)	+	***Low Viability*** Embryonic /larval lethality (N=32)
	CG5278	+	***Lethal*** (0%)$_{N=171}$ Larval /pharate lethality	-	WT (N=126)	-	WT (N>100)	+	***44% flies have a wing phenotype***$_{(N=87)}$
	CG5326	+	***Low Viability*** (3.3%)$_{N=122}$	-	WT (N=120)	-	WT (N>100)	-	WT (N=108)
	CG33110/ 6926	+	***Lethal*** (0%)$_{N=155}$	+	***Pharate lethality*** 5 escapers Normal movement	+	***Pharate lethal***	+	***Pharate lethal***
	CG32072/ 6261	+	***Male lethal*** (0% M & 65% F)$_{N=66}$	-	WT$_{(N=127)}$	-	WT (N>100)	-	WT$_{(N=182)}$
B	CG11801	-	Viable (91%)$_{N=42}$	-	WT$_{(N=83)}$	-	WT (N>100)	-	WT$_{(N=173)}$
	CG6921	+	***Lethal*** (0%)$_{N=38}$	-	WT (N=207)	-	***Low viability*** WT chorions$_{(N>100)}$	-	WT$_{(N=63)}$
C	**CG6660**	+	Reduced viability (53%)$_{N=92}$	-	WT$_{(N=145)}$	-	WT (N>100)	+	7/160 flies have ***one bristle less***$_{(N=160)}$
	CG17821	-	Viable (175%)$_{N=102}$	-	WT$_{(N=138)}$	-	WT (N>100)	+	WT$_{(N=185)}$
	CG8534	+	***Low Viability*** (2%)$_{N=53}$ pharate lethality	-	WT$_{(N=159)}$	-	WT (N>100)	+	WT$_{(N=102)}$

Elongase (CG)	RNAi Mediated Elo Knockdown							
	Act GAL4[1] General expression		**C155 GAL4[1,2] Neuronal expression**		**CY2 GAL4[1,3] Follicle cells expression**		**Ptc GAL4 [1,4] Segmantal expression**	
	Mutant Ph.	Observation	Mutant Ph.	Observation	Mutant Ph.	Observation	Mutant Ph.	Observation
CG18609	+	***Low Viability*** $(23\%)_{N=86}$ some pharate lethality	-	$WT_{(N=83)}$	-	WT $_{(N>100)}$	+	7/171 have *wing defects*$_{(N=171)}$
CG16904/ *CYO*	-	Viable $(91\%)_{N=99}$	-	$WT_{(N=150)}$	-	WT $_{(N>100)}$	-	$WT_{(N=175)}$
CG9458	-	Viable $(84\%)_{N=83}$	-	$WT_{(N=179)}$	-	WT $_{(N>100)}$	-	$WT_{(N=138)}$
CG9459	-	Viable $(137\%)_{N=144}$	-	$WT_{(N=147)}$	-	WT $_{(N>100)}$	-	$WT_{(N=161)}$
CG16905	+	***Lethal*** $(0\%)_{N=37}$ pharate lethality	+	***Wing phenotype*** (unfirled wings) Pharate lethality Movement $WT_{(N=48)}$	-	WT $_{(N>100)}$	+	***pharate lethality*** Female lethality small shriveled wings with crossvein defects (missing ACV)$_{(N=31)}$
CG31141	-	Viable (110%) $_{N=125}$	-	$WT_{(N=124)}$	-	WT $_{(N>100)}$	-	$WT_{(N=172)}$
CG30008/ 12138	-	Viable $(70\%)_{N=85}$	-	$WT_{(N=152)}$	-	WT $_{(N>100)}$	-	$WT_{(N=177)}$
CG3971	+	***Lethal*** $(0\%)_{N=155}$	-	$WT_{(N=207)}$	+	***CC*** $_{(N>100)}$	-	$WT_{(N=144)}$

1- Adult knockdown F1s were scored for any gross morphological defects and viability. The original parent vial was also observed for larval/pupal lethality. The percent viability was calculated by dividing the number of total progeny trans-heterozygotes for the indicated elongase and the GAL4 driver by the number of progeny of the trans-heterozygous for the GAL4 and the indicated elongase. N indicates the total number of progeny scored (Duffy and Gergen, 1991).

2- Adult knockdown F1s were observed for overt behavioral defects and assayed using Flip Over Assay. Numbers in the parenthesis indicate the total progeny assayed (materials and methods and supplementary Movie 4.3A).

3- Chorions from adult knockdown F1 females were observed for defects. Numbers in the parenthesis indicate the total eggs scored (materials and methods).

4- Adult knockdown F1s were scored for wing and bristle defects. Numbers in the parenthesis indicate the total progeny scored for viability and wing and bristle defects.

WT- wild type

CC- Collapsed chorions

DISCUSSION

Comparative analyses of *Drosophila* and vertebrate elongases revealed specific phylogenetic relationships suggesting functional roles may have been conserved from flies to humans. To gain insight on these roles and to determine if there are functional distinctions between family members in *Drosophila* I undertook functional studies. Using RNAi mediated tissue specific knockdown, I addressed the role and functional specificity of fatty acid elongases in *Drosophila* development. All twenty members of the elongase family in *Drosophila* were screened for their role in viability, neuronal development, fertility and wing/bristle development.

Sequence analysis of Drosophila Elongases

Both phylogenetic analysis and sequence alignments of *Drosophila* and vertebrate elongases revealed high sequence conservation both within and outside of putative functional domains. Specific *Drosophila* elongases formed clades with vertebrate elongases, while other elongases were restricted only to *Drosophila*, hinting both at functional homology between species and functional diversity within a species. For example, Bals is more closely related to vertebrate elongases than other fly elongases, while clade C represents a fly specific clade with eleven members.

Expression and Functional Analysis of Drosophila Elongases

RNA seq data, as well as the *in situ* data, on *Drosophila* elongases revealed spatio-temporal differences in their expression patterns during development (Chertemps et al., 2007; Jung et al., 2007; Szafer-Glusman et al., 2008). This is a direct indication of tissue

specific functions of these elongases and was supported by my functional analysis. For example, knockdown of only two of the twenty elongases, *bals/CG3971* and CG31523, resulted in collapsed chorions supporting specific roles for these elongases in oogenesis. Tissue specificity of function was also observed in neuronal development as only three elongases (CG31522, CG33110, and CG16905) exhibited effects with neuronal knockdown. Knockdown of each of these three elongases had effects on viability, while knockdown of CG31522 also affected adult locomotor behavior. Evidence of sex-specific roles was present, consistent with previously published work. Knockdown of CG32072/elo68alpha, which is predominantly expressed in males, resulted in male lethality and knockdown of CG16905 (*eloF*), which has been linked to the production of female specific pheromones, led to female specific lethality (Chertemps et al., 2007)

Lending support to the notion that the sequence conservation observed across species is indicative of functional significance, elongases conserved from flies to vertebrates were more likely to perform vital functions, as knockdown of these elongases more often resulted in lethality than elongases found only in *Drosophila*. Since only a limited number of processes/tissues were tested in this screen, it is possible that functions of elongases were missed. Knockdown of an elongase could have been viable, but might have produced specific defects affecting behaviors like aggression or courtship that were not tested here. Based on the phylogenetic and expression analyses, it is also possible that some elongases have overlapping functions and therefore the single gene knockdown would not show any overt phenotypes. To address that issue, it would be interesting to use the phylogenetic relationships to guide multigene knockdowns of some elongases to

see if this uncovers more overt phenotypes than what were observed, similar to what's been observed for yeast elongases. Yeast *elo-2* and *elo-3* single mutants are viable whereas *elo2, elo-3* double mutants are lethal (Oh et al., 1997).

The developmental roles of fatty acid elongases are coming under more scrutiny and even though they have been implicated in development and some diseases, in many cases their roles are not clearly understood. The results of this rapid RNAi mediated screen to look for loss-of-function defects during *Drosophila* development hints at the conservation of some of the basic elongase functions. The importance of elongases for viability has been seen both in mice and *Drosophila* (Li et al., 2007) and the *Drosophila* elongase Bals seems to be playing a role in maintaining epidermal barrier function just like its vertebrate counterparts Elovl3, Elovl4, and Elovl1 (Aldahmesh et al., 2011; Cameron et al., 2007; Sassa et al., 2013; Westerberg et al., 2004). In addition, roles for lipids in neuronal development have long been known, and their involvement in neurodegenerative diseases is coming under increasing scrutiny. Lipids have been implicated in diseases such as Huntington's (Desplats et al., 2007), Tay-Sachs (Friedman, 1971), Adreno-leukodystrophy (Ferrer et al., 2010), Parkinson's (Ruiperez et al., 2010). With respect to elongases, there is indirect evidence of involvement of human ELOVL1 in X-linked adrenoleukodystrophy (Ofman et al., 2010), and ELOVL4 has been identified as a cause of Stargadt disease, an early onset form of macular dystrophy (Zhang et al., 2001). The fact that several of the neurodegenerative diseases listed above have been recapitulated in *Drosophila*, along with the presence of conserved lipid metabolic genes, including elongases, suggests that *Drosophila* may be a useful system to decipher the

lipid connections of the diseases. In this regard, it was interesting that my RNAi screen identified an elongase, CG31522 or *sit still* (*sits*), that exhibited a striking behavioral phenotype upon neuronal specific knockdown. This neuronal phenotype included a lack of coordination, reduced locomotion, and premature death symptoms somewhat analogous to those observed in patients suffering from above mentioned neurodegenerative disorders. Whether or not this analogy is functionally relevant remains to be determined, but it is intriguing that *sits* is conserved across species, being most closely related to vertebrate Elovl1 and Elovl7. It is tempting to speculate that Sits represents a previously unknown, but conserved role in neuronal development.

MATERIALS AND METHODS

***Fly genetics*:** All the flies were maintained at room temperature in regular food. Crosses were set up at 28 degrees unless noted otherwise.

Phylogenetic and Sequence Analysis: Full length protein sequences were aligned using Clustal W2 (http://www.ebi.ac.uk/Tools/msa/clustalw2/) using Gonnet type protein matrix, Gap open 10, Gap extend 0.1and Neighbor joining clustering. For Figure 2.2, the sequences were cropped to highlight the more conserved domains. All the sequences used for alignment can be found in Appendix B.

Flip Over Assay: Progeny of the right genotype is sorted and placed overnight in the vials without the yeast. The progeny is shifted into a new vial without yeast the next day and the vial is tapped and inverted and again tapped (flipped over) (Supplementary Movie 4.3A) and the flies are observed for any locomotion. Displacement of a fly in a given direction (except circling) is considered as locomotion. The number of flies performing the locomotion as well as number of non movers (flies sitting at a fixed location or circling) is counted for every set of flies.

Fertility Assay/Chorionic Assay: Flies of the correct genotype were made to lay eggs overnight on apple juice agar plates (standard Duffy lab recipe). Flies were removed in the morning and the laid chorions were scored for collapsed chorion phenotype or other overt morphological defects.

***Fly stocks*:** All the RNAi lines were acquired from Vienna *Drosophila* Resource Center (VDRC), Austria. Following table lists all the lines used in this chapter.

Table 2.3: List of VDRC stocks for elongases RNAi.

CG	Trans-formant ID	Construct ID	RNAi library	ON Targets	OFF Targets	Viability	Inserted Chromo-some
CG31522	106652	108786	KK	1	0	lethal	2
CG2781	102543	111950	KK	1	0	viable	2
CG5278	107919	106859	KK	1	0	viable	2
CG6921	102051	110522	KK	1	0	viable	2
CG3971	101557	109085	KK	1	0	viable	2
CG5326	106540	112190	KK	1	0	viable	2
CG6660	101046	106710	KK	1	0	viable	2
CG17821	107255	105782	KK	1	0	viable	2
CG8534	106515	111518	KK	1	0	viable	2
CG18609	100172	105151	KK	1	0	viable	2
CG16904	103434	112025	KK	1	0	lethal	2
CG9458	102418	111629	KK	1	0	viable	2
CG9459	102715	112257	KK	1	0	viable	2
CG30008	6760	419	GD	1	0	viable	3
CG31141	100460	104411	KK	1	3	viable	2
CG32072 (Elo68 α)	9206	3869	GD	1	2	viable	2
CG16905 (EloF)	103269	112719	KK	1	1	viable	2
CG11801 (Elo68 β)	103506	112353	KK	1	1	viable	2

CG	Trans-formant ID	Construct ID	RNAi library	ON Targets	OFF Targets	Viability	Inserted Chromo-some
CG31523	45226	4631	GD	1	1	viable	1
CG33110	29689	15094	GD	1	350	viable	2

Chapter 3

Molecular and Genetic characterization of *sits* locus

ABSTRACT

In the screen described in chapter three we identified a fatty acid elongase, *sit still* (*sits*), that showed a behavioral phenotype where the adults exhibit locomoter defects. In order to further characterize its function in *Drosophila* behavior we analyzed *sits* role throughout development using a variety of molecular and genetic techniques and behavioral assays. In this chapter, I report that the *sits* genomic locus is transcriptionally complex, that *sits* is expressed in a tissue specific manner during *Drosophila* development and that *sits* is a vital gene.

INTRODUCTION

Among *Drosophila* elongases Sit still is the most orthologous to mammalian ELOVL1 and ELOVL7. In mice an *elovl1* knockout is embryonic lethal due to impaired epidermal barrier function, whereas a knockout has not been reported for *elovl7* and thus little is known about its the function. As described in chapter two an RNAi screen in flies involving the tissue specific knockdown of elongases suggested that knockdown of *sits* in the nervous system leads to overt locomotion defects. This is the first report of a role for an elongase in locomotion and raises the question as to whether this function is unique or conserved among other fly elongases. The ability to dissect the role of *sits* in an amenable model system like *Drosophila* provides the opportunity to better understand the basis for this function and, eventually, if it is indicative of a broader role for elongases in vertebrates.

This chapter focuses on genetic and molecular characterization of the *sits* genomic locus. Utilizing the already available genetic information it was inferred that *sits* genomic locus exhibits some degree of molecular complexity with respect to the number of transcripts, promoter region and encoded proteins. RNA *in situ* hybridizations revealed that *sits* is expressed in embryonic and larval tissues, while mutational analysis demonstrated that *sits* is a vital gene.

RESULTS

The genetic locus of Sits is complex

sits genomic region is located at the 82B cytological location on the third chromosome (3R) and covers around 21.5 Kb. Seven putative transcript isoforms have been predicted

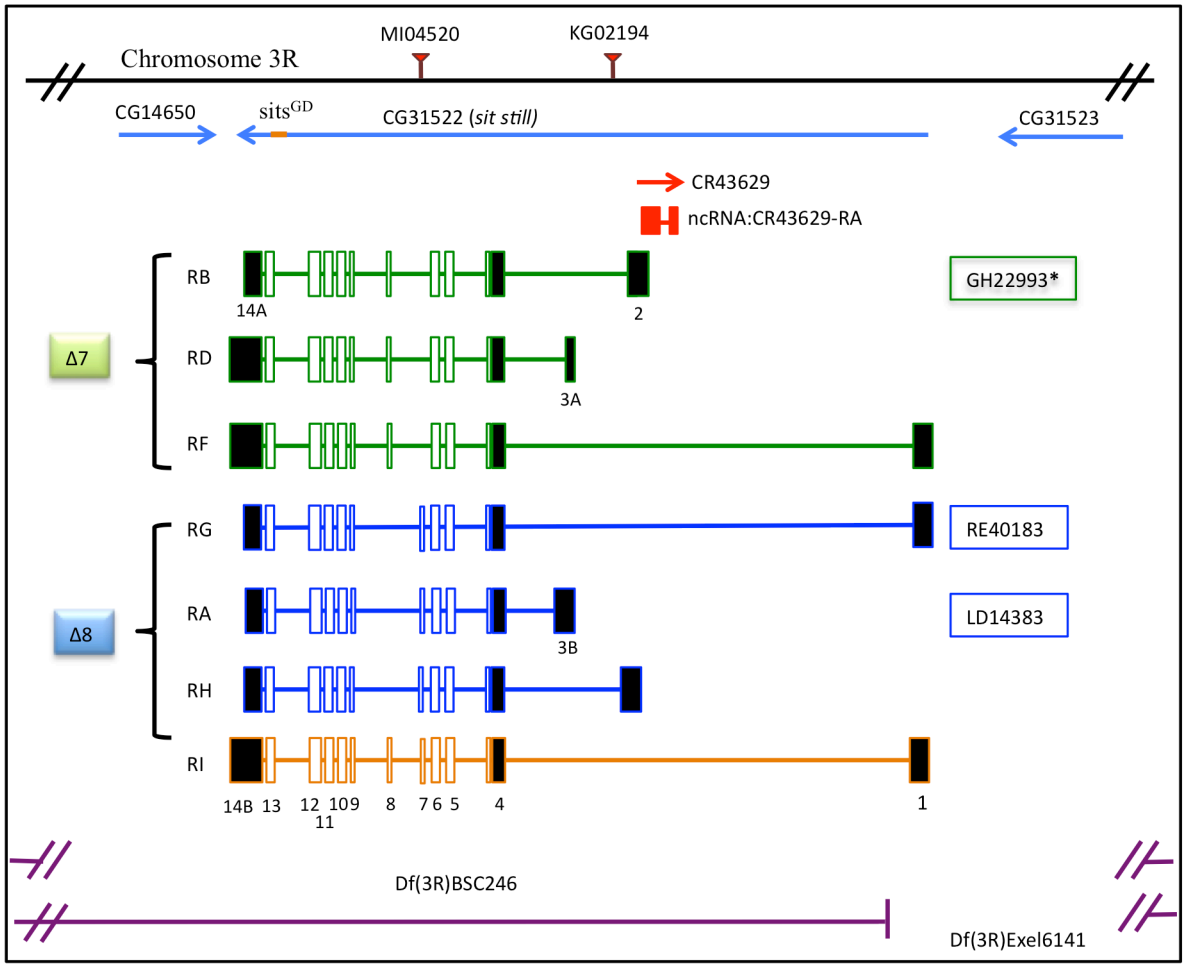

Figure 3.1: Schematic representation of *sits* (CG31522) genomic locus at 82B1-82B2. The coding sequences are represented by white boxes and the untranslated regions are indicated by black boxes. The transcript variants are color coded based on the presence or absence of exon 7 and 8. Corresponding cDNA clones are listed on the right of the transcripts. * = cDNA clone used in this study. Approximate site for insertion for the P-element alleles is indicated on the chromosome. The red arrow (CR43629) represents a noncoding RNA within the *sits* genomic region. The deficiencies uncovering the chromosomal region of 82B are depicted below the transcription units. The neighboring genes CG31523 (a closely related elongase) and CG14650 (unknown function) are also shown. The red line on the *sits* genomic region represents the *sits*^{GD} RNAi trigger. The entire schematic is approximately to scale.

that encode for three putative protein variants. The coding variants differ from each other based on the absence of exon 7 ($RB^{\Delta 7}$, $RD^{\Delta 7}$ and $RF^{\Delta 7}$) or exon 8 ($RA^{\Delta 8}$, $RG^{\Delta 8}$ and $RH^{\Delta 8}$) or presence of both (RI) and all of these exons are supported by the presence of corresponding cDNA clones and/or RNA seq data ((Tweedie et al., 2009), data not shown). No cDNA is available for the longest transcript RI, which encodes the third predicted Sits isoform. There are 14 putative exons encoded by *sits* transcript variants, 10 of which contain coding sequences for Sits. GH22993, the cDNA corresponding to RB, RD and RF transcript variants encodes a 365 amino acid protein and was the one used in this thesis for rescue and misexpression studies. Interestingly, although they are non-overlapping exons 7 and 8 have a conserved core sequence that might have a functional relevance since it is present in both the variants (Figure 3.2).

Figure 3.2: Sequence similarity between two exons present in different Sits variants. PB* is used in this study. Magenta indicates the region common between the isoforms. Yellow indicates the extra amino acid present only in PI.

As there are multiple transcript variants of the *sits* gene, it is possible that there are different regulatory elements involved in *sits* expression and thus its function (Chapter four). The gene region also contains a noncoding snRNA of unknown function.

sits exhibits tissue specific expression during development

To gain insight on the function of *sits,* RNA *in situs* were carried out to determine its expression profile *in vivo* with greater cellular resolution than the RNA seq expression data obtained by the *Drosophila* genome project. High throughput RNA seq data indicates high expression of *sits* in the larval hindgut, the fat body, trachea, and the adult head, thoracic ganglion, midgut and hindgut (Tweedie et al., 2009). High levels of expression were also detected in embryos (stage 14-20), the pupal central nervous system (Stage P8), and the adult female and male head and adult digestive system (Tweedie et al., 2009). To get cellular level insight to *sits* expression during development, I designed an antisense RNA probe using *sits* cDNA, GH22993 and performed *in situ* hybridizations

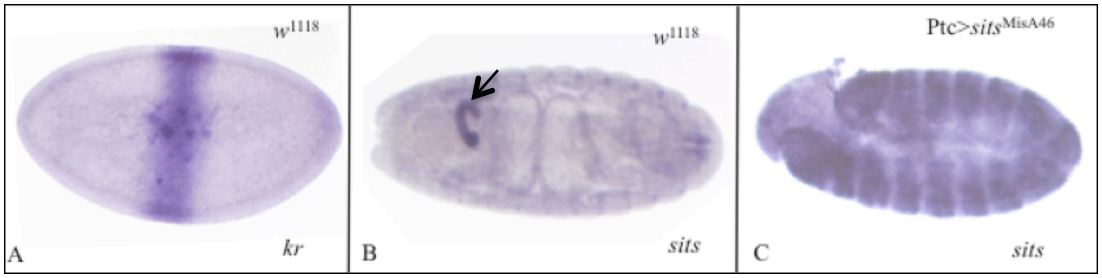

Figure 3.3: *sits* mRNA expression. A) Control w^{1118} embryo hybridized with a probe for the gap gene *kruppel* (*kr*). B) w^{1118} embryo with *sits* probe. C) Ptc>$sits^{MisA46}$ embryo *with* sits probe. Anterior is to the left and dorsal is up. Arrow points to the esophageal staining.

on embryos and larval tissues (Figure 3.3, 3.4). In stage 16/17 embryos, high levels of specific expression are detected in what is likely the esophagus with lower levels detectable in the posterior hindgut.

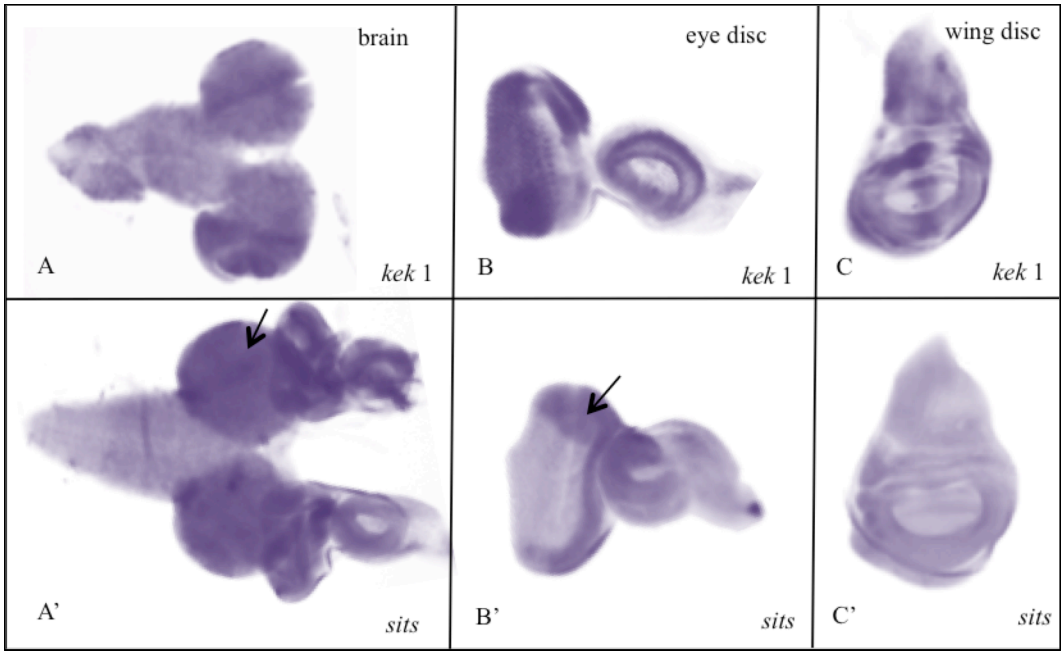

Figure 3.4: *sits* expression in larval tissues. Arrow indicates Sits expression. w^{1118} discs A, B & C are probed for *kek1* whereas A'B' & C' are probed for *sits*.

In order to prove that the probe is specific to *sits*, I misexpressed *sits* using a GAL4 driver, Ptc-GAL4, that expresses in a segmental pattern in embryos, and observed positive segmental staining for *sits* (Figure 3.3). In third instar larvae, expression is observed in various patterns in the eye and wing discs, as well as in the nervous system, with expression being more prominent in the optic lobes than in the ventral ganglion in the brain.

sits activity is essential for viability

As shown in Figure 3.1 there are two P-element insertions mapping within the *sits* genomic region that are available through Bloomington Stock Center. Analysis of both the P-element insertions suggested that they have reduced viability (Table 3.1).

Complementation tests with each P-element insertion and a large deletion that uncovers *sits* (*Df(3R)BSC246*) resulted in even lower viability suggesting that the P-elements are hypomorphic *sits* alleles and that *sits* is important for viability. In order to generate

Table 3.1: Complementation crosses of *sits* genomic region. Highlighted percentages indicates the percent viability and numbers in the bracket indicate the number of flies scored.
* indicates an accessory lethal
R7= cleaned $sits^{KG02194R7}$

	$sits^{KG02194*}$	$sits^{KG02194R7}$	$sits^{MI04520}$	*Df(3R)BSC246*	*Df(3R)Exel6141*
$sits^{KG02194*}$	**0%** (n=130)			**3.3%** (n=245)	**119 %** (n=102)
$sits^{KG02194R7}$		**47%** (n=104)		**1.2%** (n=333)	
$sits^{MI04520}$			**11%** (n=111)	**0%** (n=97)	
Df(3R)BSC246	**3.3%** (n=245)	**1.2%** (n=333)	**0%** (n=97)	**0%** (n>500)	**0%** (n=190)
Df(3R)Exel6141	**119%** (n=102)			**0%** (n=190)	**0%** (n>500)

additional, hopefully stronger, alleles of *sits* to further understand *sits* loss-of-function, I employed a method of creating imprecise excisions of the original P-element insert. Through the imprecise excisions I hoped to obtain small-scale deletions in *sits* generating

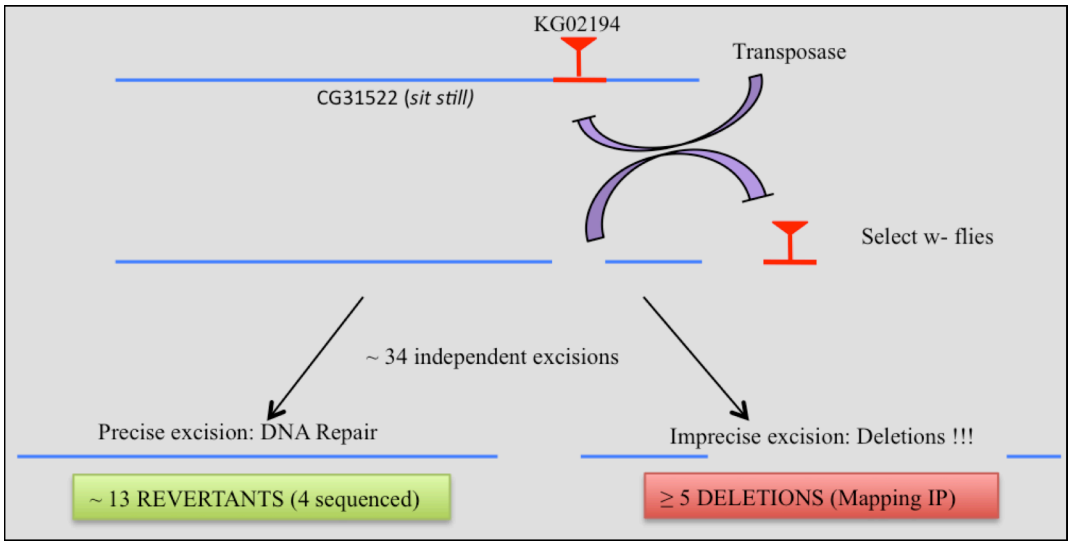

Figure 3.5: *sits* P ($sits^{KG02194}$) element excision scheme. KG02194 is the *sits* transposon selected for excision. Out of 34 independent excisions generated, both the revertants and the revertants and the deletions have been recovered.

a null allele (Figure 3.5). One of the two P-element insertions, *sits*^{KG02194}, was selected to generate excisions and crossed to a strain providing a source of transposase. Resulting individual flies lacking the transgene (identified by the absence of the w^+ eye marker) were then selected to generate balanced stocks. During this process it was determined that there was an accessory lethal mutation also present on the starting chromosome, in addition to the original P-element insertion (*sits*^{KG02194*}). Unfortunately, due to this accessory mutation all of the resulting excisions were homozygous lethal. However, upon performing complementation tests between these excisions and the large deletion for the *sits* region, *Df(3R)BSC246*, a percentage of excisions showed wild type viability (Table 3.2). Molecular analyses of four excision lines that are viable over *Df(3R)BSC246*, was consistent with reversion events suggesting they represent precise excisions that restored the chromosome to wild type (data not shown). The isolation of these revertants indicated a number of important points. First, the reduced viability of the original P-element insertion over the large deletion was due to the insertion (and not the accessory lethal) as clean excision of the P-element restores viability to wild type levels when placed over *Df(3R)BSC246*. This analysis confirmed that *sits* was important for viability. It also indicated that the accessory lethal, which was still present in the revertant lines (as they were homozygous lethal), did not map to the region uncovered by *Df(3R)BSC246*, the large deficiency for the *sits* region. This confirmed that the accessory lethal was not affecting *sits* function. To further demonstrate this, I removed the accessory lethal from original P-element insertion stock by recombining it with the wild type chromosome and obtained a clean insertion strain (*sits*$^{KG02194\mathbf{R7}}$). Using this strain I repeated the

complementation crosses and it recapitulated the original results that *sits* is important for viability.

In contrast to the revertant alleles, a second class of excisions was lethal over *Df(3R)BSC246* consistent with imprecise excisions that have generated deletions in *sits*. Although the precise breakpoints of these lines have not been defined, at least two of these lines appear to represent deletions within *sits*. Such lines again confirm the requirement of *sits* for viability and represent useful genetic tools for further analysis of *sits* role in development.

Table 3.2: Complementation analysis of *sits*^{KG02194} excisions.

	Df(3R)BSC246	*sits*$^{KG02194\Delta 17*}$	*sits*$^{KG02194\Delta 92*}$	*sits*$^{KG02194\Delta 23*}$	*Df(3R)Exel6141*
Df(3R)BSC246	**0%**(n>500)	**138%**(n=385)	**0%**(n=321)	**7%**(n=279)	**0%** (n=190)
sits$^{KG02194\Delta 17*}$	**138%**(n=385)	**0%**(n>300)			**414%**(n=43)
sits$^{KG02194\Delta 92*}$	**0%**(n=321)		**0%**(n>500)		**119%**(n=281)
sits$^{KG02194\Delta 23*}$	**7%**(n=279)			**0%**(n>200)	**333%**(n=16)
Df(3R)Exel6141	**0%** (n=190)	**414%**(n=43)	**119%**(n=281)	**333%**(n=16)	**0%**(n>500)

* = accessory mutation
Δ= excision

DISCUSSION

Analysis of the *sits* genomic region revealed molecular complexity involving seven transcript variants and three putative protein isoforms, which differ from each other with respect to two internal exons (exons 7 and 8). Interestingly, although representing distinct exonic sequences at the nucleotide level, these two exons both contain a conserved nine amino acid stretch suggesting that those amino acids might have some functional relevance. Given its conservation in all protein isoforms, it is tempting to speculate that this conserved sequence is critical for *sits* function, but that the distinct versions of this region provide for functional specificity between isoforms.

Consistent with distinct isoforms and the possibility of unique developmental functions, data from my RNA *in situ* hybridization and RNA seq from the *Drosophila* genome project indicated that *sits* expression is both temporally and spatially regulated. The absence of a ubiquitous expression pattern in embryos or larvae provides further support for a specific role for *sits* during development, arguing against it acting as a general metabolic enzyme required in all cells.

Mutational analysis demonstrated that *sits* is essential for viability, with lethality of *sits* mutants occurring predominantly at 1^{st} and 2^{nd} instar larval stages. Interestingly, although the majority of *sits* mutants don't survive, a small percentage of *sits* mutants "escapers" survive to adulthood and appear overtly normal. This was a bit surprising given that RNAi mediated knockdown of *sits* results in locomotor defects and suggests that there is a certain threshold level for *sits* function and once that is reached flies appear wild type.

MATERIALS AND METHODS

Fly stocks: All the information regarding the genomic region, number of transcripts and protein variants was obtained from Flybase. The cDNA clone GH22993 was obtained from DGRC (*Drosophila* Genomic Resource Center). All the crosses were carried at 25°C unless mentioned otherwise. Stocks were ordered from Bloomington stock center. Δ2-3 transposase (y^1 w^*; ry^{506} Sb^1 P{Δ2-3}99B/TM6)- B.S# 3664, P{SUP}$sits^{KG02194}$*= B.S# 14183, Mi{MIC}$sits^{MI04520}$ = B.S#37818, Deletions *Df(3R)BSC246* and *Df(3R)Exel6141* = B.S# 9720 and B.S#7620. The stocks were rebalanced on TM3Sb for ease of scoring.

in situ hybridization: cDNA GH22993 was used to make digoxygenin labeled *sits* probe by adding T7 promoter on the 3' end. The resulting 1.25 Kb fragment was then hydrolyzed for 19 minutes. Embryos from w^{1118} and *Ptc>*$sits^{MisA46}$ were collected and fixed as described earlier (Patel, 1994). *in situ* hybridization procedure was adapted and from (Tautz and Pfeifle, 1989) with hybridization temperature of 65°C and 3X 15minute washes with Hybe-B near the water bath. 1µl of the final probe was used for each hybridization reaction. The larval tissue was dissected from w1118 larvae in PBT (PBS+.1% Tween20+.1%DEPC) and fixed in 3.7% formaldehyde/PBT for 15 minutes. The tissue was serially rinsed 5X in PBT, 30%, 50% in PBT and 100% methanol (in PBT) and stored at -20°C till the *in situ* was performed.

P element excisions: P element excisions were carried out by crossing P{SUP}$sits^{KG02194}$ to the Δ2-3 transposase Δ2-3. The resultant progeny with the P and the transposase was selected based on their mosaic eye colors. The individual males of the right genotype

were taken and crossed to virgin females of the third chromosome balancer *LY/TM3Sb* and the resulting progeny was scored for white eyes (*w*-) and *TM3Sb*. The individual flies with the right genotype were then further crossed back to the third chromosome balancer *LY/TM3Sb* and select for non Ly flies to make the balanced stock of the excision. All the excisions generated using P{SUP}*sits*^{KG02194} were homozygous lethal because of the presence of an accessory mutation and hence the lines were tested with the available deletions to determine the revertants vs the deletions. This was further verified using molecular analysis.

Molecular characterization of P-element excisions: Genomic DNA of the putative revertants (excisions viable with the deletion) over the deletion *Df(3R)BSC246* was prepared using Qiagen DNA extraction kit. 5' W180 and 3' W181 primers were used to perform the PCR on that DNA as template to cross over the location where the P was originally inserted (primer sequences listed in appendix C). The band hence recovered was gel purified using Qiagen kit and the DNA was sent for sequencing to a company called Genewiz. Similarly DNA was generated using the similar strategy for the putative deletions over the *Df(3R)BSC246* (from escapers) and the breakpoints are verified using PCR.

ACKNOWLEDGEMENT

Work on *sits* was started with the help of an MQP student Shreelekha Mandal. Initial molecular characterization of *sits* P-element excisions were carried out with the help of an undergrad Corbyn Lamy.

Chapter 4

Analysis of *sits* function in locomotor control

ABSTRACT

Locomotion is a critical requirement for animal survival. From searching for food, avoiding predators or pain to mating, animals have developed complex motor behaviors. Underlying these motor behaviors are neural circuits that control decision making, selection, initiation, and execution. Not surprisingly, motor defects are often associated with neurodegenerative disorders, including Alzheimers and Parkinson's. In this chapter, I have focused on an elongase, conserved from flies to humans, that is required in flies for locomotor behavior. Reducing the activity of this elongase (CG31522), Sit Still (Sits), in the nervous system led to inactivity, lack of coordination, twitching, circling, and premature death. Additionally, it was found that misexpression of Sits in the nervous system results in a larval behavioral/locomotor phenotype. Taken together, my work provides the first direct link between an elongase and locomotor activity in any organism.

INTRODUCTION

In the prior chapter, Sits (CG31522) was one of the twenty *Drosophila* elongases that were screened for their function during development. Of the twenty, only *sits* affected locomotor behavior, representing the first direct involvement of a fatty acid elongase in regulating locomotor activity.

Lipids in brain development, behavior and neurodegeneration

Lipids form an important constituent of the brain both structurally and functionally. In the mammalian brain, lipids constitute 50-60% of the dry weight, phospholipids being the most predominant lipid class (Youdim et al., 2000). Omega-3 PUFAs such as docosahexaenoic acid (DHA) and eicosapentaenoic acid (EPA) are major constituents of neuronal membranes and function in neuromodulation and neuroprotection (Zhang et al., 2011). Additional links come from neurological diseases such as Tay-Sachs and Niemann Pick that are also known as lipid storage disorders because they involve excessive lipid accumulation. There are also proposed roles for lipids in cognition and behavior. Altered lipid composition has been associated with several psychiatric and neurodegenerative disorders (Gul et al., 1970; Khan et al., 2010).

Neuronal /behavioral studies in Drosophila

The fact that basic neuronal machinery is conserved between flies and humans (Figure 4.1), means it is possible to study a vast repertoire of neuronal functions in flies and gain insight to vertebrate systems. For example, work on the neuronal basis of learning (Ren et al., 2012), decision-making (Certel et al., 2010), memory formation (Dubnau and Chiang, 2013), nociception (Xu et al., 2006), olfaction (Apostolopoulou et al., 2013), courtship &

mating (Le et al., 2012), sleep patterns (Beaver et al., 2012), aggression (Zwarts et al., 2011), and locomotion (Slawson et al., 2011) has been carried out using *Drosophila* as a

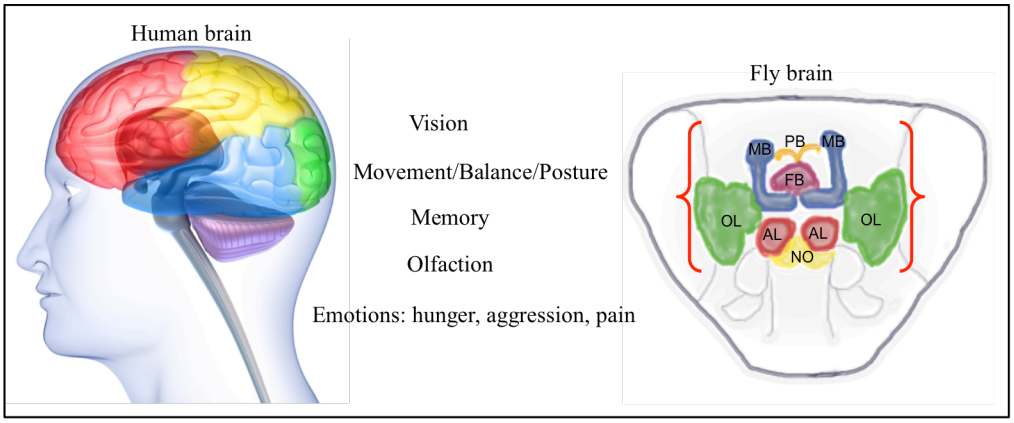

Figure 4.1: Similarity between the fruit fly and human brain. The processes in middle are common functions of human and fly brain. Different regions of *Drosophila* brain performing these functions are highlighted. PB= Protocerebrum bridge, FB= Fan shaped body, OL= Optical lobe, AL= Antennal lobe, NO= noduli, MB= Mushroom body.

model system. In many cases different regions of the brain have been shown to be responsible for carrying out these tasks. In flies, the mushroom bodies have been implicated in learning and memory (Huang et al., 2012), whereas the central complex has been shown to function in locomotor control (Poeck et al., 2008). There are several advantages to using *Drosophila* to study complex behavioral processes because of the increasing repertoire of tools and reagents. Several efforts are being made to map the complete neuronal population of *Drosophila* brain. Recently, a collection of 7000 GAL4 lines was generated that allows the expression of exogenous genes in specific subsets of the adult nervous system and thus helps in identifying novel neuronal cell types and manipulating the function of existing cells (Jenett et al., 2012).

Locomotor behavior

Locomotion is the act or the ability to move from one point to another. It is an indispensable aspect and a fundamental requirement for an individual that enables it to find food, escape from predators, defend its territory or find a mate. Locomotion is a highly coordinated process involving neural circuits that process sensory information and guide appropriate behavioral responses. In humans, voluntary movements are initiated in motor cortex that sends the electrical signals through the motor neurons and the brain stem to the spinal cord and ultimately to the muscle (Ghez et al., 1991). In *Drosophila*, the Central Complex (CC) is one of the most prominent structure that has been associated with locomotion (Strauss and Heisenberg, 1993). The CC is comprised of four distinct structures, namely the ellipsoid body, the fan-shaped body, the noduli and the protocerebral bridge. Mutations affecting the different structures of the CC components have defects in walking speed, leg coordination and straightness of walking (Strauss and Heisenberg, 1993). Specifically, mutations in the protocerebral bridge affect locomotion (Poeck et al., 2008) and ellipsoid body defects affects the flight behavior (Ilius et al., 2007). Other than the CC, mushroom bodies are the most extensively studied structure of the *Drosophila* central nervous system and it has clear roles in learning and memory (Akalal et al., 2010; Lee et al., 2011). Mushroom bodies have also been implicating in controlling some aspects of locomotion (Helfrich-Forster et al., 2002; Serway et al., 2009).

My screen of elongase family functions revealed a strong link between *sits* activity and locomotor behavior. Knockdown of *sits* in the nervous system led to locomotor defects

accompanied with lack of coordination and premature death. To confirm this phenotype and better understand the ties between fatty acid elongation and neural function I set out to characterize the role of *sits* in locomotor behavior in *Drosophila*.

RESULTS

Knockdown of sits in Drosophila nervous system affects locomotor behavior

siRNA mediated knockdown of sits suggests a role in adult locomotor behavior

RNAi mediated knockdown of one particular elongase, Sits (CG31522), in the *Drosophila* nervous system resulted in a behavioral phenotype with locomotion defects (Chapter 3, Movie 4.1 A & B). Adult flies with pan neural knockdown of *sits* (C155>*sits*^{GD}) showed very limited mobility, lack of coordination, twitching and premature death. The behavior was initially quantified using general methods of startle induced negative geotaxis, such as vortexing and a flip over assay (Featherstone et al., 2008; Gargano et al., 2005; Homyk, 1977; Jordan et al., 2012)(Movies 4.2 A, B & Movie 4.3 A & B). These assays, though useful, were somewhat subjective and less robust. To enable a more quantitative analysis of the behavioral defects I adapted an automated machine vision based method of behavior quantification developed for *Drosophila* using Ctrax (Branson et al., 2009). This approach involves automated tracking of a group of flies in a closed arena and generating trajectories that contain the position and orientation of each fly in each frame of a recorded video that can be converted into quantifiable data (Movie 4.4 A & B). A specialized chamber was constructed which allowed the flies to move around freely and each fly is denoted as a colored oval. The flies are detected as dark images on the light background and they are assigned certain pixels, which are picked up by the software for every frame. Figure 4.2 shows the video frame snapshot of control (C155>*mCD8*::GFP) and *sits* knockdown flies (C155>*sits*^{GD}). The control flies move around freely in a specialized circular area (adapted from (Simon and Dickinson, 2010)), whereas *sits* knockdown flies don't show any significant movements. Panel C

shows the tracks made by the control flies in the first five hundred frames of the video, while in panel D, for the *sits* knockdown flies there are no visible tracks. The control flies tend to move more towards the edge of the chamber possibly due to the air draft. Additional information about fly movement, including speed and distance traveled, was also generated using the same software, thereby providing direct objective quantification of underlying aspects of the locomotion defects.

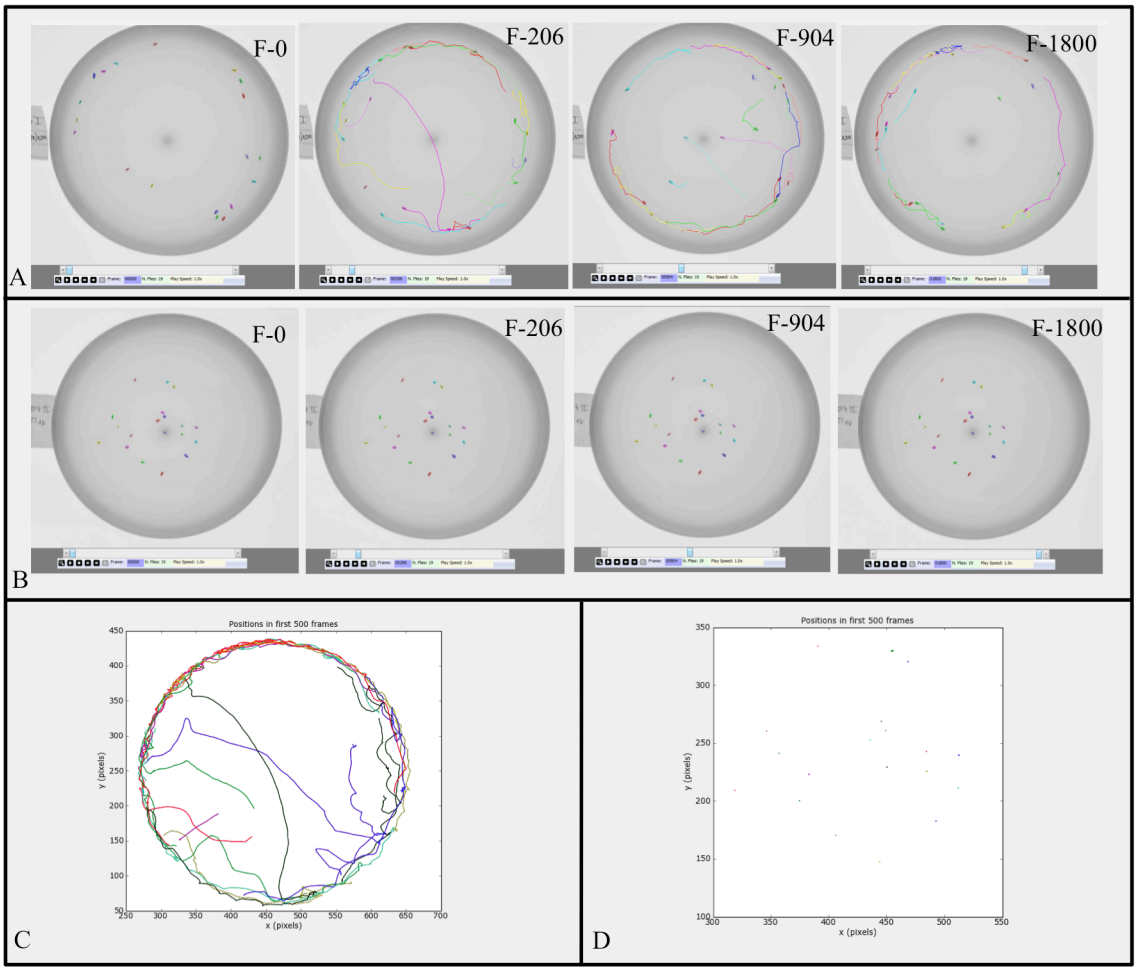

Figure 4.2: *sits* knockdown results in locomotion defects. Video frame captures of (A) control flies (C155>*mCD8*::GFP) and (B) *sits* RNAi flies (C155>*sits*^{GD}). Each colored oval represents an individual fly and the corresponding colored line is the track it traveled in previous 150 frames at the time of snapshot. Frame numbers are listed on top right corner of each snapshot. (C) and (D) are snapshots of the cumulative trajectories made by the control flies (C) and *sits* mutants (D) in first five hundred frames as calculated by Ctrax.

The tracking results indicate that flies with *sits* knockdown showed minimal locomotion as depicted by their near zero speeds as compared to their control counterparts (Figure 4.3).

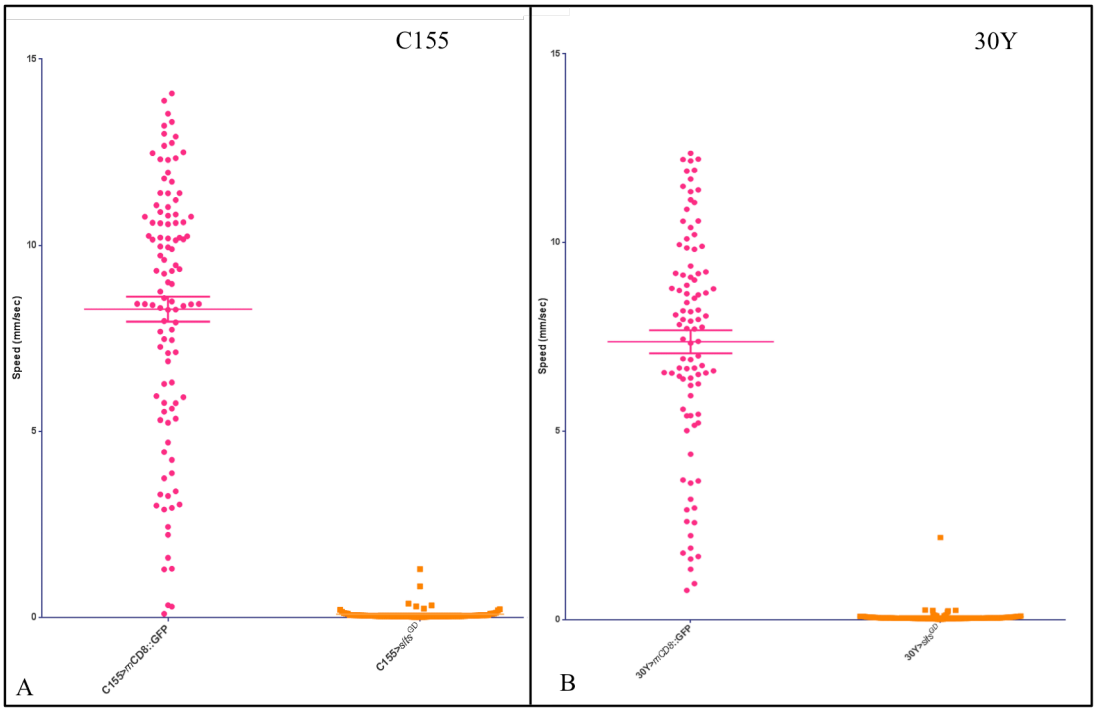

Figure 4.3: Neuronal knockdown of *sits* affects locomotion. Each point represents the speed of an individual fly. Pink dots are the control flies and orange squares are the *sits* mutants. A) C155>*m*CD8::GFP (n=106) and the C155>*sits*^{GD} (n=90). There is a significant difference between the control and the mutant flies (Unpaired t test, p <0.0001). B) Means differ significantly between the controls and the experiment (p<000.1), N= 95 & 107 for 30Y>*m*CD8::GFP & 30Y>*sits*^{GD} trigger respectively. The speeds depicted on the graph are for males. Similar phenotype was observed in the females at higher temperatures (Appendix).

This reduction in movement was quite strong and the effect was seen in both males and females. Knockdown with a more restricted neuronal driver pGawb-30Y (30Y, adult expression including but not limited to mushroom, ellipsoid and fan shaped bodies, subesophageal ganglion, antennal & optic lobes, protocerebrum & median bundle) was able to robustly recapitulate the *sits* locomotor phenotype without significant effects on

viability making it easier to recover adults for analysis (Movie 4.5 A & B). Thus, 30Y was used for carrying out majority of my experiments.

Genetic and molecular validation of the role of sits in adult locomotor behavior

As described previously in Chapter three the RNAi trigger used for *sits* knockdown

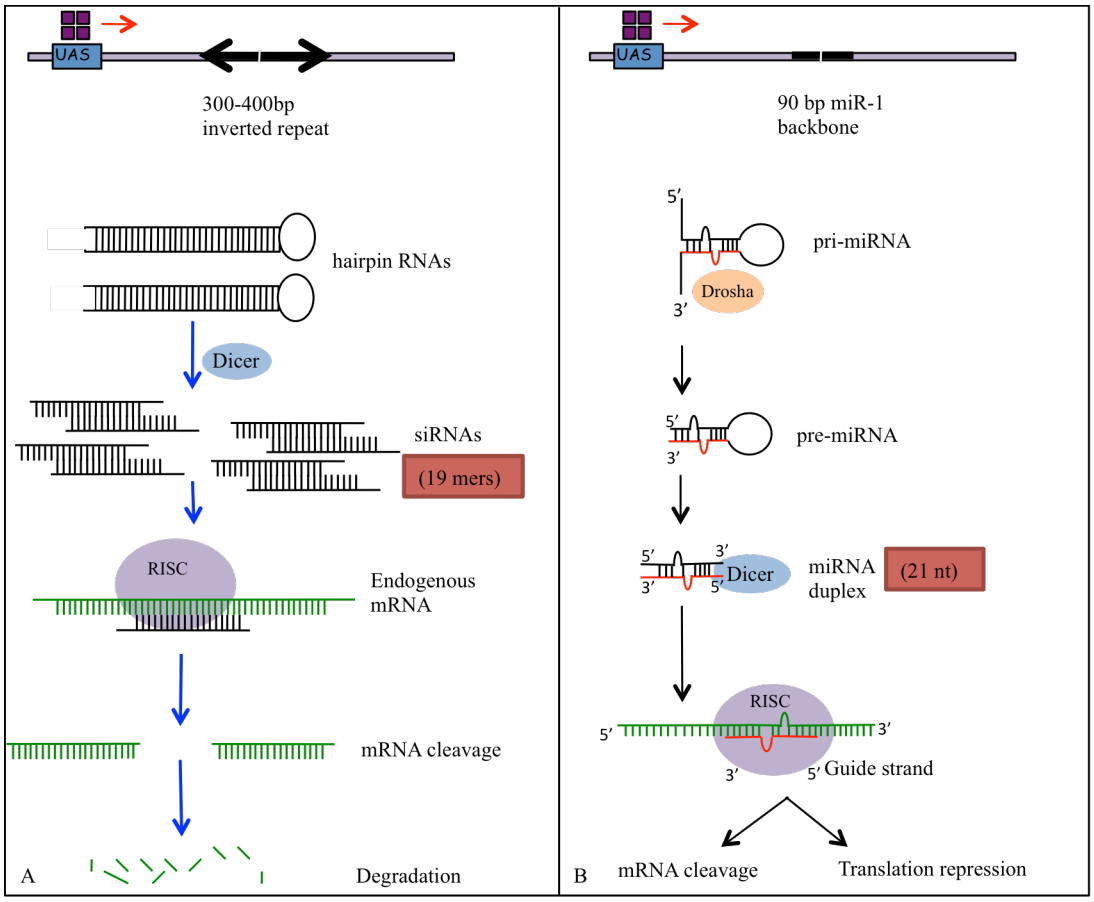

Figure 4.4: Two separate pathways of RNA interference (RNAi). Panel A is long hairpin mediated siRNA pathway and B is short hairpin mediated miRNA (shmiR) pathway. The miRNA based approach used for this study utilized miR-1 backbone and the 21 bases of the target sequence from *sits* 3', 5' UTRs and coding region.

(UAS-*sits*^{GD}) was obtained from the Vienna *Drosophila* Resource Center (VDRC). These triggers were designed using an inverted (IR) method where the resulting hairpin RNA is 'diced' *in vivo* to generate all possible combinations of 19-mers targeting the *sits* RNA (Dietzl et al., 2007)(Figure 4.4, Panel A). The biggest shortcoming of this method is the

possibility of 'off-target' effects where a potential 19-mer can target an off-target gene for degradation as well. For *sits*^{GD} trigger, out of 282 possible 19-mers that targeted *sits*, one also targeted the gene CG9265, which is predicted to have a putative nucleotide binding activity (Tweedie et al., 2009). Knockdown of the putative off-target gene, CG9265 did not appear to affect locomotor activity, supporting the notion that locomotor phenotype of the UAS-*sits*^{GD} construct is dependent on *sits*.

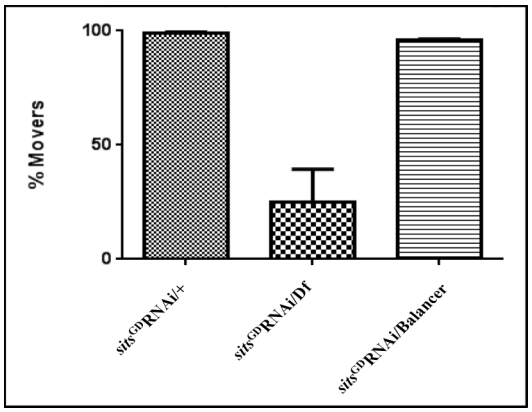

Figure 4.5: Reducing *sits* RNA pool results in mutant phenotype. The experiment was performed at 21°C. The genotypes from left to right: C155>*m*CD8::GFP>*sits*^{GD};+/+, C155>*m*CD8::GFP>*sits*^{GD}; *Df(3R)BSC246*/+, C155>*m*CD8::GFP>*sits*^{GD};*TM3Sb*/+. N= 692, 353 and 235 respectively. P<0.05, Ordinary One Way ANOVA.

In order to confirm this, I utilized three different approaches. First, I used a sensitized genetic background that combined the *sits* knockdown with a deficiency, *Df(3R)BSC246*, that uncovers *sits*, thereby reducing the target pool of *sits* mRNA by 50%. At 21°C, GAL4 activity is reduced leading to reduced expression of the *sits* RNAi trigger, less efficient knockdown and normal locomotor activity among females. Addition of the deficiency to the same genetic background should reduce the *sits* RNA pool by 50%, leading to enhanced knockdown and induction of the locomotor phenotype. As predicted if the target is indeed *sits*, addition of the deficiency to this genetic background led to a reduction in percentage of moving flies (Figure 4.5).

The second approach was a more direct approach for gene specific knockdown using miRNA based shmiR (short hairpin miRNA) triggers that have been recently used as an

effective way of gene silencing (Figure 4.4, Panel B) (Ni et al., 2011). *The most important advantage of using an miRNA based approach over an siRNA approach is the increased specificity and reduced probability of off-target effects as only one 21mer specific to the target sequence is synthesized and used to target the gene of interest.* In addition each trigger can be individually targeted to distinct regions (5'UTR, ORF, 3'UTR) of the same gene. Using this miRNA based approach, I generated three different shmiR triggers to the 3'UTR, ORF and 5'UTR of *sits* gene using a modified scaffold of the endogenous microRNA miR-1 (Materials and Methods). Consistent with the effects of *sits*^{GD} knockdown locomotor effects were observed with all three shmiR *sits* triggers (Figure 4.6). Together the ability of three distinct trigger sequences targeting the *sits* gene to induce the locomotor phenotype confirmed the activity of *sits* is essential for normal locomotor activity. Adding more support, I was able to partially rescue the locomotor phenotype by expressing Sits (isoform PB) to flies also carrying 5'UTR shmiR trigger (Figure 4.7).

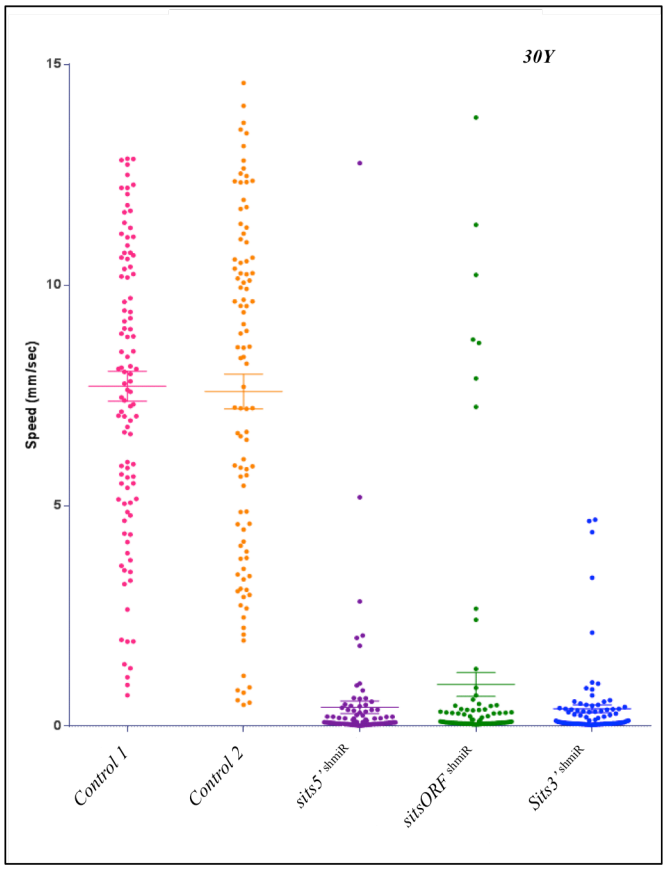

Figure 4.6: *sits* specific shmiRs induce locomotion defects. Genotypes from left to right: Control 1 30Y>w^{1118} (n=102), Control 2 (30Y>*bond*^{shmiR}) (n=100), *sits*5'shmiR (30Y>*sits*5'UTR^{shmiR}) (n=99), *sits*ORFshmiR (30Y>*sits*ORF^{shmiR}) (n=93), *sits*3'shmiR (30Y>*sits*3'UTR^{shmiR}) (n=96). P<0.0001, Kruskal Wallis test.

As mentioned in chapter four, *sits* encodes for three putative protein isoforms and isoform PB was used for rescue. The partial rescue observed could be attributed to distinct functions between isoforms or alternatively the level of expression of the transgene due to chromosomal effects due to insertion position. Regardless of the level of rescue, the combined results from all of the experiments above confirm the requirement of *sits* in regulating normal locomotor behavior in *Drosophila* adults and suggest some level of dose dependence in this process. Misexpression of just the *sits* transgene (UAS-*sits*^{MisA46}) does not have any effect on the locomotor behavior and functions similar to the control flies (Figure 4.7).

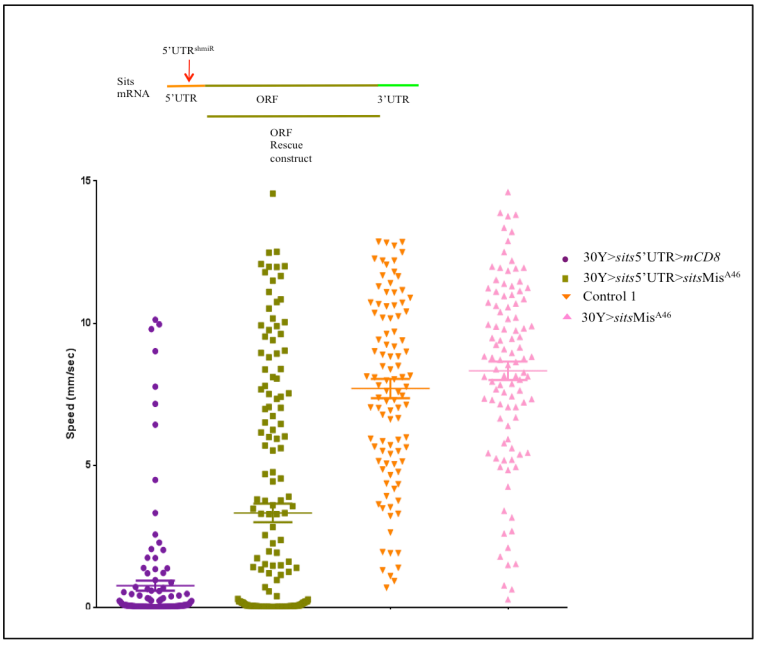

Figure 4.7: *sits* locomotion defects are partially rescued by adding Sits isoform PB. *sits* knockdown (30Y>sits5'UTR>*m*CD8, n=155), *sits* rescue (30Y>*sits*5'UTR>*sits*^{MisA46}, n=168), Control 1 30Y>w^{1118} (n=102) added for reference from figure 4.6 and *sits* Misexpression (30Y>*sits*^{MisA46}, n~100) . P<0.0001, Kruskal Wallis test. The schematic on top outlines the rescue approach.

Sits knockdown induces additional adult behavioral phenotypes

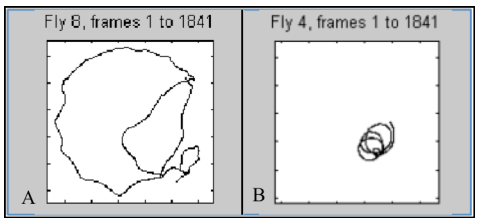

Figure 4.8: A circling phenotype is associated with *sits* knockdown. Tracks of A) Control (30Y>w^{1118}) B) *sits* miRNA mutant (30Y>*sits*5'UTR^{shmiR} fly).

Careful observation of *sits* knockdown flies revealed additional behavioral phenotypes. Apart from lack of movement, I observed that *sits* mutants showed other phenotypes, including

twitching, circular movement, disorientation, and problems with balance and coordination, as well as premature death (Figure 4.8) (Movies 4.6, 5.7, 5.8 and 5.9). Approximately 30-40 % of movers showed circling for shmiR based *sits* knockdown. Interestingly though, the flies seem able to groom and can also hop when stimulated (Movies 4.10 & 4.11).

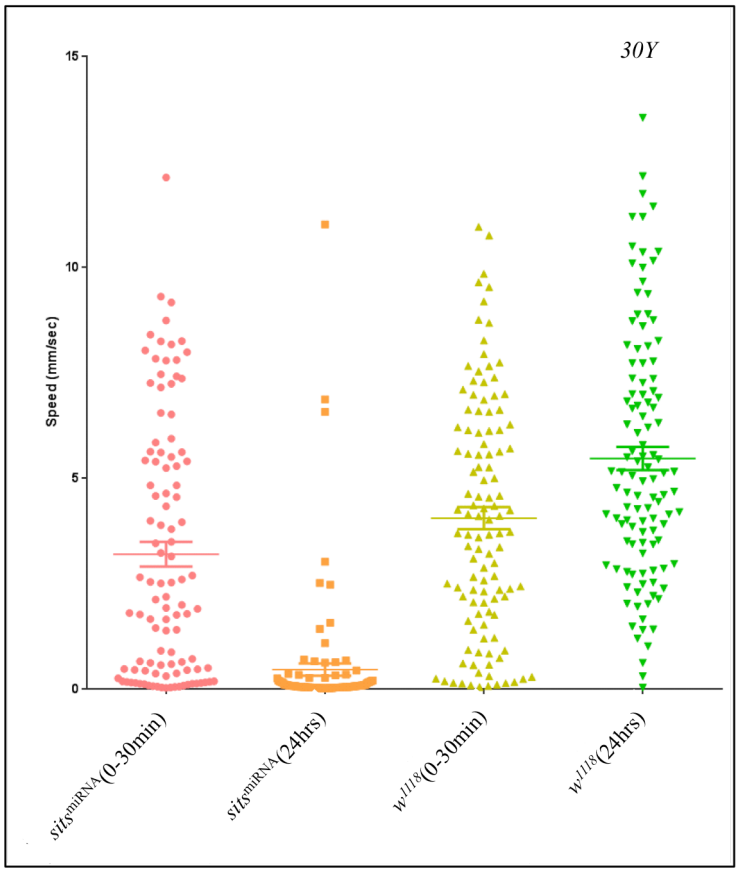

Figure 4.9: *sits* affect on locomotion is temporally dependent. Gal4 used is 30Y. sits miRNA trigger is 5'UTR. Time is calculated post eclosion. Genotypes from left to right: 30Y>*sits*5'UTR^{shmiR}(0-30min) PE, 30Y>*sits*5'UTR^{shmiR}(24hrs) PE, 30Y>w^{1118}(0-30min) PE, 30Y>w^{1118}(24hrs) PE. N= 100 each. $p<0.0001$, Kruskal Wallis test. Dunn's post hoc test shows significant difference between the first two groups (****) whereas there is no difference between the control and the mutants early on (0-30min flies). Test also show the two controls being different to each other (*). Similar temporal requirement was observed with 30Y>*sits*^{GD} (Appendix B, Figure B.).

During the process of collecting adults for behavioral studies, I noted differences in activity that appeared to be age dependent. This suggested the locomotor phenotype might in fact be temporally dependent. To analyze this, the locomotor activity of newly eclosed *sits* flies (0-30') was compared to day old *sits* flies (24hrs). Strikingly, *sits* knockdown mutants appear to move with close to normal frequency immediately after eclosion (Figure 4.9, Movie

4.12 A). They then show a decline in locomotion over time and within 24 hours of eclosion the majority of flies exhibited the classic *sits* locomotor phenotype (Figure 4.9, Movie 4.12B). Thus, knockdown of *sits* induces a temporally dependent/progressive reduction in locomotor activity.

Finally, *sits* knockdown flies also exhibited a significant reduction in lifespan as compared to the control flies (Figure 4.10). Surviving knockdown flies show some degree of locomotion.

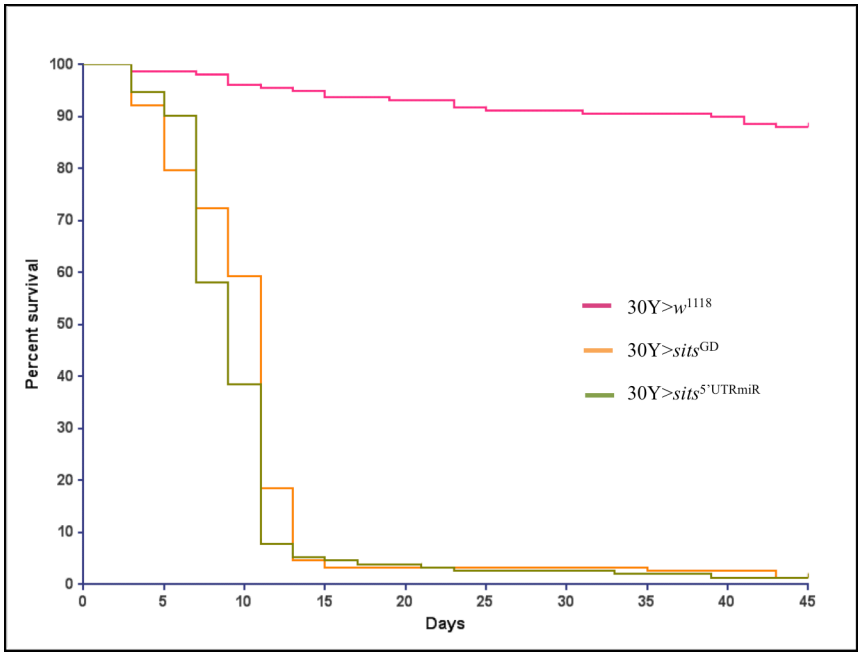

Figure 4.10: Reduced *sits* activity affects the normal lifespan in adults. For both RNAi triggers (30Y>$sits^{GD}$ and 30Y>$sits^{5'UTRmiR}$), there is a steep reduction in percent of flies alive as compared to the control flies (30Y>w^{1118}). N= ~ 150 per genotype. Graph made by Kaplan Meier method.

Pupal activity of sits is required for normal adult behavior

Although knockdown of *sits* produces a temporally dependent effect on adult locomotor behavior, the phenocritical period for knockdown was unknown. All experiments involved continuous induction of the RNAi triggers from embryogenesis through adulthood. I tested the induction of *sits* RNAi only in the adult nervous system and found that it did not result in locomotion defects. This suggests that *sits* activity is required prior to adult stages for normal behavior and that *sits* might be playing a developmental role in the *Drosophila* nervous system (n>70, data not shown). In order to determine the phenocritical period for *sits* activity, I performed the temperature shift assay that utilizes the temperature dependence of GAL4 activity. At 20^{o}C GAL4 activity is low leading to inefficient *sits* knockdown and normal motor activity in females. Knockdown was then induced at different developmental stages by shifting to 26^{o}C to increase GAL4 activity and expression of the *sits* RNAi trigger. It was found that triggering RNAi by shifting the vials after pupal stages P5-P7 does not induce

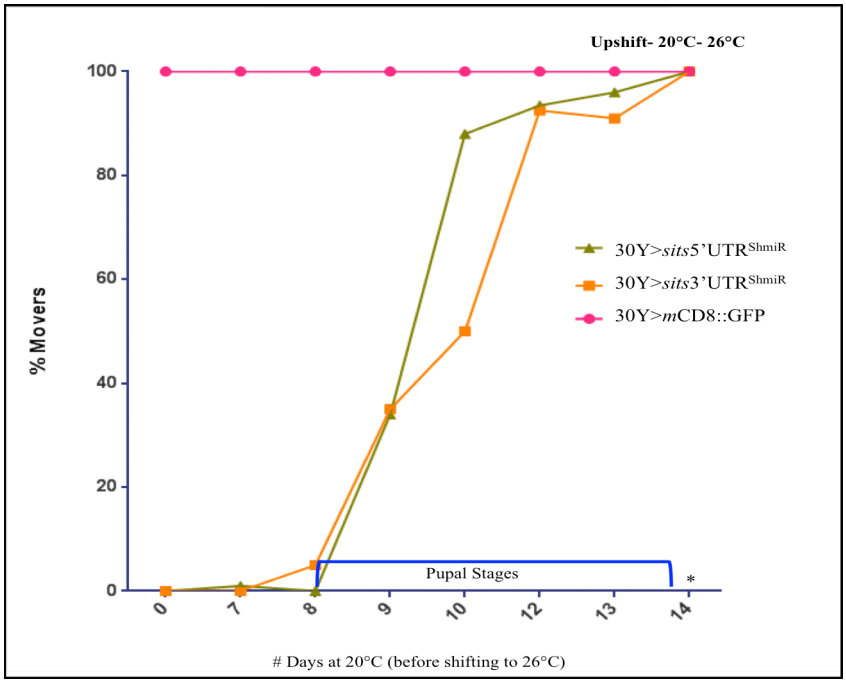

Figure 4.11: sits activity is required during pupal stages.
N = 318, 237 & 420 for mutants 30Y>*sits*3'UTR^{ShmiR}, 30Y>*sits*5'UTR^{ShmiR} & control 30Y>*m*CD8::GFP respectively. Blue bracket indicates the pupal stages and * indicates the day of eclosion.

sits phenotype (Figure 4.11). Additionally, *sits* knockdown in larvae doesn't show any overt locomotor (n=10, Movie 4.13) or behavioral (feeding, data not shown) defects as compared to the control. *sits* mutant embryos also didn't show any gross morphological defects in the ventral nerve cord or the CNS, when stained by the neuronal markers αID4 (marker for Fasciclin II) and αBP102(marker for CNS axons) (Appendix B, Figure B.5). This result along with temperature shift data suggests that *sits* expression during pupal stages is critical for normal adult locomotor behavior and survival.

Sits activity is required in the central nervous system for wild type behavior

As mentioned in earlier chapters, the behavioral phenotype observed using RNAi knockdown of *sits* was initially observed with a pan-neural (entire nervous system) GAL4 driver (C155). In *Drosophila*, the nervous system is broadly divided into the Central Nervous system (CNS) and Peripheral Nervous System (PNS) and contains a myriad of cellular populations including neurons, glia and other specialized cell that form a part of an organized neural circuit. The PNS is comprised of sensory neurons that innervate external sensory organs like chemosensory or mechanosensory organs (bristles, sensilla etc), and chordotonal organs (e.g. hearing organs) located in stretch receptors. The CNS is divided in the central brain, Sub-esophageal Ganglion (SOG) and the Ventral Nerve Cord (VNC). The cellular population of the CNS is comprised of motor neurons (axons to innervate muscles), interneurons (axons innervate other neurons) and neurosecretory neurons (secrete neuropeptides and hormones). Glia act as the support cells and help in axonal pathfinding (Hidalgo and Booth, 2000), axon fasciculation

(Spindler et al., 2009), neuronal survival (Booth et al., 2000) and neuronal ensheathment (Leiserson et al., 2000).

The induction of locomotor defects by pan-neural knockdown of *sits* using C155 GAL4 did not provide specific clues as to the specific type of cells, motor neurons, interneurons, glia, etc., underlying this phenotype. In order to understand the tissue requirement of *sits* activity, I tested a broad set of cell type specific GAL4 drivers to mediate *sits* knockdown and assessed their ability to induce the locomotor phenotype. Table 4.1 shows a subset of GAL4 drivers tested for their requirement for *sits* function (A complete list of all the drivers tested can be found in Appendix B, Table B.1). No effect on locomotor activity was observed with glia, motor neuron, astrocyte, or PNS specific knockdown, which

Table 4.1: Lack of effect with Muscle, Glia, Motor Neuron and PNS GAL4 drivers support CNS role for *sits*.

Driver (GAL4)	*Expression Pattern*	*sits mutant phenotype*
P{GawB}elav[C155]	Pan neural	Yes
y[1] w[*]; P{w[+mC]=GAL4-Mef2.R}3	Muscle	No
w[*]; P{w[+mW.hs]=GawB}D42	Motor Neurons	No
Repo GAL4/TM3, Sb[1]	Glia	No
Alarm GAL4	Astrocytes (Glia)	No
w[*]; P{w[+mW.hs]=GawB}43	Glia and subset of PNS	No
GMR GAL4	Eye	No
P{GawB}neur[GAL4-A101]	Sensory organs and their precursors	No

together ruled out a role for glia, motor neurons and the PNS and supported a role for the CNS for *sits* function in locomotor behavior.

The *Drosophila* CNS is made up of the brain and the ventral nerve cord, which develop and mature throughout the life cycle (Figure 4.12, Panel A). The brain is composed of several neuropils that are defined as the synapse rich regions formed because of dense interconnectivity between neurites in the localized region versus the adjacent area (Yu et al., 2013). These neuropils have distinct anatomical distinctions that help in dividing the brain circuitry into sub-circuits. Some of the most well characterized neuropils in *Drosophila* brain are the Antennal Lobes (AL), the Mushroom Bodies (MBs) and the components of the Central Complex (CC) (Figure 4.12, Panel B). As mentioned in the introduction, these neuropils have been associated with locomotor behavior. In addition, several bio-amines are present in the nervous system, mostly localized to the Sub-esophageal Ganglion SOG, which consists of fused ganglia and is located just below the esophagus in the brain, acting as neurotransmitters and thus regulating behaviors. *Drosophila* brain utilizes all the canonical neurotransmitters such as acetylcholine, dopamine, glutamate, GABA,

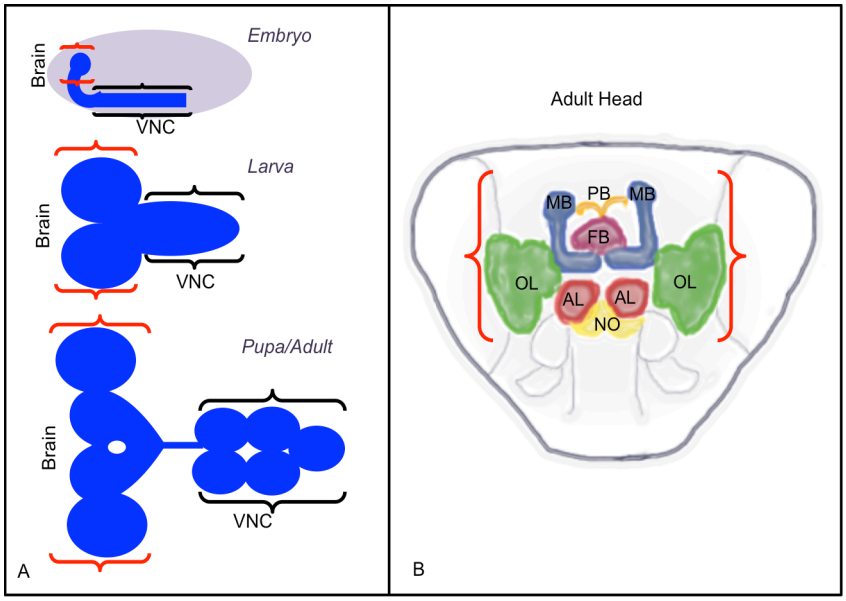

Figure 4.12: Schematic representation of *Drosophila* CNS. A) brain and ventral nerve cord during development B) adult brain divided into distinct anatomical regions called neuropils. VNC= ventral nerve cord, PB= Protocerebrum bridge, FB= Fan shaped body, OL= Optical lobe, AL= Antennal lobe, NO= noduli, MB= Mushroom body. Red parenthesis= brain, black parenthesis = VNC

tyramine, octopamine, serotonin, and histamine. Dopamine has been shown to be an essential neuromodulator for both vertebrates and invertebrates affecting processes like motivation, movement control, cognition and attention (Gaffori et al., 1980). In *Drosophila*, mutants lacking dopamine synthesis specifically in nervous system show reduced activity, locomotion deficits that increase with age, and extended periods of sleep (Riemensperger et al., 2011). To better define what cells within the CNS were mediating Sits function and therefore its role in locomotor behavior, I screened a diverse set of GAL4 drivers reflecting distinct expression patterns involving the cell types described above for the ability to mediate *sits* dependent locomotor defects (Appendix B, Table B.1).

Table 4.2: Gal4 Drivers that showed the *sits* phenotype.

Driver (GAL4)	*Expression Pattern (Flybase)*
P{GawB}30Y	mushroom, ellipsoid and fan shaped bodies, subesophageal ganglion, antennal & optic lobes, protocerebrum & median bundle
P{GawB}129Y	antennal nerve & subesophageal ganglion
P{GawB}SG18.1	antennal olfactory receptors, neurons and processing centers in CNS, also imaginal precursors
Sli Gal4	MP1 neurons and Midline Glia
P{GawB}OK376	Oenocytes (and larval CNS)
w[*]; P{w[+mW.hs]=GawB}MT14	olfactory, gustatory and mechanosensory neurons, as well as photoreceptor cells R2, R5 and R8

However, while some specific lines were able to induce the locomotor phenotype, no common pattern or specific neuronal structure could be discerned from the combined results with all the drivers tested (Table 4.2, Figure 4.13, Appendix B, Table B.1). These results did, however, indicate that particular regions, including the individual components of the central complex or the SOG alone, were unlikely to play a critical role (data

not shown). Thus while corroborating the CNS dependence of the phenotype, the cellular basis remained unclear.

Furthermore, I analyzed the expression of some of the abovementioned GAL4 lines that

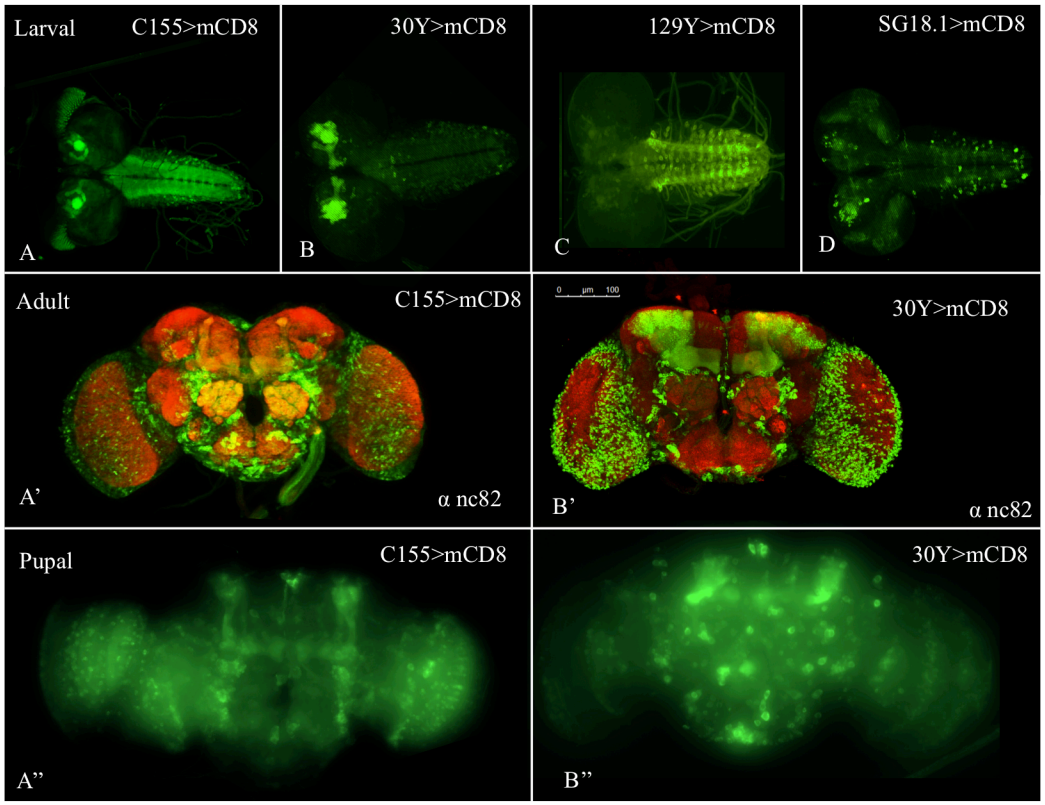

Figure 4.13: Expression patterns of GAL4s that are required for *sits* function are non-overlapping. A, A'&A'' are C155>mCD8::GFP larval, adult and pupal brains respectively. B, B'&B'' are 30Y>mCD8::GFP larval, adult and pupal brains respectively. C) 129Y>mCD8. D) SG18.1>mCD8. Adult brains are stained with α nc82 neuropil marker.

did trigger the phenotypic effects were analyzed in larval, adult and pupal brains by tagging them with a reporter (GFP) (Figure 4.13). It was hypothesized that expression pattern in larval and adult brain might give us some insight on the cellular population requirement in pupal stages, which is when the *sits* expression is necessary for normal behavior but is a very difficult stage to analyze neuronal expression. Expression patterns

in both the larval and adult nervous system did not show overlapping patterns between the different GAL lines, thus making it difficult to deduce specific tissue/ cellular requirement for *sits* function.

In addition to the lines above, I also screened a set of GAL4 lines from the FLY LIGHT project for their ability to induce the *sits* knockdown phenotype (Jenett et al., 2012). These lines express GAL4 under the control of regulatory fragments from neuronal genes that act as transcriptional enhancers in well-defined subsets of the adult nervous system (Jenett et al., 2012; Pfeiffer et al., 2008). These lines were tested based on specific expression in individual components of central complex or subesophageal ganglion or other subparts of *Drosophila* CNS, but none were able to recapitulate the phenotype (data not shown).

Regulatory analyses of sits supports a role for CNS based function in adult behavior

Rather than use regulatory elements from unrelated loci to map the cellular requirement for *sits*, I chose to screen the regulatory elements of *sits* as an alternative approach. The putative regulatory

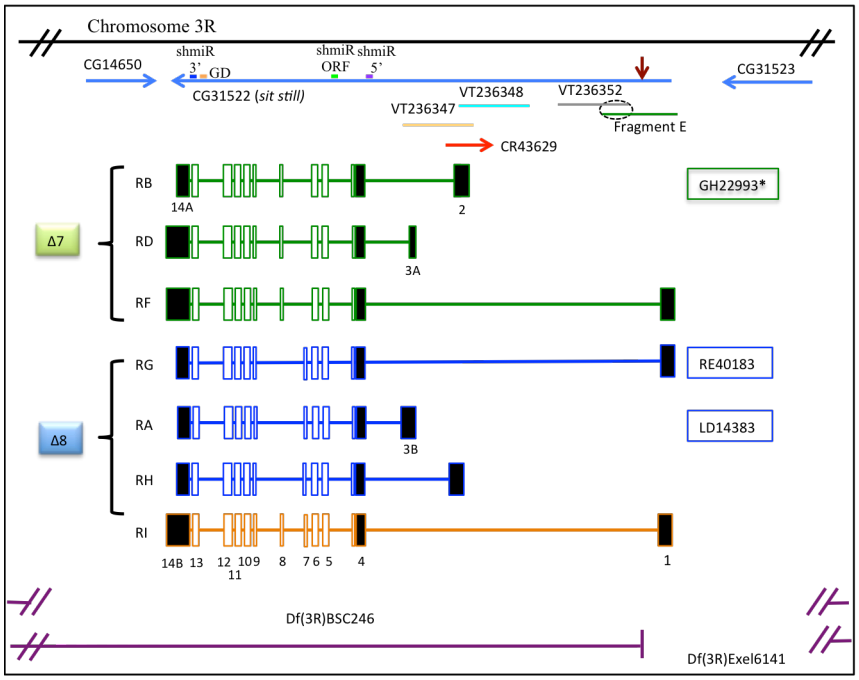

Figure 4.14: Schematic of *sits* genomic locus with regulatory element fragments. Fragment E is the RE-GAL4 generated in house. VT lines were obtained from VDRC. The encircled region in Fragment E and VT236352 is the ~900 bp stretch that should contain *sits* regulatory elements. Arrow in maroon represents the breakpoint for deletion *Df(3R)Exel6141*. Different RNAi triggers (3', ORF, 5' and GD) are marked on top of the genomic region.

region of *sits* was divided into six overlapping PCR based fragment of ~2.5 kb each. All fragments were cloned into the GAL4 expression vector pBPGuw that contains a *Drosophila* synthetic core promoter (C. Jain personal communication, DSCP). Clones containing each putative *sits* regulatory fragment were then co-transfected with a UAS-GFP tagged responder in *Drosophila* S3 cells and tested for the ability to induce GFP expression. Of the putative regulatory elements fragment E was selected to create transgenic flies based on its ability to trigger GFP expression in cell culture, suggesting it contained regulatory sequences capable of promoting expression.

Transgenic lines containing Fragment-E GAL4 (RE-GAL4) were established and then tested for the ability to induce the *sits* knockdown phenotype. Expression of both *sits*^{GD} and *sits*5'UTR^{shmiR} mediated by Fragment-E GAL4 (RE-GAL4) resulted in the *sits* dependent locomotor phenotype (data not shown). This suggests that fragment E contains regulatory elements that are necessary for *sits* expression and function in locomotor behavior, providing a critical tool for mapping of the cellular basis of this function. Concurrently with our work, the Vienna Drosophila Resource Center had also generated a set of GAL4 lines under the control of putative *sits* regulatory fragments. These three additional putative regulatory region fragments fused to GAL4 were obtained and tested for their effect on *sits* knockdown (Figure 4.14). Two of them were able to recapitulate *sits* knockdown phenotype, whereas one had no effect. Interestingly, one of the two (VT236352) positive VDRC lines partly overlaps our positive fragment RE-GAL4. This suggests that *sits* regulatory elements necessary for its endogenous expression and function in locomotor behavior are present in the ~900 bp overlapping region just downstream of its first exon. Consistent with this, a chromosomal deletion in the region,

Df(3R)Exel6141, uncovers a small region of *sits* 5'UTR, but leaves this 900bp region intact and is viable and displays no locomotor phenotype in combination with *sits* alleles (Figure 4.14). Preliminary expression analyses (larval and adult stages) of the regulatory element lines capable of inducing the *sits* phenotype, fragment E, VT236352, and VT236347, indicate neuronal expression, but it is unclear to what, if any, overlap in expression exists among the lines. Thus, we have identified *sits* specific regulatory fragments that define expression critical to its role in locomotor behavior, providing a key tool for uncovering the cellular basis for the *sits* phenotype.

Cellular basis of sits phenotype

sits knockdown in the CNS leads to locomotion defects in adult flies. In order to gain

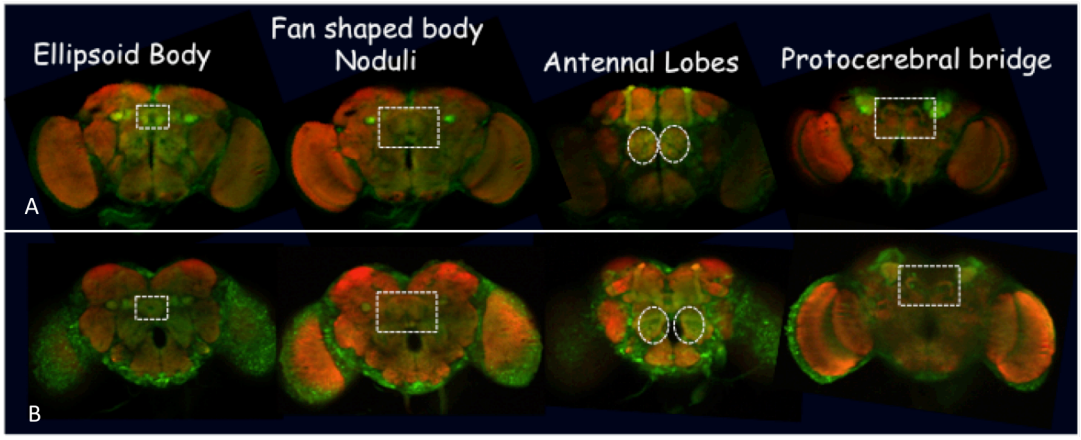

Figure 4.15: No overt morphological defects were seen in *sits* mutant brains. Central complex structures of A) control (C155>*m*CD8::GFP) & B) *sits* mutant (C155>*m*CD8::GFP>*sits*^{GD}) adult brains. The selected neuropils are highlighted in the brain slices. The brains are stained with α nc82 antibody to stain different neuropils.

insight into the cellular basis of the phenotype, I screened adult brains for overt defects. Dissections were carried out for both knockdown and control flies. Anatomical examination of brains derived from knockdown adults (C155>*m*CD8::GFP>*sits*^{GD} &

30Y>*m*CD8::GFP>*sits*^{GD}) did not show any overt morphological defects (Figure 4.15). However, while specific cells underlying the defects remain to be identified, additional support for their function was provided by expressing the pro-apoptotic molecule reaper (UAS-Rpr) using lines capable of inducing the *sits* locomotor phenotype (30Y-GAL4 and RE-GAL4). Induction of cell death with 30Y-GAL4 led to adults displaying locomotor defects, while the effects of RE-GAL4 could not be assessed due to lethality when combined with UAS-Rpr (Charu Jain, personal communication). While not confirming neuronal death or degeneration as the underlying cause of locomotor defects in *sits* knockdown, this suggests at the importance of the cells identified by the 30Y-GAL4 line. Further analysis with the cell death specific markers in the mutant brains should be able to help us better understand if cell death is playing a role in inducing *sits* mediated locomotion defects.

Level of sits is important for behavior

Although no overt effects on larval behavior were detected in *sits* knockdown experiments, I found that misexpression of Sits using pan neural driver C155-GAL4 triggered aberrant larval behavior. Control larvae exhibit normal behavior and go up the vial to pupate. In order to understand the basis behind this unusual larval phenotype, I tested the hypothesis the larvae go down because of gravity (positive geotaxis). To test for possible geotaxis defects vials with eggs of the right genotypes were kept upside down and observed for larval lethality. It was observed that putting the vials upside down does not affect the larval lethality and they die in the food (Figure 4.16, Panel B).

Next, I tested the hypothesis that the larvae exhibit light avoidance behavior by burrowing deep in the food (negative phototaxis). A second set of vials with eggs of the correct genotype was covered with foil paper to test this hypothesis (Figure 4.16, Panel C). Larvae were observed dead in the food suggesting that defects in neither mechanism underlies the observed behavior (Figure 4.16, Panel C'). Ptc>GAL4 and Act>Gal4 are other GAL4 drivers that showed varying degree of the phenotype with *sits* misexpression whereas 30Y did not show any effect on this larval behavior. This is suggestive of a differential cellular requirement for *sits* activity in this larval behavioral and the adult locomotor defects. Another interesting observation was that at higher temperatures (28°C, efficient GAL4, high misexpression) this burrowing phenotype was not as prominent as at lower temperatures (25°C & RT, medium efficiency for GAL4, medium misexpression) (Appendix B, Figure B.6). Regardless of the mechanism, the induction of phenotypes upon misexpression of *sits* indicates that regulation of its levels are essential for normal development and is consistent with the overall rate limiting role of elongases in the production of VLCFAs.

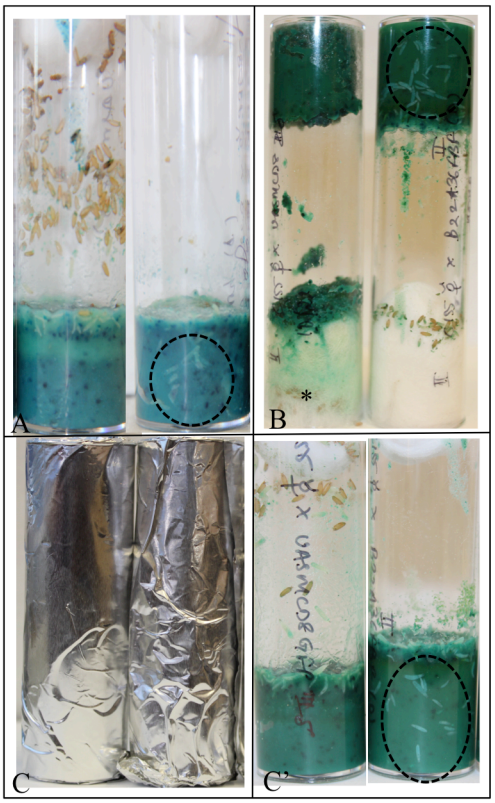

Figure 4.16: *sits* misexpression in the nervous system leads to a larval behavioral phenotype. Control (C155>mCD8::GFP, left vial of each pair) and *sits* misexpression (C155>*m*CD8::GFP>*sits*^{Mis2X}, right vial of each pair). Black dashed circle highlights dead larvae in food after subjecting the vials to different stimuli. (A) vials at RT. (B) vials upside down. (C) & (C') vials covered in foil.

DISCUSSION

sits plays a behavioral role in *Drosophila* development

Recently, *Drosophila melanogaster* has become a model system for a variety of behavioral and neurological diseases with the hope that it can be used to understand the underlying molecular mechanisms behind these neuropathies. Diseases that have been modeled in fruit flies include Parkinson's, Huntington's, spinocerebellar ataxia–1 (SCA-1). Most of these neurological diseases have been associated with altered lipid/fatty acid composition, making these macromolecules and the enzymes involved in their synthesis and processing targets to study for their possible roles in these disorders. For example, ELOVL1 has been indirectly implicated in ALD, thus understanding ELOVL1 function may provide greater insight to the cause of ALD. A second link between elongases and neural dysfunction was recently uncovered with the discovery that recessive mutations in *ELOVL4* in humans have been associated with intellectual disability and seizures (Aldahmesh et al., 2011).

Here I've demonstrated a direct tie between elongases and neural function by characterizing in detail the role of a *Drosophila* fatty acid elongase, *sit still*, in behavior. To my knowledge this is the first report directly implicating an elongase in controlling locomotion.

There are several possible hypotheses about how *sits* activity might be regulating locomotor behavior in flies. The phenocritical time period for Sits activity coincides with the remodeling of the *Drosophila* brain during metamorphosis. Metamorphosis is initiated at the onset of larval-pupal transition into the late pupal stages. Several new adult specific neurons are added to the already existing larval neurons and persistent

neurons are modified (reviewed in (Levine et al., 1995). One wave of programmed cell death also occurs during metamorphosis that helps in sculpting the adult CNS from larval structures (Truman, 1990). Based on the temporal requirement for *sits* during pupal stages one possible mechanism of action would be through effects on this neuronal remodeling and suggests that sits plays a developmental role rather than physiological/maintenance role in the nervous system. While the functional requirement for Sits activity is during pupal stages, I uncovered a striking temporal aspect to the appearance of strong locomotor defects in adults – activity immediately post eclosion was similar to wild type and decayed dramatically within 24 hours. One interpretation of this temporal delay is that the initiation of locomotor activity upon eclosion of the adults triggers degeneration of a locomotor circuit due to its underlying dysfunction. In this scenario, the dysfunction in locomotor control was created during the absence of Sits activity in pupal development, but would not be apparent until its requirement was temporally triggered by eclosion and movement of the adult.

Identifying the specific neurons would provide an important step towards clarifying this model and identifying any such putative circuit. To get at this, Sits activity was knocked down in likely players at the cellular level (Motor neurons, Central complex, Glia), but did not lead to the identification of the responsible cells. Possible explanations could involve Sits function in interneurons. Alternatively, given the association of elongases in vesicular trafficking (yeast) and as the regulators of membrane proteins (worms), it is possible that Sits is also important for the transport or synthesis of some molecule (bioamine or metabolite) important for locomotion throughout the nervous system. Regardless of the underlying molecular mechanism having the right tools in hand to

address these hypotheses is essential to define how *sits* might be regulating locomotor behavior in flies. With this in mind, it will be critical going forward to define the neuronal population that requires *sits* expression (using the RE-GAL4 and VT236352 lines) during pupal stages. Identifying these neurons will be the most important step to defining the circuitry involved and elucidating the role of this elongase in locomotor function.

MATERIALS AND METHODS

Flies- The flies were kept at room temperature in the regular cornmeal media. The crosses were set at 26°C unless otherwise mentioned. The males have bee used for the experiments unless specified. The complete list of stock used can be found in the Appendix B, Table B.1.

miRNA synthesis- *sits* shmiRs were synthesized using the miR-1 backbone and the Valium 20 vector as described previously(Ni et al., 2011). The 21 nucleotide sequence was selected based on no off target effects, CG concentration and seed region complementarity following the criterion listed by others (Birmingham et al., 2007; Griffiths-Jones, 2004; Vert et al., 2006). The selected 21 mers were further subjected to testing from existing siRNA software (Dharmacon, DSIR, Ambion) to select the best candidate sequence. More information about the primer sequences used is available in Appendix C.

Chamber specifications and video setup: Chamber was synthesized as described before (Simon and Dickinson, 2010) with some modifications in overall size to suit our requirements.

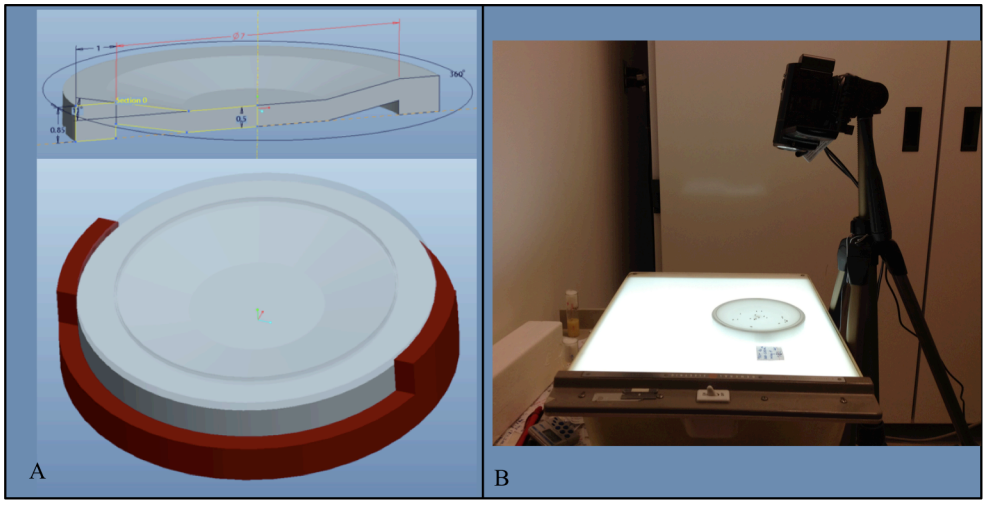

Figure 4.17: The chamber specifications and the video setup for locomotion analysis. A) CAD software images of the desired chamber specifications. B) The apparatus used to take video recordings of the flies in the chamber.

Video Analysis and data collection- Around 20 flies (15-25 depending upon the genotype) 12-48 hr post eclosion are collected in a vial and used for a single video. 80-100 total number of males are assayed per genotype. The chamber lid was cleaned with 70% ethanol an evening before taking the videos for every experiment and wiped with moist kimwipe (dH_20) before putting in the new set of flies each time between the videos. The flies to be videotaped are placed in an ice bucket for about 5 minutes till they are unconscious. They are then transferred to the chamber and are allowed to recover for 15 minutes. After the end of the 15 minutes the chamber top is tapped thrice. Each set of 20 flies was recorded three times (1 minute each) with a break of 2 minutes between each recording and the chamber was tapped before the start of recording.

The camera takes the video in .MOV format, which is not compatible with ctrax. The first step is to convert the video in .Avi format using AVS Video Converter. The .Avi file thus generated is then uncompressed using VirtualDub software. The file generated can finally be used as input file in Ctrax. Ctrax can be downloaded online for free. Ctrax version 3.3 was used for this study as per the directions (Branson et al., 2009). After the completion of tracking, the video was exported as a .MAT file that was imported in matlab with a bunch of specialized matlab scripts provided by the Ctrax developers. The script was modified to give the necessary data. In our case we get the total distance travelled in a minute by an individual fly and the average speed with which the fly was walking in that minute. It also generates a graph depicting the tracks of each fly for the entire length of video.

Immunohistochemistry- Adult and larval nervous systems were dissected in PBT (PBS+ .2% Triton X) and fixed in 4% formaldehyde in PBT. Samples were washed with PBT 6X for 10 min each on the rocker. They were then incubated in blocking buffer (5% normal goat serum in PBT) for 1 hour at room temperature. The blocking buffer was replaced with 100 ul of primary antibody α nc82 (Developmental Studies Hybridoma Bank, Iowa City, IA) at the concentration of 1:200 in blocking buffer and was left overnight at 4°C with rocking. After the primary antibody incubation, samples were returned to room temperature and were given 3X 1 hour washes in PBT. The last wash solution was replaced with 100 ul of a secondary antibody solution consisting of a 1:400 dilution of Alexa Fluor 568 goat anti-mouse in blocking buffer and the samples were incubated overnight with rocking at 4°C. After the secondary antibody treatment, tissues were washed several times with PBT. Samples were stored in 70% glycerol.

Antibody staining of embryos was carried out using the prefixed embryos at -20°C in methanol. Embryos were rehydrated by rinsing them once and washing them twice (5 minutes each) with PBT (1XPBS+.1%Tween-20). Embryos were blocked using (5% NGS, 2%BSA in PBT with .1% Tween-20) for 30 minutes at RT. Primary antibody (αBP102 (1:500) and αID4 (1:100)) was added after removing the antibody block and the sample was left at 4°C overnight on a rotator. The embryos were rinsed thrice and washed twice with PBT. Secondary antibody (Alexa fluor 488 and 568 (1:400)) was added to the embrys for 2 hours at RT with rotation. After rinsing the embryos thrice and washing them with PBT, they were rinsed with PBS and re-suspended in 70% glycerol. Imaging was carried out using Zeiss Axio Imager equipped with Apotome.

The adult brain staining of 30Y>mcd8::GFP was imaged using confocal microscope.

Vortexing Assay: Newly eclosed flies of correct genotype were collected and kept at appropriate temperature for 24 hrs after which the assay was done. Briefly flies were transferred in empty vials and vortexed for 10 seconds. After vortexing they were observed for 15 seconds and the number of flies climbing up the vial were counted.

Flip Over Assay: Adult flies 24 hrs post eclosion were transferred to a new vial and the vial was flipped over a couple of times. The flies are observed for movement from one point to another in a direction. The flies that were circling were not considered moving.

Graphs and Stats: All the graphs have been generated using GraphPad Prism 5 and 6.

ACKNOWLEDGEMENTS

Work on sits was initiated with the help of an MQP student Shreelekha Mandal. *sits* RE-GAL4 has been cloned and mapped by Charu Jain. Daniel Huang and Jeeva Jacob helped in testing of the Janelia Farm GAL4 lines. Erica Stults and Neil Whitehouse helped with the chamber construction. Ivan Ivanov, an undergrad in chemical engineering helped with the matlab script.

Chapter 5

Developmental characterization of *baldspot* (*bals*)

ABSTRACT

Elongases are a conserved family of enzymes that are instrumental in synthesis of specific lipids *in vivo*, but whose developmental roles are little understood. Previously, the *Drosophila* elongase, *baldspot* (*bals*), was identified as a target of epidermal growth factor receptor (EGFR) signaling in an enhancer trap screen (Doetsch, 2004). This chapter reports the further investigation of role of *baldspot* during *Drosophila* development. Using a variety of molecular, genetic and cellular approaches, *bals* was confirmed to play a role in viability, oogenesis and Programmed Cell Death (PCD). Specifically, loss of *bals* activity in follicle cells of developing egg chambers disrupts barrier function associated with the protective layers of the oocyte and developing embryo, the chorion and vitelline membrane, respectively. Loss of barrier function results in dessication of the developing embryos causing maternal-effect lethality. In contrast to loss-of-function, misexpression of Bals can triggers PCD in multiple tissues in a caspase dependent fashion.

INTRODUCTION

The *bals* gene was initially identified in an enhancer trap screen as a target of EGFR (Doetsch, 2004). It is expressed during oogenesis in both the germline and the somatic, follicle, cells and broadly during embryogenesis (Doetsch, 2004; BDGP(Tomancak et al., 2002)). Sequence analysis suggests that *bals* codes for a seven pass trans-membrane protein that function as a fatty acid elongase (HMMTOP, (Tusnady and Simon, 2001)). Prior work using loss-of-function *bals* alleles suggests that *bals* is a vital gene and acts in eggshell biogenesis/maintenance (Doetsch, 2004).

Lipids and Elongases in Epidermal barrier

One central function lipids perform is that of providing structural integrity to a cell (i.e. plasma membrane). In addition, lipids perform additional functions, of which one is acting as protective barrier. In the epidermis the topmost layer is known as stratum corneum (SC), which plays a key role in the barrier function of the skin. Compromised skin barrier is easily susceptible to microbes and allergens and increased water loss (Figure 5.1) The lipid composition of a stratum corneum primarily

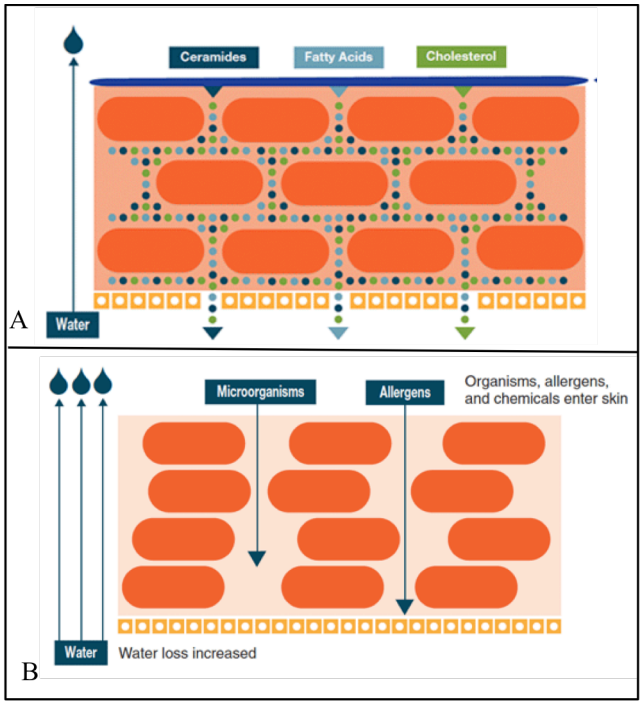

Figure 5.1: Stratum Corneum lipids form a protective barrier against pathogens and water loss. A) Schematic of a normal SC with lipids and no water loss. B) Loss of lipids causes defective barrier and water loss. Source (http://www.epiceram-us.com/patient.html)

consists of cholesterol, triglycerides, free fatty acids and sphingolipids (in form of ceramides) and alterations in the lipid composition have been found to be responsible for barrier defects in the mammalian epidermis (Feingold, 2007). Mice with null mutations in *elovl1*, *elovl3* and *elovl4* have been found to have impaired barrier function leading to lethality in cases of *elovl1* and *elovl4* (Cameron et al., 2007; Sassa et al., 2013; Westerberg et al., 2004). In accordance to whats depicted in Figure 5.1, studies have also shown a link between lipid induced barrier defects and skin diseases such as psoriasis and atopic dermatitis (Cork et al., 2009; Kopytova et al., 2007; Proksch et al., 2003). In addition to their role in barrier function, lipids have also been associated with the differentiation process of keratinocytes and thus formation of the fully functional epidermis (Proksch et al., 2003; Sporl et al.).

Interestingly, VLCFAs have also been found to be an important constituent of plant epidermis (Millar et al., 1998; Qi et al., 2004; Todd et al., 1999). Plants have a protective barrier made up of long chain hydrocarbons and waxes that protects them from dessication (Riederer and Schreiber, 2001). Enzymes, including elongases, involved in biosynthesis of these VLCFAs and hydrocarbons have been directly implicated in barrier function in Arabidopsis. Mutations in *kcs1* and *kcs9* have been associated with waxless stems and leaves, suggesting an analogous role to some mammalian elongases (Li et al., 2008; Millar et al., 1999; Reina-Pinto et al., 2009; Todd et al., 1999).

Drosophila and barrier function

As in plants and mammals, barrier function in *Drosophila* is also critical to maintaining homeostasis. From the multilayered *Drosophila* eggshell to the epidermis/cuticle of the

larvae and adults, barriers are essential for normal development and viability. Similar to the mammalian skin, lipids form an integral part of the epidermal barrier in insects (Nelson and Lee, 2004; Papassideri et al., 1993). During *Drosophila* oogenesis, a barrier is

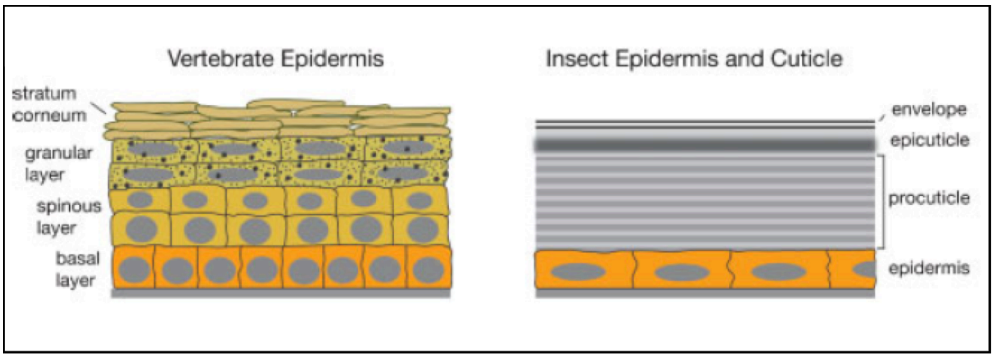

Figure 5.2: Structural conservation of invertebrate and vertebrate epidermis. Both the vertebrates and invertebrates have a multilayered epidermis made up of specialized lipids and proteins that protect the underlying organism. (Moussian et al., 2005)

formed through the action of the somatic follicle cells. Early in oogenesis, the germline derived oocyte is surrounded by a layer of somatic follicle cells. The follicle cells are responsible for the secretion of eggshell components, before they undergo cell death (Papassideri and Margaritis, 1996; Waring, 2000). Eggshell components are secreted from the follicle cells in a temporal manner; the first layer to be formed is the vitelline membrane, followed by the wax layer and the inner and outer chorion layer respectively (Margaritis et al., 1980; Papassideri et al., 1993; Waring, 2000). Mutations in different layers of the eggshell have been associated with a variety of phenotypes, including collapsed chorions and barrier defects. For example, absence of the chorion protein (*cor36*) has been associated with structural abnormalities of the eggshell, whereas loss of the vitelline membrane proteins (*fs(2)Qj42, dec-1, nudel protease*) has been implicated in permeability barrier defects (LeMosy and Hashimoto, 2000; Savant and Waring, 1989).

Similar to the multilayered eggshell, *Drosophila* embryos, larvae, and adults are also surrounded by an organized barrier, known as the cuticle (Locke, 2001). In embryos and larvae, the topmost layer of the cuticle is termed the envelope or cuticulin and is believed to be comprised of lipids, such as wax and fatty acids, and this layer has been proposed to account for waterproofing properties of the cuticle (Wigglesworth, 1985). Underlying the envelope are two proteinaceous layers comprising of a bipartite epicuticle and an innermost procuticle that also form a part of the epidermal cuticle. Recently it has been found that defects in the cross linking of the extracellular components of the cuticle can lead to barrier disruption in embryos and larvae, confirming the role of the cuticle in barrier function (Shaik et al., 2012).

In this chapter I describe further characterization of the role of *baldspot* in *Drosophila* development using both loss-of-function and gain-of-function studies. I have recapitulated the collapsed chorions phenotype using targeted gene knockdown via RNA interference (RNAi) and shown that this can be rescued by providing Bals activity specifically in the follicle cells. I provide further work demonstrating that the collapsed chorion phenotype is likely due to defective barrier function (wax layer and/or vitelline membrane). I also show that the defective barrier function could be responsible for the embryonic lethality observed in *bals* mutants, suggesting a conserved function for *bals* in barrier maintenance similar to its vertebrate counterparts (mice Elovl3, Elovl4 and Elovl1).

RESULTS

Genetic structure of bals

The gene *bals* (CG3971) is located at 73B on the third chromosome (3L) and contains two transcripts that code for the same protein of 316 amino acids (Figure 5.3). Of the two *bals* transcripts, the full length cDNA, LD11132 represents the transcript used for misexpression studies (Doetsch, 2004). Neighboring genes, *abl*, coding for a tyrosine Kinase, and *Galpha* are also shown and the entire schematic is approximately to scale. There is an snRNA gene with one transcript and unknown molecular function overlapping the *bals* genomic sequence. Various P element insertion alleles, enhancer trap alleles and EMS induced point mutation alleles that are used in this study are indicated accordingly on the genomic region.

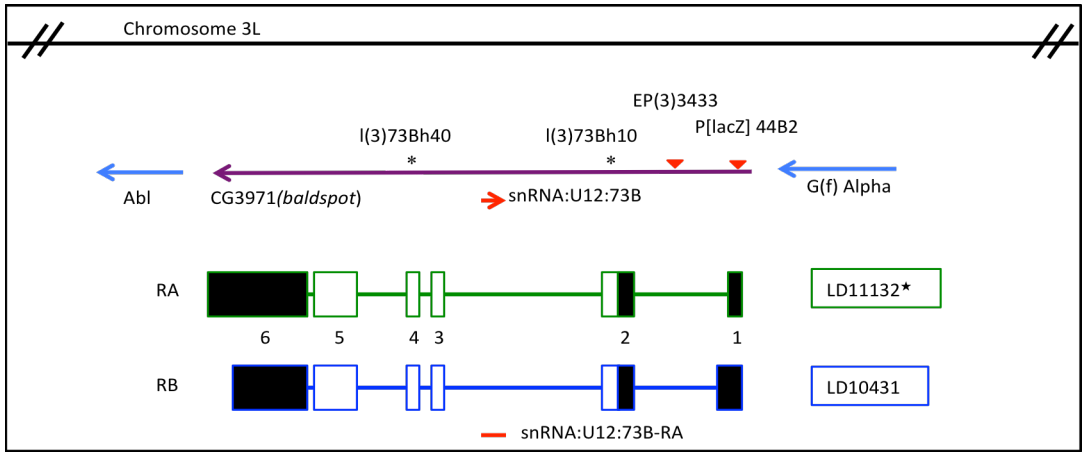

Figure 5.3: Genomic locus of *baldspot*. *bals* Genomic region is represented by purple arrow and the neighboring genes are in blue. Two transcript variants RA and RB are shown below the genomic region. ★ represents the cDNA clone used in this study. All the P-element mutations are marked as red triangles on the genomic region. The EMS mutations are denoted by *.

bals – identification and rescue of a highly penetrant chorion phenotype

Prior work had shown that absence of *bals* in female ovaries leads to collapsed chorions (Doetsch, 2004). To confirm this phenotype was indeed *bals* dependent, I set out to rescue the collapsed chorion phenotype using targeted expression of a *bals* cDNA. I therefore screened for a *bals* allelic combination (hypomorphs and amorphs), which had high viability for trans-heterozygous females, and that showed a highly penetrant collapsed chorion phenotype. Based on the complementation and phenotypic analyses, the allelic combination of *l(3)73*Bh40/*EP(3)3433* was selected as the genotype to rescue the collapsed chorion phenotype (Table 5.1). This trans-heterozygous combination gave moderate viability, 47%, and a fully penetrant, 100%, collapsed chorion phenotype.

Table 5.1: *bals* complementation and collapsed chorion penetrance.
The bolded genotypes (and percents) are the selected combination that was used for rescue**.**

	% Viability							
	EP(3)3433		*P[lacZ]44B2*		*l(3)73Bh10*		*l(3)73Bh40*	
	F	M	F	M	F	M	F	M
EP(3)3433	-	-	>100$_{(n=49)}$	>100$_{(n=71)}$	18$_{(n=72)}$	57$_{(n=78)}$	***47***$_{(n=80)}$	82$_{(n=78)}$
P[lacZ]44B2	>100$_{(n=49)}$	>100$_{(n=71)}$	-	-	15$_{(n=153)}$	52$_{(n=164)}$	12$_{(n=143)}$	21$_{(n=191)}$
l(3)73Bh10	18$_{(n=72)}$	57$_{(n=78)}$	15$_{(n=153)}$	52$_{(n=164)}$	0	0	0	0
l(3)73Bh40	***47***$_{(n=80)}$	82$_{(n=78)}$	12$_{(n=143)}$	21$_{(n=191)}$	0	0	0	0
	% Collapsed chorions							
	EP(3)3433		*P[lacZ]44B2*		*l(3)73Bh10*		***l(3)73Bh40***	
	% Collapse	# Chorions	% Collapse	# Chorions	% Collapse	# Chorions	% Collapse	# Chorions
EP(3)3433	-	-	94	220	100	78	***100***	**186**
P[lacZ]44B2	94	220	-	-	100	52	100	220
l(3)73Bh10	100	78	100	52	0	0	0	0
l(3)73Bh40	***100***	**186**	100	220	0	0	0	0

If this phenotype was because of absence of *bals*, providing back *bals* coding sequence in the mutant background should rescue the phenotype. With a penetrant *bals* phenotype in hand, inducible *bals* expression was assessed for the ability to restore the collapsed chorion phenotype to wild type. Using the genotype *l(3)73*Bh40/*EP(3)3433* and UAS-GAL4 system, *bals* expression was induced in the follicle cells of the mutant flies. In the absence of inducible transgene, *bals* mutants laid ~100 % collapsed chorions. Expressing Bals by inducing the transgene at 29°C was found to be sufficient to rescue the collapsed chorion phenotype, as compared to 0% wild type in the mutants, up to ~90% wild type chorions were observed for the rescue genotype (Figure 5.4, Materials and Methods). This corroborates that absence of *bals* specifically is responsible for collapsed chorions.

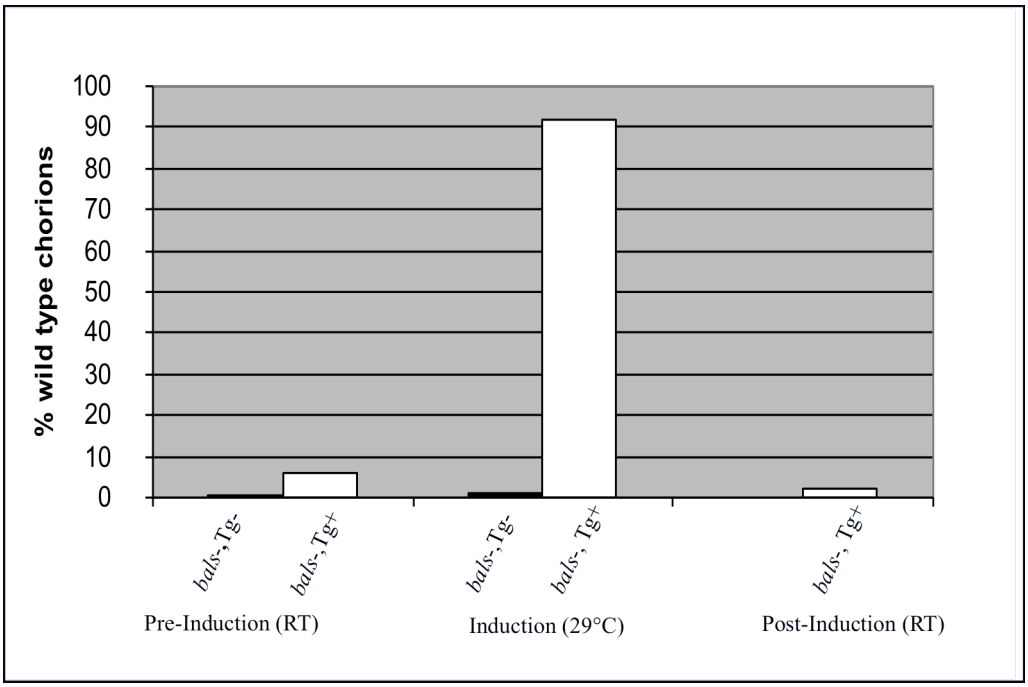

Figure 5.4: Rescue of the *bals* collapsed chorion phenotype. The eggs were scored after the flies had been acclimatized to the corresponding temperatures (>24hrs). *bals*$^{-}$;Tg^{-} = *l(3)73*Bh40/*EP(3)3433* and *bals*$^{-}$;Tg^{+} = *l(3)73*Bh40/*EP(3)3433;CY2-GAL4>GAL80^{ts}>UASbals^{2-1F}* . The number of chorions scored for each genotype >200./.

RNAi mediated knockdown of bals mimics the collapsed chorion phenotype shown by loss-of-function alleles

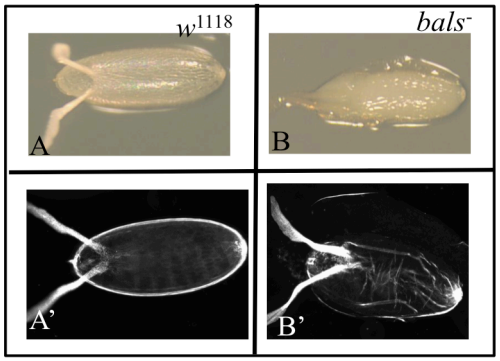

Figure 5.5: RNAi mediated *bals* knockdown in the soma leads to the collapsed chorion phenotype. Panels A&B shows the DIC images whereas panel A'&B' are the dark field images. A&A'= wildtype B&B'= CY2>$bals^{siRNA\#47519}$ (follicle cell knockdown using *bals* RNAi)

After confirming the chorion phenotype was dependent on *bals* activity, I set out to identify an efficient method to generate larger numbers of *bals* dependent collapsed chorions to simplify additional mechanistic studies. In order to do this, I utilized an entirely different approach using RNA knockdown in the oogenesis (Dietzl et al., 2007). Using RNAi mediated *bals* knockdown specifically in the follicle cells (CY2>$bals^{siRNA\#47519}$), I recapitulated the collapsed chorion phenotype (Figure 5.5). I further confirmed that Bals activity only in the soma (follicle cells) is necessary for its function, as germline knockdown of *bals* (using triple maternal GAL4 driver MTD-GAL4 and $bals^{siRNA\#47519}$) had no effect on the chorion morphology, producing only wild type chorions (Figure 5.6).

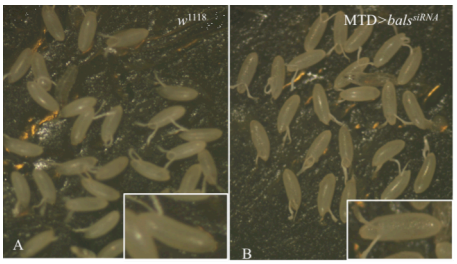

Figure 5.6: Germline knockdown of *bals* does not lead to collapsed chorions. A) Wild type (w^{1118}) and B) Germline driver mediated *bals* RNAi (MTD-GAL4>$bals^{siRNA\#47519}$) chorions have similar appearance.

Thus, RNAi mediated knockdown of *bals* allowed for larger homogenous pools of females lacking *bals* in a tissue specific manner for a better characterization of the phenotype.

In order to understand the basis of the collapse, the chorions lacking *bals* were observed under the microscope for gross morphological defects. The

chorions lacking *bals* appeared to have normal overall morphology.

Furthermore, consistent with what has been shown previously, it was observed that the deposited eggs from *bals* RNAi knockdown collapse gradually likely due to dessication (Figure 5.7, Doetsch, 2004). This temporal aspect is distinct and makes the observed collapsed phenotype different than that previously reported for the mutants, *fs(2)Qj42, dec-1,* and *nudel, s*uggesting a different underlying mechanism. Figure 5.7 shows the temporal progression of the collapsed egg phenotype as compared to the wild type control. Both the wild type and the mutant chorions have similar appearance immediately after they are laid and gradually the mutant chorion starts loosing its firm structure. Within 24 hours, the wild type embryo hatches and moves away from the chorion but the mutant chorion is completely collapsed.

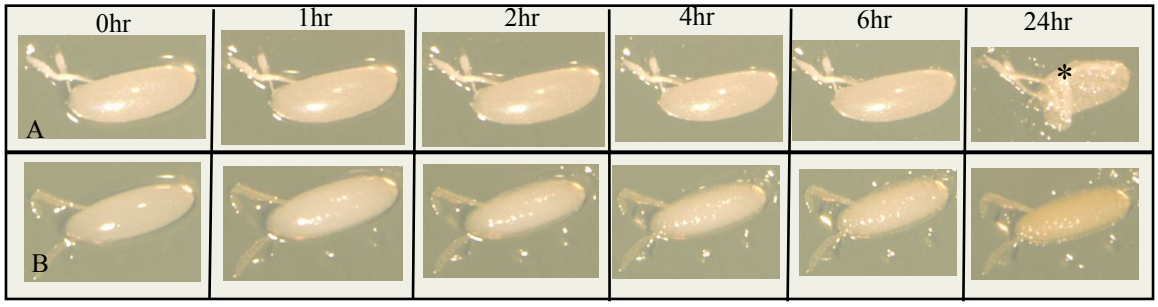

Figure 5.7: The deposited chorions dessicate overtime. Representative images of (A) wild type (w^{1118}) and (B) *bals* mutant (CY2>$bals^{siRNA\#47519}$) chorions taken at different time intervals. * = the embryo has hatched leaving an empty chorion. This image has been converted to black and white image.

This temporal progression of the collapsed chorion phenotype, likely due to dessication, pointed towards the possibility of defective protective barrier of the eggshell which was tested next.

Compromised barrier function underlies the collapsed chorion phenotype

To determine the underlying cause of the collapsed chorions, barrier function was assessed using a permeability barrier assay involving the dye neutral red (LeMosy and Hashimoto, 2000). Previously it has been found that *bals* mutant chorions can readily take up neutral red dye indicating barrier properties are affected (Doetsch, 2004). In order to better understand the phenotype and how the integrity of the eggshell is affected, I repeated the neutral red dye assay on *bals* RNAi eggs chorions from *bals* knockdown females and obtained similar results, the mutant egg chorions readily take up neutral red, while wild type chorions are impermeable (Figure 5.8). Furthermore, additional chemical treatments were carried out on wild type chorions to test the barrier function of different layers in preventing neutral red uptake. Dechorionation, (removal outer chorionic layer) using bleach (50%) did not result in permeability to the dye, indicating either the wax layer and/or the vitelline membrane are providing barrier function with respect to neutral red. In contrast, after dechorionation, treatment with organic solvents (2:1 v/v, chloroform:methanol) to remove the wax layer lead to neutral red dye uptake (Figure 5.8). This result suggests that wax layer was protecting the wild type chorion from taking up the neutral red dye and the mutants lack that protection because of lack of wax layer and hence they take up the dye. Dewaxing did not appear to disrupt the integrity of the vitelline membrane as it seemed uncompromised and the underlying embryos remained intact (data not shown).

Furthermore, in wild type longer exposure of the chorion to bleach only affects the chorionic layer, while the underlying structure (vitelline membrane/wax layer) appears unaffected (N=60). In contrast, exposure of *bals* chorions to bleach completely dissolves

the entire egg within minutes (N=50). This suggests that in wild type eggs the wax layer/ and possibly vitelline membrane are impervious to bleach, providing a protective function for the embryo. The wax layer appears to be the primary barrier to bleach. Removal of the wax layer by treating wild type chorions to bleach followed by organic solvents (2:1 chloroform:methanol) and then bleach again results in the eggs being dissolved (similar to the bleach only treated *bals* mutant chorions, N>200). Thus, compromising the wax layer in wild type triggers a bleach dependent phenotype analogous to that observed in *bals* mutants, consistent with the hypothesis that the wax layer is compromised in the mutant. Together my data strongly suggest that the wax layer is the permeability barrier

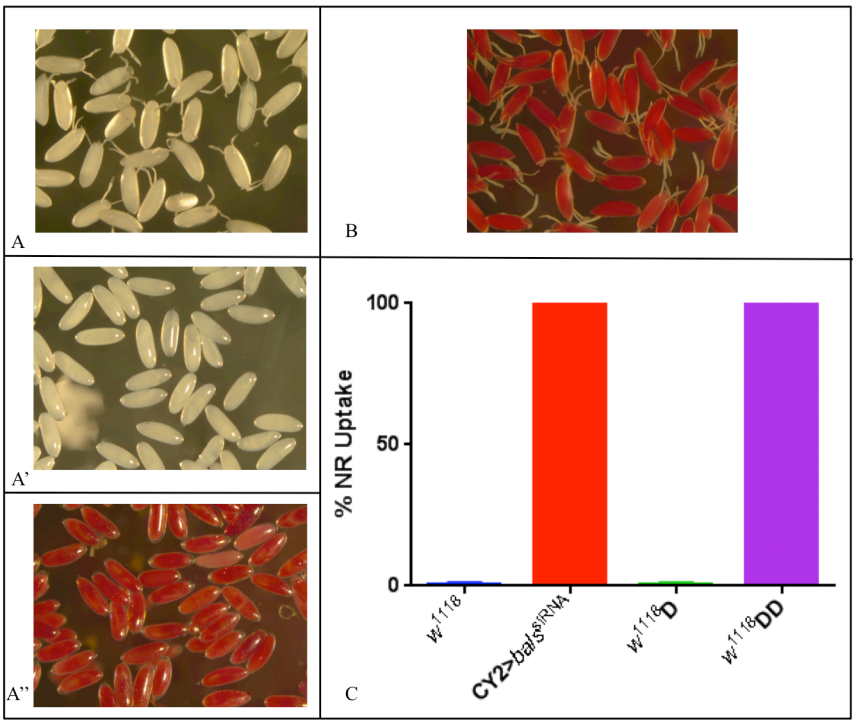

Figure 5.8: Structural integrity of the eggshell is compromised in *bals* mutants. Images were taken after the neutral red dye assay. Panel A, A'&A'' are the wild type chorions (w^{1118}) Wild type chorions (A) were treated with bleach to remove top chorionic layer (A') and treated with 2:1v/v chloroform:methanol (A'') before being subjected to the dye. Panel B shows *bals* mutant chorions (CY2>$bals^{siRNA}$) without any chemical treatment. Panel C represent the graphic representation of the % chorions that took up neutral red dye for a given genotype and treatments. w^{1118}= wild type chorions (N=703), CY2>$bals^{siRNA}$ = *bals* mutant chorions (N=674), *w*1118D= wild type dechorionated chorions (N=648), w^{1118}DD= wild type dechorionated and dewaxed chorions (N=647).

disrupted in the *bals* mutant chorions. However, it is unclear if the vitelline membrane or the chorion layer are compromised as well.

Loss of bals during embryogenesis leads to embryonic lethality possibly due to barrier defects

Previously it has been found that *bals* is a vital gene as amorphic mutations in *bals* lead to embryonic lethality (Doetsch, 2004). This result was confirmed using *bals* knockdown mediated by ubiquitous GAL4 drivers (Actin and Tubulin) (Appendix A, Table A.1). It was observed that the *bals* mutants hatch out of the chorion and die shortly thereafter, often remaining partially within the chorion (Figure 5.9). No overt morphological defects were observed in those larvae as compared to the control (Figure 5.9). Interestingly, over time the appearance of the hatched larvae looked flaccid suggesting that it might be undergoing dessication similar to the *bals* chorions, possibly due to defective cuticular barrier function. To test if *bals* mutant embryo/larvae are dessicating due to barrier defects, I knocked down *bals* specifically in embryonic epidermis using 69B GAL4 driver. My results closely mimic the phenotype of loss-of-function alleles, providing some evidence for *bals* function in cuticular barrier function (Galko and Krasnow, 2004; Gangishetti et al., 2012). To further test the hypothesis that the barrier function might be compromised in the *bals* mutant embryos, a neutral red permeability assay was performed. Wild type and *bals* larvae were treated with neutral red dye and it was observed that the wild type larvae do not take up any dye whereas variable degree of dye uptake was seen for *bals* mutant larvae, consistent with a role in cuticular barrier function

(Figure 5.9). This result suggests that *bals* might be playing some role in maintaining the barrier function during embryogenesis as well.

Alternatively, given that Bals is expressed in the nervous system during embryogenesis, one hypothesis was that *bals* activity in the embryonic nervous system was necessary for viability. To test this hypothesis, RNAi mediated knockdown of *bals* in the nervous system (C155 GAL4) was carried out and it did not lead to embryonic lethality (Appendix A, Table A.1). This result further corroborates that the embryonic lethality in the *bals* mutant embryos is due to disrupted barrier function and not due to requirement *of bals* in the nervous system.

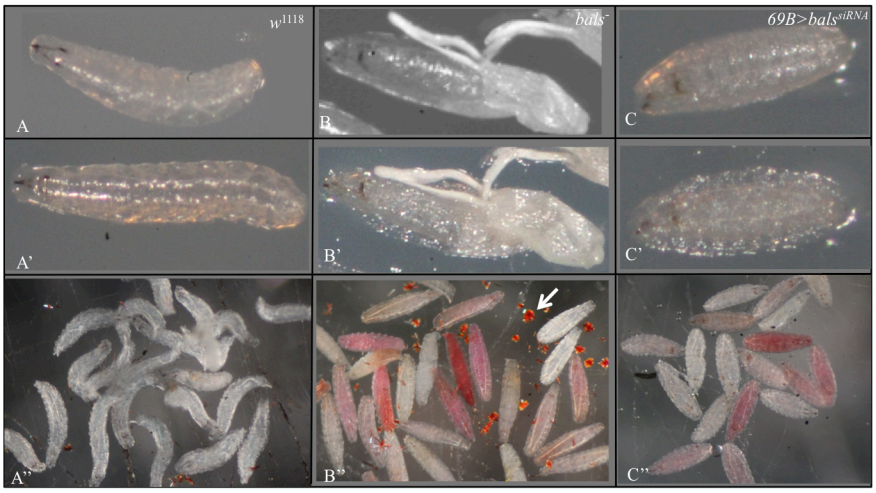

Figure 5.9: Absence of *bals* during embryogenesis leads to lethality possibly due to defective cuticular barrier function. Panels A, A'& A'' are w^{1118}. Panels B, B' & B'' are *bals* trans-het allelic combination (*l(3)73bh10/l(3)73bh40*). Panels C, C' & C'' are 69B>*bals*$^{siRNA\#47519}$. The top row shows newly hatched embryos (~ 2-4 hrs). The middle row represents the same embryos after 24 hrs. The bottom row shows the embryos /larvae treated with neutral red dye. Arrow in B'' is neutral red dye crystal.

Misexpression of Bals triggers caspase dependent programmed cell death

Along with loss-of-function studies, gain-of-function studies can also provide valuable insight into the gene function. Therefore as a complement to the loss-of-function studies

described above gain-of-function studies have also been carried out for *bals* and are extended here (Doetsch, 2004).

As mentioned earlier in the introduction (chapter one), gain-of-function mutations in human ELOVL4 have been implicated in the autosomal dominant macular degeneration. It has been suggested that apoptosis (a type of programmed cell death, PCD) resulting from dominant negative effects of the truncated and mislocalized ELOVL4 mutant protein might be the underlying cause for STGD3/macular degeneration (Karan et al., 2004). Previous work in lab on *bals* gain-of-function studies (*bals* misexpression) implicated Bals in Programmed Cell Death (PCD). It was found that *bals* misexpression in the eye leads to a rough eye phenotype that can be modified by the members of PCD pathway suggesting that *bals* misexpression triggers PCD (Doetsch, 2004). Thus, understanding the mechanism underlying *bals* induced cell death might give us an insight into the roles of elongases in apoptosis and possibly macular degeneration. This section of the chapter addresses the role of Bals misexpression in inducing PCD in multiple tissues.

Programmed Cell Death (PCD) and lipids

Cell death is an innate phenomenon that is responsible for tissue patterning and organogenesis during development (Vaux and Korsmeyer, 1999). There are different mechanisms by which a cell can die via PCD, such as apoptosis, autophagy or necrosis (Clarke, 1990). Apoptosis is the most extensively studied PCD pathway and is conserved from flies to mammals (Figure 5.10). Even though it is generally believed that apoptosis depends on caspases to bring about cellular demise (Taylor et al., 2008), evidence also

exists that suggests that apoptosis can take place without the involvement of caspases (Stefanis, 2005). Lipid molecules such as cholesterol (Li et al., 2006), sphingosine (Ullio et al., 2012), ceramides (Thon et al., 2005) have been implicated in PCD. *In vitro* assays using neuronal cell cultures and free fatty acids also suggest a role of fatty acids in inducing cell death consistent with the proposal that dysregulation of ELOVL4 activity and fatty acid dependent PCD underlies autosomal dominant macular degeneration (Ulloth et al., 2003). This is also consistent with the hypothesis that *bals* misexpression is triggering PCD.

Apoptosis studies in Drosophila

Since *Drosophila* contains all the canonical apoptosome proteins (Figure 5.10), it has been routinely used to study the regulation and role of cell death during development and diseases. Apoptosis is responsible for normal development and tissue homeostasis in *Drosophila* (Lee and Baehrecke, 2000). Similar to vertebrates, different stimuli can trigger the cell death pathway in *Drosophila* via the activation of HID, GRIM or REAPER family of proapoptotic proteins. These proteins then act on the downstream inhibitor of apoptosis (DIAPs) molecules,

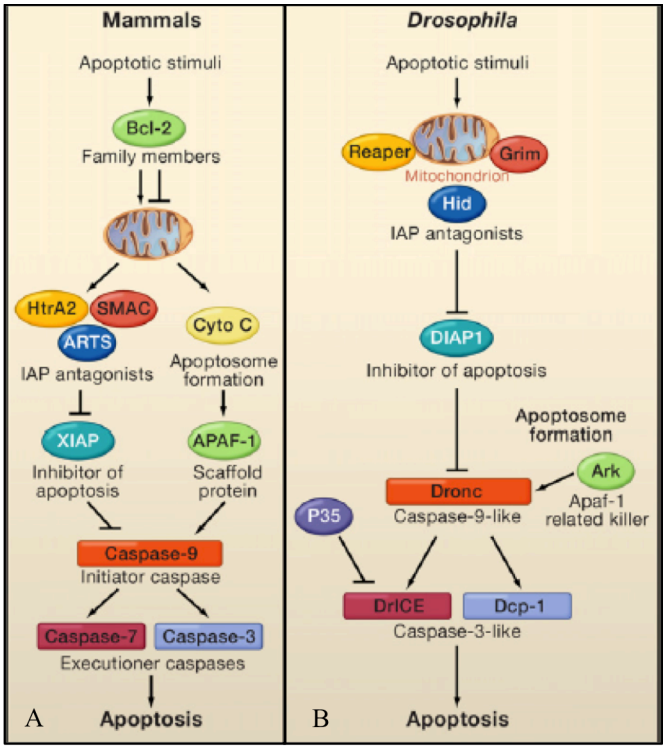

Figure 5.10: Core Apoptotic machinery is conserved across species. Mammalian (A) and *Drosophila* (B) apoptosis pathway (Fuchs and Steller, 2011)

thus starting a cascade of events that leads to the activation of executioner cystine proteases (caspases) and cell death.

In the section below, I have recapitulated the effects of *bals* misexpression on the eye (rough eye phenotype) and provided further evidence of the involvement of caspase dependent cell death as the underlying molecular mechanism. I have also shown that *bals* misexpression is capable of inducing PCD in multiple tissues in *Drosophila*.

Baldspot can trigger Programmed Cell death (PCD) in caspase dependent manner

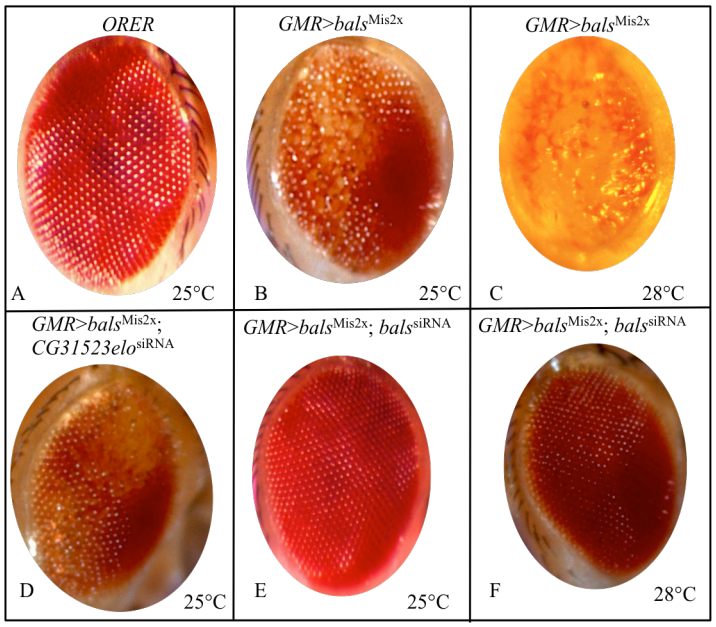

Figure 5.11: *bals* mis-expression leads to rough eye phenotype in *Drosophila*. A) Control ORER (Oregon R) B) & C) GMR>*bals*^{Mis2X} at 25°C and 28°C respectively. D) GMR>*bals*^{Mis2X} ; CG31523*elo*^{siRNA} E & F GMR>*bals*^{Mis2X} ; *bals*$^{siRNA\#47519}$ at 25°C and 28°C respectively. GMR= Glass multiple repeat GAL4 driver specifically driving in the photoreceptors, *bals*^{Mis2X}= *bals* misexpression UAS transgene, *bals*$^{siRNA\#47519}$ = *bals* RNAi line and CG31523*elo*^{siRNA}= RNAi for a related elongase CG31523.

Prior work has shown that misexpression of *bals* leads to a rough eye phenotype caused by triggering of PCD. A modifier screen revealed that molecules of the PCD pathway (HID/Grim/RPR & DIAPI, II) affect the *bals* misexpression eye phenotype supporting the role of PCD. In order to confirm and further understand the role of *bals* in the PCD pathway, I recapitulated the rough eye phenotype induced by *bals* misexpression. I showed that the rough eye

phenotype is specific to *bals* misexpression, as reducing the levels of *bals*, by using *bals* specific RNAi, represses the phenotype (Figure 5.11E, F), whereas RNAi for a related family member CG31523 has no discernible effect on the phenotype (Figure 5.11, D). Additionally, I performed antibody staining for a specific cell death marker (cleaved caspase3) on the eye discs of wild type and *bals* misexpression third instar larvae. Positive staining for the cleaved caspase antibody only in the *bals* misexpression background confirms that *bals* misexpression leads to PCD in the eye. This was a better approach than the previously used TUNEL staining, that can give false positives and thus can't be completely relied on (Grasl-Kraupp et al., 1995). DIC imaging of the eye discs with *bals* misexpression also exhibited cellular extrusion and these extruded cells stained positive for caspase3

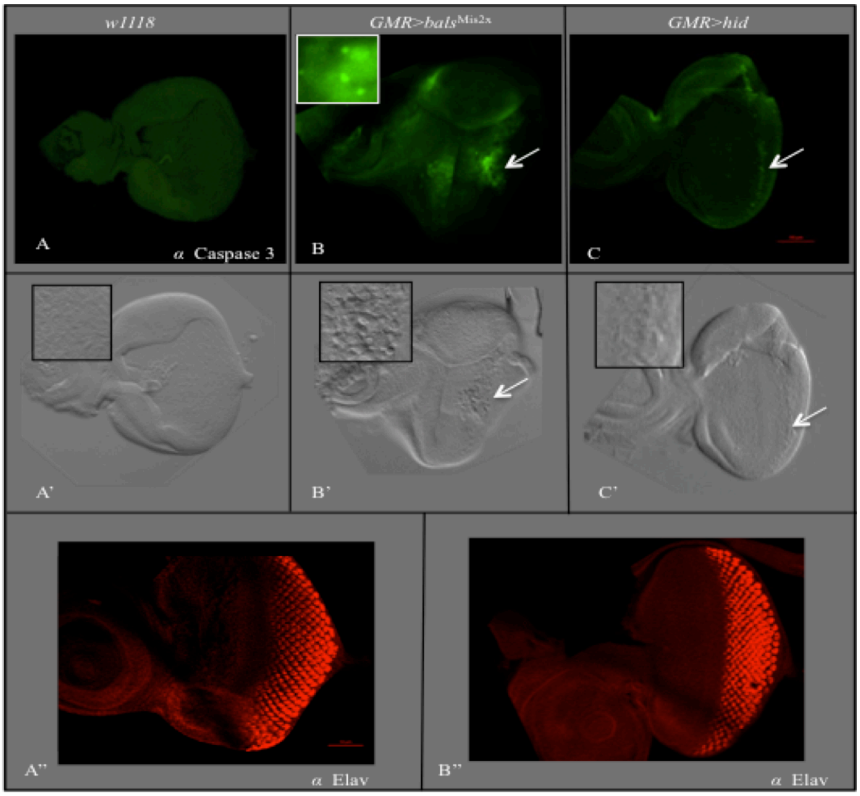

Figure 5.12: *bals* misexpression induces caspase dependent cell death in *Drosophila* eye discs after neuronal specification. A, A'&A'' are the w^{1118} eye discs, B, B' & B'' are misexpressing *bals* (GMR>$bals^{Mis2X}$). Top panels A, B & C are stained with α caspase 3 (positive staining indicated by white arrow, Inset shows magnifying section of the stained region). Panels A', B' & C' are DIC images. Arrows show cellular extrusion. Inset images show magnified middle region of the disc. Panel A'' & B'' are stained for neuronal fate marker α Elav.

confirming the role of *bals* in caspase dependent cell death (Figure 5.12). Furthermore, to determine if *bals* misexpression induced PCD in the eye was due to a failure of cells to adopt a neuronal fate, I tested the neuronal specification of the photoreceptors with a neuronal fate marker (Embryonic lethal abnormal vision (ELAV)). Positive ELAV staining in *bals* misexpressed eye discs, similar to the control discs, suggests that the neuronal specification is indeed taking place and *bals* is directly implicated in triggering PCD/Apoptosis.

Misexpression of bals can lead to PCD in multiple tissues

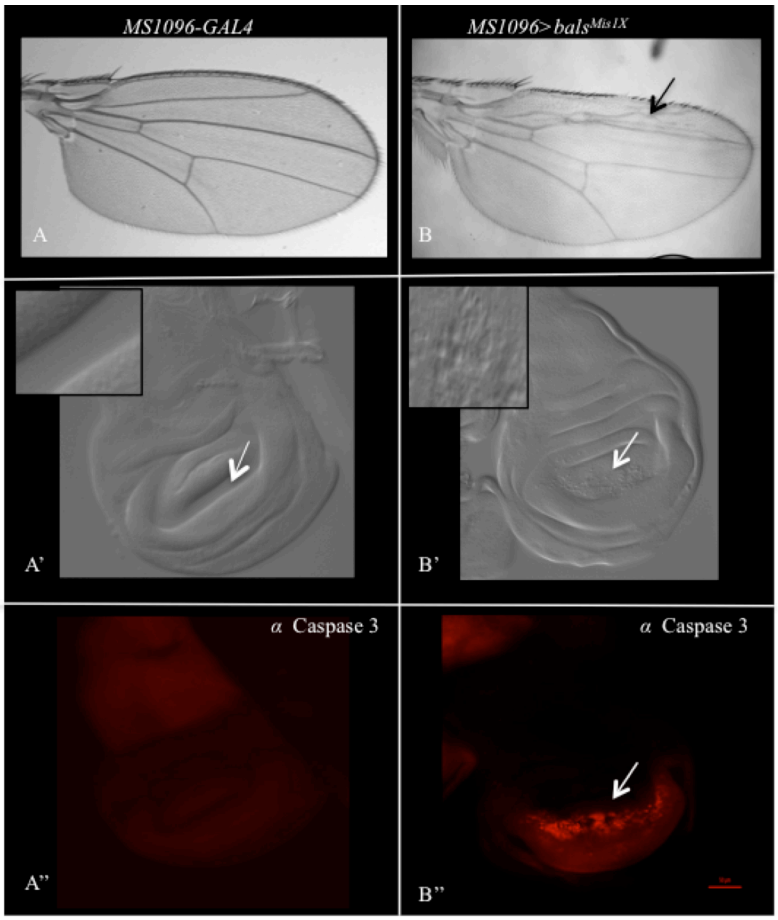

Figure 5.13: *bals* misexpression induces PCD in *Drosophila* wing discs. Panels A, A' & A'' are the control discs (MS1096-GAL4) and B, B' & B'' are the bals misexpressing discs (MS1096>*bals*^{Mis2X}). The top row shows the adult wings. Black arrow indicates the vein defects. The middle row shows the DIC images of the wing discs. The insets are magnified regions of the discs (white arrow). The bottom row shows staining for proapoptotic marker, caspase 3.

In order to understand the mechanism of *bals* involvement in PCD, I tested to see if this effect was limited to the eye or occurred in other tissues as well. *bals* misexpression using UAS-GAL4 in several *Drosophila* tissues led to lethality (Appendix A, Table A.2). One particular GAL4 driver (MS1096 – wing disc expression) gave viable

flies with vein defects. Further analysis of the wing discs from those flies showed cellular extrusion similar to eye discs and also tested positive for cleaved caspase3 (Figure 5.13). This result suggested that misexpression of a fatty acid elongase, Bals, is capable of inducing PCD in multiple tissues. Taken together, our gain-of-function studies on *bals* lend further support to the idea that misregulation of elongases and VLCFA profiles *in vivo* can trigger caspase dependent PCD and pathologies, such as autosomal dominant macular degeneration.

DISCUSSION

baldspot and barrier function

Lipids form an integral part of an epidermis and provide it with barrier properties that help maintain organismal homeostasis by protecting against environmental insults including dessication. Recent work on vertebrate and plant elongases supports a conserved barrier function for elongases across species. In this study, we have identified and characterized a fatty acid elongase (*bals*) that seems to be playing a similar role in barrier maintenance in *Drosophila*. Following on previous work done in lab, using transgene mediated rescue, I confirmed that the collapsed chorion phenotype was dependent on Bals activity and utilized RNAi as an efficient method to generate larger numbers of *bals* dependent collapsed chorions to simplify additional mechanistic studies. This was helpful in carrying out studies addressing barrier function in the chorions and will be useful for future studies aimed at identifying the effect loss of *bals* has on lipid profiles. Wild type chorions are impermeable to neutral red because of the integrity of the chorion layers. In mutations affecting this, neutral red can penetrate and stain the underlying embryo red, thus emphasizing on the protective barrier properties of these layers (LeMosy and Hashimoto, 2000; Savant and Waring, 1989; Tootle et al., 2011). Removing different layers of the wild type egg using chemical treatments suggests that compromising the chorion, wax layer and/ or vitelline membrane makes the otherwise impermeable egg permeable to the dye.

Since *bals* is a fatty acid elongase, it is possible that it is involved in the synthesis of the chorion components by the somatic follicle cells during oogenesis. *bals* expression in follicle cells coincides with the synthesis of the vitelline membrane and wax layer

consistent with such a role in chorion biogenesis (Doetsch, 2004). Additionally, it is also possible that *bals* activity is somehow required for maintenance of the functional barrier rather than synthesizing it. There is a possibility that *bals* might be required for the transport or lipid based modifications of the chorion components.

In the *Drosophila* embryo, *bals* have been shown to be important for viability (Doetsch, 2004). Based on the appearance of the dead embryos (flaccid over time), it was speculated that *bals* might be playing a similar barrier function in the cuticle of embryos/larvae as well. This was tested using an epidermal driver to knockdown *bals* during embryogenesis, which also resulted in lethality and uptake of neutral red by *bals* mutant larvae. This is similar to *elovl4* mutant mice which are neonatal lethal and have a compromised epidermal barrier. Additionally, treating the wild type embryo/larvae with the organic solvent (2:1 v/v chloroform:methanol) makes them somewhat susceptible to neutral red (data not shown). This is consistent with the reported presence of a lipid based protective barrier, and a potential role for *bals* in its synthesis and/or maintenance (Nelson and Lee, 2004; Papassideri et al., 1993).

baldspot and PCD

Lipids have long been considered as central players in mediating cell death. Here, I have a shown that misexpression of a putative lipid elongase, Bals, is capable of triggering caspase dependent PCD in the developing *Drosophila* tissues. This is similar to the study in *Arabidopsis*, where misexpression of FAE1 (KCS1) elongase in the epidermis leads to PCD (Reina-Pinto et al., 2009). Since cell death can occur with or without the involvement of caspases, this brings us one step closer in understanding the mechanistic

regulation of an elongase induced cell death. In order to understand Bals position in the cell death pathway, epistasis experiments with the other players of the pathway were carried out but yielded variable results. It would be helpful to try a different approach to get a better idea about placement of Bals and its role in cell death. Interestingly, gain of function mutations in human ELOVL4 has been associated with STD3/macular degeneration, possibly via apoptosis. Having a similar PCD phenotype for *bals* misexpression gives us the opportunity to gain a better understanding on the possible mechanism by which elongases and specifically ELOVL4 are involved in PCD.

MATERIALS AND METHODS

Fly Stocks and Genetics

Flies were raised at room temperature on standard media. All the crosses were carried out at 25°C and 28°C unless mentioned otherwise. The following stocks were used: *l(3)73Bh10*/TM6B, *Ep(3)3433/*TM3Sb, *l(3)73Bh40*/TM6B, *Ep(3)44B2/*TM3Sb, MTD-GAL4 (B.S# 31777), *bals*^{siRNA} 47519 and 3241 (VDRC).

Rescue Assay: Double balancer stock carrying the CY2>GAL4>GAL80^{ts}; *l(3)73Bh40 was crossed to* UAS*bals*$^{2\text{-}1FMis}$; *Ep(3)3433*; to get the final genotype of CY2-GAL4>UAS*bals*$^{2\text{-}1FMis}$; *l(3)73Bh40/ Ep(3)3433*. *l(3)73Bh40/Ep(3)3433* was used as the control. The flies of both the genotypes were made to lay eggs at RT before they were shifted to 29°C. The flies were allowed to acclimatize to the high temperature before scoring the eggs for rescue. The same group of flies was then shifted back to the RT and the eggs were scored for collapse.

Dehydration/Dessication Assay: Flies were made to lay eggs for an hour after which the eggs were collected and observed and imaged after every hour for first 6 hours and then at 10th and 24th hour for eggshell collapse. Similar to the chorions, newly hatched embryos and larvae were observed for the dessication over the span of 24 hours.

Permeability assay using Neutral Red dye: Permeability was tested as a factor of neutral red dye uptake by the egg as done previously(LeMosy and Hashimoto, 2000). Eggs were collected from six hour egg lay plate and neutral red dye solution (5mg/ml in 1X PBS) was added for two minutes after which the eggs were rinsed with PBS to remove the dye and imaged using the dissection scope. Eggs were also dechorionated with 50% bleach and then subjected to neutral red dye. w^{1118} eggs were further de-waxed using chloroform

and methanol solution (2:1v/v) for one minute and washed with PBS before performing the neutral red uptake assay.

Immunohistochemistry: Larval imaginal discs were dissected in 1XPBS and fixed in 4% formaldehyde in PEMP for 15 minutes. The fixed tissue was washed with antibody wash thrice (30 minutes each) after which antibody block was added and tiddue was rotated at RT for 2 hours. Primary antibody was added (αElav-7E8A10 rat monoclonal antibody from DSHB (1:500), αCaspase3-rabbit polyoclonal antibody (Asp175 from cell signaling technologies), 1:250) and left overnight on a rotator at 4°C. The tissue sample was washed thrice with antibody was (30 minutes each) and secondary antibody (Alexa 488 or 568 (1:400)) was added for 2 hours at RT. Sample was washed with antibody wash and couple of times with 1XPBS. Remove the buffer and add 70%glycerol and one drop of slowfade to the sample and leave it overnight. The images were taken using Zeiss.

ACKNOWLEDGEMENT

Work on *baldspot* was initiated by Amy Doetsch. She identified and generated *bals* mutant alleles and the misexpression constructs that have been used in this study.

Chapter 6

Developmental analysis of components of the VLCFA biosynthetic pathway

ABSTRACT

Fatty acid biosynthesis is a highly specialized pathway that takes places in different cellular compartments and utilizes various enzymes to synthesize and elongate a fatty acid. Given the distinct developmental roles uncovered across the elongases, I sought to assess the roles of additional components of the fatty acid metabolic machinery. One would anticipate reducing the activity of enzymes critical for the production of a given fatty acid species would result in related developmental effects. To investigate this, I identified various members of the lipid biosynthetic pathway based on their sequence homology to known yeast or vertebrate counterparts and tested their roles in *Drosophila* using RNAi mediated knockdown. Results suggest that most of them are important for viability, whereas there seems to be some overlap in their roles in individual tissues.

INTRODUCTION

As briefly mentioned in the introduction, fatty acid biosynthesis *in vivo* occurs in different compartments of a cell. Fatty acid chains with C18 (acquired via diet) or C16 (generated by Fatty Acid Synthase, FAS) present in the cytoplasm are shuttled to the ER for further elongation. A series of sequential reactions takes place in the ER by enzymes of the fatty acid elongation machinery resulting in the synthesis of very long chain fatty acids (VLCFA). In a condensation reaction, elongases trigger the cyclical process of elongating in two carbon increments in the first and the rate-limiting step, while other enzymes including keto acyl reductases, dehydratases and enoyl reductases, sequentially act act on the FA substrate to yield a VLCFA. All the genes encoding the enzymes of the pathway have been characterized in yeast and their sequence has been used to identify mammalian counterparts (Riezman, 2007).

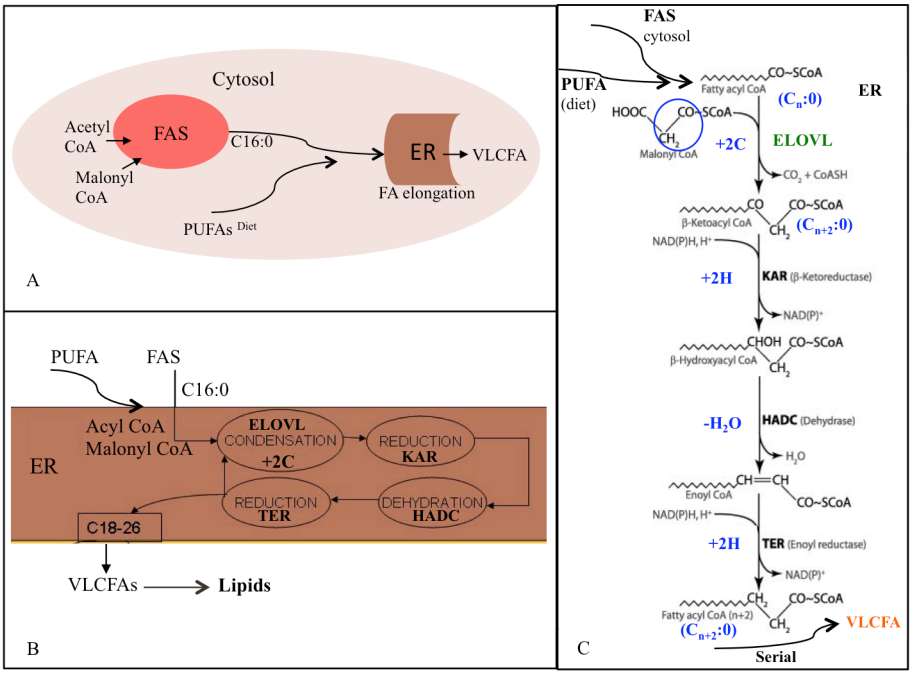

Figure 6.1 (Fig. 1.3 reprinted from chapter 1): VLCFA biosynthesis *in vivo*. FAS in cytosol synthesizes C16:0 which acts as the substrate for elongation machinery present in the ER. ELOVL (Elongase), KAR (β Keto Acyl Reductase), HADC (Dehydratase) and TER (Tertiary Enoyl Reductase). PUFA are the dietary polyunsaturated fatty acids.

In an organism, *de novo* fatty acid synthesis initiates in the cytosol by FAS. It is a multimeric enzymatic complex that catalyzes the synthesis of a C16:0 by utilizing malonyl-CoA. There are two types of fatty acid synthases Type I and Type II. Type I FAS is further divided into animal and fungi FAS based on the architecture and organization of the structure. Type II FAS are present in bacteria and plant plastids (White et al., 2005). Type I FAS are giant multifunctional proteins and even though the catalytic domains are conserved between the two FASs, FAS II are dissociated mono-functional proteins (Smith et al., 2003). FAS levels have been found to be abnormally elevated in numerous cancers like breast, thyroid, ovary and skin making it a potential anticancer drug target (Chakravarty et al., 2004; Lu and Archer, 2005). Consistent with an essential role, *fas* null mutants die during embryonic stages in mice (Chirala et al., 2003). Sequence analysis suggests that *Drosophila* has Type I animal FAS, but not much is known about it's role in development (Leibundgut et al., 2008).

After the C16:0 is synthesized and shuttled to the ER, elongases perform the first condensation reaction leading to the addition of two carbon atoms. The intermediate product is then reduced (addition of hydrogen) in the presence of NADPH by the second enzyme in the process - β-Ketoacyl Reductase (KAR). YBR159wp is the first KAR identified in budding yeast because of its homology to the known reductases and because its inactivation led to expected intermediates in the ER (Beaudoin et al., 2002; Han et al., 2002). Similar studies led to the identification of the enzyme required for the fourth step of elongation - tertiary reductase trans-2, 3-enoyl-CoA (TER) or Tsc13p in yeast (Kohlwein et al., 2001). Based on sequence homology, their mammalian counterparts were identified with having multipass transmembrane domains (Moon and Horton, 2003).

Overexpression and RNAi mediated inhibition of both the reductases has been shown to affect fatty acid elongation in *in vitro* assays (Moon and Horton, 2003).

The most recently discovered members of the fatty acid elongation pathway are the dehydratases (HADC). They are a family of multipass transmembrane enzymes acting on the third step of the reaction by removing the water molecule from the elongated fatty acyl substrate. The first dehydratase was characterized in yeast (PHS1) and homology studies identified four mammalian dehydratases (HADC1-4) (Denic and Weissman, 2007; Ikeda et al., 2008). These dehydratases have tissue specific expression patterns and exhibit some preference for interacting with specific ELOVLs (Ikeda et al., 2008). Genetic depletion of yeast HDAC, Phs1p, led to defective elongation and accumulation of an intermediate fatty acid substrate for third step of the reaction (Kihara et al., 2008).

One other family of proteins that plays an important role in fatty acid metabolism and thus possibly VLCFA biosynthesis/elongation is the Fatty acid transport protein (Fatp) family implicated in fatty acid uptake (Gimeno, 2007). FATp members have highly conserved sequence signature spanning 311 amino acids (Hirsch et al., 1998) and show specific expression patterns in mammals (Herrmann et al., 2001; Schaffer and Lodish, 1994). Functionally, they have been implicated in thermogenesis, obesity and restrictive dermopathy in mice, a skin defect caused by altered fatty acid composition (Guignard et al., 2010; Herrmann et al., 2003; Klar et al., 2009). In *Drosophila*, CG7400 has been identified as a *Drosophila* fatty acid transport protein based on its homology to mammalian *fatp1* and *fatp4* and is implicated in Rhodopsin-1 metabolism and photoreceptor neuron survival (Dourlen et al., 2012).

Even though some of the components of fatty acid elongation machinery are known in *Drosophila*, their individual roles have not been extensively studied. This chapter aims at the identification and functional characterization of these individual components in *Drosophila* to gain a better understanding of their developmental and physiological functions.

RESULTS

Identification of Drosophila components of the VLCFA biosynthetic pathway

In order to identify components of *Drosophila* VLCFA biosynthetic machinery, sequences of known yeast and mammalian counterparts were used to perform a BLAST search on *Drosophila* genome. Putative enzymes of fatty acid elongation machinery in *Drosophila* are listed in Table 6.1 with their percent sequence identities shown. From this analysis, *Drosophila* appears to contain only a single putative Fatty acid synthase (FAS), three putative fatty acid transporters (FATp), five putative Keto Acyl Reductases (KAR),

Table 6.1: Sequence homology between VLCFA biosynthetic enzymes. (*Sc) Saccharomyces cerevisiae, (Mm) Mus musculus, (Hs) (Homo sapiens), (Dm) (Drosophila melanogaster).* Highlighted and italicized CGs were tested for their function using knockdown. No percentage means the CG was not pulled up in the blast.

Enzyme Name	*Yeast (Sc)*	*Mouse (Mm)*	*Human (Hs)*	*Drosophila (Dm)*	*% Identity Mm-Dm*	*% Identity Hs-Dm*	*% Identity Sc-Dm*
Fatty Acid Synthase	FAS1 (YKL182 W)	FAS	FAS	***CG3523***	***49%***	***48%***	
Fatty Acid Transporter protein FATp	Fat1p (FAT1)	FATp-4 Slc27a4	FATP	***CG7400***	***47.4***	***45.1***	***30.2***
				CG30194	46.7	43.5	30.7
				CG3394	41.9	41.6	29.7
Keto Acyl Reductase KAR	Ybr159w p	3-ketoacyl-CoA reductase	KAR	***CG1444***	***50.6***	***50.2***	***32.7***
				CG13284	42.7	42.5	29.8
				CG31809	37.8	36.3	28.6
				CG31810	40.1	38.7	
				CG6012	32.9	32.6	
Dehydratase HADC	Phs1p (PHS1)	3-hydroxyacyl -CoA dehydratase 2	3-hydroxyacyl -CoA dehydratase 2	***CG6746***	***39***	***39***	***36.5***
				CG9267	***29.3***	***29.8***	***24.3***
Enoyl Reductase TER	Tsc13p	TER	TER	***CG10849 (Sc2)***	***53.1***	***53.4***	***31.9***
				CG3248 (Cog3)			39.3
				CG7840	*33.9*	*32.8*	

two Dehydratases (HADC), and three Enoyl Reductases (TER), to go along with the twenty elongases described previously. Those putative enzymes with the highest conservation were selected for further analysis, including functional studies in *Drosophila* development using RNAi mediated knockdown.

Expression of putative Drosophila VLCFA biosynthetic pathway members

Expression profiles for the genes representing putative *Drosophila* VLCFA components was compiled from Fly Atlas anatomical data, available on Flybase (Table 6.2, (Tweedie et al., 2009)).

Table 6.2: Expression and function of selected members of VLCFA biosynthetic machinery. Expression and functional data compiled from Flybase, including Fly Atlas Anatomical Expression Data (Chintapalli et al., 2010.9.17). Only the tissues exhibiting the highest mRNA expression for a particular enzyme are listed.

Enzyme	*Expression (Flybase)*	*Known Functions*
FAS CG3523	Adult head, adult eye, larval/adult central nervous system, adult crop, larval/adult midgut, larval/adult hindgut, adult Malpighian tubules, adult heart, larval/adult fat body, larval trachea, adult spermathecae, adult carcass.	Viability (Flybase)
FATp CG7400	Adult head, adult eye, adult crop, larval/adult midgut, adult hindgut, adult heart, adult fat body, adult male accessory gland, adult carcass	Photoreceptor neuron survival (Dourlen et al., 2012), triglyceride homeostasis (Sujkowski et al., 2012)
KAR CG1444	Adult male, gut, fat body, heart, head, brain, eye, thoracic ganglion	Unknown
HADC CG6746	Adult head, adult crop, adult midgut, adult hindgut, adult Malpighian tubules, adult heart, adult fat body, adult spermathecae, larval/adult carcass	Unknown
HADC CG9267	larval central nervous system, adult heart, larval/adult fat body	Unknown
TER CG10849 (Sc2)	Adult head, larval central nervous system, adult crop, adult midgut, adult hindgut, adult heart, adult fat body, larval salivary gland, larval trachea, adult female reproductive system, larval/adult carcass	Viability (Flybase)

As with elongases, distinct spatial and temporal expression patterns are also observed during *Drosophila* development for these additional putative VLCFA components.

Putative enzymes of Drosophila VLCFA biosynthetic pathway are important for viability and other physiological functions

Ubiquitous knockdown of almost all the putative enzymes tested, five of the six, led to lethality or decreased viability (Table 6.3). In two cases this appeared to affect males more than the females, however it is currently unclear if this is a true reflection of a sexually dimorphic effect or simply an artifact of the GAL4 system, which typically has stronger effects in males due to dosage compensation effects. Knockdown of *fas* and one of the putative *hadc* genes (CG9267) also seem to affect the wing development, whereas *fatp* (CG7400) appeared to be important for fertility, exhibiting the same collapsed chorion phenotype observed for *bals* and CG31523. Surprisingly, none of the putative VLCFA components tested here resulted in locomotor defects, which were uniquely associated with *sits* among all the elongases.

Table 6.3: Functional analysis of other members of VLCFA biosynthetic machinery. RNAi mediated knockdown of different enzymes in different tissues was carried out at 28°C. Numbers in the bracket indicate the total flies scored.

Enzyme^{siRNA}	*GAL4 Tested*			
	General (Act-GAL4)^{1}	***Neuronal (C155 GAL4)***^{1,2}	***Follicle cells (Cy2 GAL4)***^{1,3}	***Segmantal Wing/Bristle (Ptc GAL4)***^{1,4}
FASI (CG3523)	Lethal (n=31) some pharate lethality	WT (n=71)	WT (chorions n>100)	Held out wings (n=90)
FATP (CG7400)	Male specific lethality (n=69) Male pharate lethality	WT (n=98)	CC (chorions n>100)	WT (n=172)
KAR (CG1444)	Viable (n=61)	WT (n=108)	WT (chorions n>100)	WT (n=162)
Dehydratase (CG 6746)	Lethal Pharate lethality (n=63)	WT (n=129)	WT (Adult Flies n=65, chorions>100)	WT (n=82)
Dehydratase (CG 9267)	Lethal (n=68)	WT (n=115)	WT chorions Adult flies have wing defects (Adult Flies n=81, chorions n>100)	Shriveled, small, held out wings (n=180)
TER (CG10849)	Low viability (n=68) Male specific lethality	WT (n=69)	WT (chorions n>100)	WT (n=110)

1. Adult knockdown F1s were scored for any gross morphological defects and viability. The original parent vial was also observed for larval/pupal lethality. The percent viability was calculated by dividing the number of total progeny trans-heterozygotes for the indicated elongase and the GAL4 driver by the number of progeny of the trans-heterozygous for the GAL4 and the indicated elongase. N indicates the total number of progeny scored (Duffy and Gergen, 1991).
2. Adult knockdown F1s were observed for overt behavioral defects and assayed using Flip Over Assay. Numbers in the parenthesis indicate the total progeny assayed (materials and methods, Chapter 2 and supplementary Movie 4.3A).
3. Chorions from adult knockdown F1 females were observed for defects. Numbers in the parenthesis indicate the total eggs scored (materials and methods, Chapter 2).
4. Adult knockdown F1s were scored for wing and bristle defects. Numbers in the parenthesis indicate the total progeny scored for viability and wing and bristle defects.
    a. WT- wild type
    b. CC- Collapsed chorions

DISCUSSION

Identification of putative VLCFA biosynthetic enzymes in Drosophila

Drosophila has proved to be an important model system to study metabolic pathways and their physiological effects. Identification and characterization of the *Drosophila* enzymes important for fatty acid elongation would help in our understanding of their functions and developmental contributions, both conserved between species and unique to a species. While some of these enzymes have been identified and their biochemical functions studied in yeast and mammals, not much is known about their specific *in vivo* roles. To address this, I used a sequence-based approach and identified putative representatives in *Drosophila*. While each of these enzymes shares significant sequence similarity to their known vertebrate counterparts, supporting these assignments, it is important to note that barring biochemical confirmation of their enzymatic activities these assignments must be considered tentative.

Functional analysis of the putative VLCFA biosynthetic enzymes during Drosophila development

Conservation of these VLCFA components from flies to vertebrates provides support for critical functional roles. Supporting this my functional studies revealed that five out of the six VLCFA components tested here were essential for viability, a result similar to that observed for elongases conserved in *Drosophila* and vertebrates (Chapter three). Additional support for functions conserved across species comes from knockdown of *Drosophila fatp*. As shown earlier Bals, like its vertebrate elongase orthologs, is required for barrier function. Strikingly, knockdown of *Drosophila fatp*, like *bals*, led to collapsed

chorions and therefore might also be playing a role in barrier function. Given the demonstration that knockout of mouse *fatp* is lethal with barrier defects, my result with *Drosophila fatp* supports this and provides further evidence for the conservation of developmental roles for members of VLCFA synthesis across species.

Conclusions

The majority of our understanding on the functions of enzymes of the VLCFA biosynthetic pathway comes from *in vitro* assays and there is limited knowledge about their developmental or physiological roles. By demonstrating these roles can be easily tested in *Drosophila* using RNAi knockdown, one can begin to decipher the contributions of each of these molecules to specific developmental processes. Unlike the large family of elongases in *Drosophila*, a limited number of each of the three additional enzymes of the elongation cycle, (KAR, HADC, and TER) are present. These could function in a promiscuous fashion partnering with any elongase or alternatively might have certain preferences towards specific elongases. Given that lethality is associated with a number of elongases (12/20), one would have anticipated that if KARs, HADCs, or TERs were promiscuous then knockdown of a single member of each family of enzymes would not result in lethality due to functional redundancy. Supporting some level of specificity among at least the HADCs, lethality was observed with knockdown of either putative HADC suggesting loss of one is not compensated for by the promiscuous function of the remaining HADC. This together with the observation that there are five putative Keto Acyl Reductases (KAR) and three Enoyl Reductases (TER) to go along with the two

Dehydratases (HADC) argues strongly for some degree of functional specificity between elongases and these other members of the fatty acid elongation cycle.

MATERIALS AND METHODS

Fly stocks: Following fly stocks from ordered from VDRC. All the crosses were carried at 28^{o}C unless mentioned otherwise.

Table 6.4: VDRC lines for enzymes knockdown.

Gene	Transformant ID	Library	On Target	Off Target
FASI (CG3523)	108339	KK	1	0
FATP (CG7400)	100124	KK	1	1
KAR (CG1444)	40949	GD	1	1
Dehydratase (CG 6746)	103625	KK	1	0
Dehydratase (CG 9267)	101546	KK	1	0
TER (CG10849)	7480	GD	1	1

Sequence Analysis: Yeast and mammalian enzyme sequences were used to BLASTP (NCBI) against the *Drosophila* genome to find the putative homologs at default settings.

CONCLUSIONS AND FUTURE DIRECTIONS

Presence of the sophisticated toolbox for genetic and molecular manipulation and the availability of elaborate genomic, molecular, and proteomic resources make *Drosophila* a model system of choice for studying the various metabolic, physiological and developmental roles of different enzymes. With these tools and resources, *Drosophila* has also become increasingly utilized to study the mechanisms underlying behavior because these tools allow for the dissection of the circuits involved.

The goal of this thesis was to gain a better understanding of the developmental roles of a family of enzymes implicated in the biosynthesis of very long chain fatty acids in *Drosophila*. The enzyme family known as elongases (elos) serve as the first and the rate limiting step (Gregory et al, 2011) of the fatty acid elongation pathway in the ER and are responsible for addition of two carbon atoms per reaction. The elongated fatty acid (VLCFA) is then shuttled to the cytoplasm where it gets incorporated into complex lipids. The lipids thus generated perform myriad of metabolic, cellular and physiological functions. Dysregulation of these lipids or the biosynthetic enzymes can lead to diseases such as Tay-sachs, Macular Degeneration, Artherosclerosis, and Diabetes.

Elongases are conserved from yeast to humans and the number of elongases present in different genus and species vary widely. Limited studies addressing their *in* vivo roles have been performed to date. *Based on their distribution across and within species, I hypothesized that some elongases have conserved functions across species, while others*

have species specific roles. Through the work described in this thesis, I have shown that elongases conserved across species are more likely to play vital roles, while species specific elos may serve functions that are unique to those species. For example, one particular elongase could be involved in the synthesis of a particular pheromone, cuticular hydrocarbon, or wax layer that is specific to a particular species of insect, plant, or vertebrate. Such knowledge could be utilized to generate bio-pesticides and herbicides by targeting and inhibiting the specific elongase that is responsible for synthesis of a given component of a wax layer. In addition insight into the role of elongases in maintaining barrier properties would be helpful in developing artificial skin with improved barrier function by ensuring the appropriate skin specific elongases, and therefore VLCFAs, are expressed during growth and culture of the skin *in vitro*.

Overall, this study shows that the repertoire of twenty elongases in *Drosophila* have varying, and in some cases conserved, developmental functions (Figure 7.1). Using *Drosophila* as a model system, I have studied the roles they are playing in development with the goal that this would help

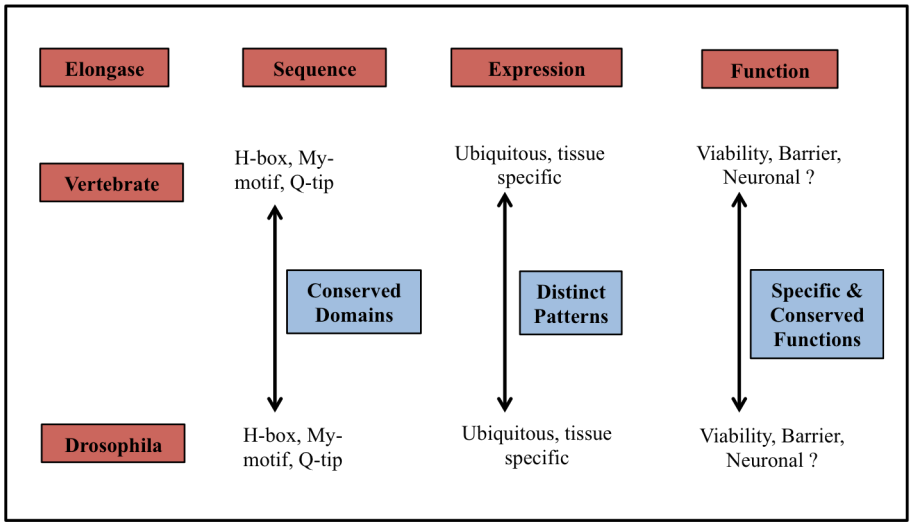

Figure 7.1: Similarities between Vertebrate and *Drosophila* elongases.

us better understand their roles in vertebrates. With respect to specific elos, I have identified the first link between an elo, Sits, and adult locomotor behavior. In addition, my work provides further insight into the role of Bals in maintaining barrier function – a role conserved with vertebrate elongases. Phylogenetically, Sits appears most closely related to vertebrate Elovl1 and Elovl7, it will be important to determine this role in behavior for Sits is also conserved in vertebrates. Consistent with a potential role, neuronal expression has been reported for Elovl1 and Elovl7 (http://www.informatics.jax.org/) and therefore analysis of these putative Sits orthologs, Elovl1 and Elovl7 is an important line of investigation for future work. Understanding the neuronal population involved in *sits* function will also give insight on the neuronal circuits that impact locomotion and may lead to insight on neurological disorders that display locomotor symptoms.

While I have provided important insight to the function of elongases in *Drosophila*, one of the next key steps in understanding the roles of elongases will be to define biochemically the lipid/ fatty acid species that these enzymes are synthesizing to help us better understand the contribution of specific lipid classes to development.

APPENDIX

APPENDIX A

Table A1: RNAi induced knockdown of *bals* by two different triggers affect various tissues in *Drosophila* development.

Driver	Expression	Phenotype with $bals^{RNAi\#47519}$ 28°C	Phenotype with $bals^{RNAi\#47519}$ 25°C	Phenotype with $bals^{RNAi\#3241X}$ 28°C	Phenotype with $bals^{RNAi\#3241X}$ 25°C
Act GAL4 [1]	General	L (1st/2nd instar) (N= 125)	L (1st/2nd instar)	L (N=227)	L
Tub GAL4[1]	Ubiquitous	L (N=106)	L	L (N=226)	L
CY2 GAL4[1,3]	Follicle cells	CC (N=>1000)	CC (N=>1000)	CC (N=>1000)	CC (N=>1000)
C155 GAL4[1,2]	Nervous System	Minor vein defect (N=181)	Minor vein defect (N=181)	Minor vein defect (N=61)	No affect (N=61)
MS1096 $GAL4^{(X)1,4}$	Wing	Pharate lethality (N=42) Strongly curled and shriveled Wings (N=210)	Pharate lethality (N=68) Strong curl in wings (N=23)	Curly, shriveled/bruised wings (N=53)	Pharate lethality (N=24) Adults with curly, shriveled wings (N=30)
Ap GAL4[1,4]	Wing	Held out wings (N=132)	Held out wings (N=132)	ND	ND
A9 $Gal4^{(X)\ 1,4}$	Wing	Curly wings (N=117)	Slight curl in the wings (50%, N=119)	Strongly curled and shriveled wings. (N=59)	Curly wings (59%, N=92)
Ptc GAL4[1,4]	Wing	Ectopic vein (67%) (N=154)	Ectopic vein (67%) (N=154)	ND	ND
En GAL4[1,4]	Wing	Black spiracles in larvae Adults with curly wings (74%, N=96)	Black spiracles in larvae Adults with curly wings (89%, N=83)	Pharate lethality Adults with slightly curly wings (N=127)	Black spiracles in larvae (N=64) Adults with curly wings (75%, N=49)
pGawb OK376[1,3]	Oenocytes, Fat body	CC	CC	CC	CC
pGawb c179[1]	Wing discs, gut region, salivary glands	Low viability (7%) Pharate Lethality (N=182)	Low viability $1^{st}/2^{nd}$ instar lethal Some pharate lethality	L	L larval/pharate lethality (N=82)
pGawb T80[1]	Larval imaginal discs	L (N= 172)	L (N= 31)	L (N=118)	L (N=103)

Table A2: Bals mis-expression in different *Drosophila* tissues induces lethality and other phenotypes.

Driver	Tissue Affected	Phenotype with UAS>*bals2X* (28°C)	Phenotype with UAS>*bals2X* (25°C)	Phenotype with UAS>*bals1X*$^{(2\text{-}1F)}$ (28°C)	Phenotype with UAS>*bals1X*$^{(2\text{-}1F)}$ (25°C)
Act GAL4[1]	General	L	L	L	L
Tub GAL4[1]	General	ND	ND	ND	ND
CY2GAL4[1,3]	Follicle cells	ND	ND	ND	ND
C155 GAL4[1,2]	Neuronal	L	L	L	L
MS1096 GAL4$^{(X)}$[1,4]	Wing	L	L	Vein Defect (missing L1) (n=58)	Vein Defect (missing L1) (n=124)
Ptc GAL4[1,4]	Wing	L	L	WT	WT
En GAL4[1,4]	Wing	L	L	L	L
pGawb OK376[1]	Oenocytes, Fat body	L (n=144)	L (n=134)	Low viability (7%, n= 151) Male lethality	Low viability (11%, n= 172) Male lethality
pGawb c179[1,4]	Wing discs, gut region, salivary glands	L (n=130)	L (n=137)	L (n=154)	L (n=88)
pGawb T80[1,4]	Larval imaginal discs	L (n=158)	L (n=210)	L (n=190)	L (n=265)

1. Adult knockdown F1s were scored for any gross morphological defects and viability. The original parent vial was also observed for larval/pupal lethality. The percent viability was calculated by dividing the number of total progeny trans-heterozygotes for the indicated elongase and the GAL4 driver by the number of progeny of the trans-heterozygous for the GAL4 and the indicated elongase. N indicates the total number of progeny scored (Duffy and Gergen, 1991).
2. Adult knockdown F1s were observed for overt behavioral defects and assayed using Flip Over Assay. Numbers in the parenthesis indicate the total progeny assayed (materials and methods, Chapter 2 and supplementary Movie 4.3A).
3. Chorions from adult knockdown F1 females were observed for defects. Numbers in the parenthesis indicate the total eggs scored (materials and methods, Chapter 2).
4. Adult knockdown F1s were scored for wing and bristle defects. Numbers in the parenthesis indicate the total progeny scored for viability and wing and bristle defects.

L= lethal
CC= collapsed chorions
ND= not done
X= transgene is on X chromosome

APPENDIX B

This section contains the additional data confirming and supporting *sits* requirement in locomoter behavior.

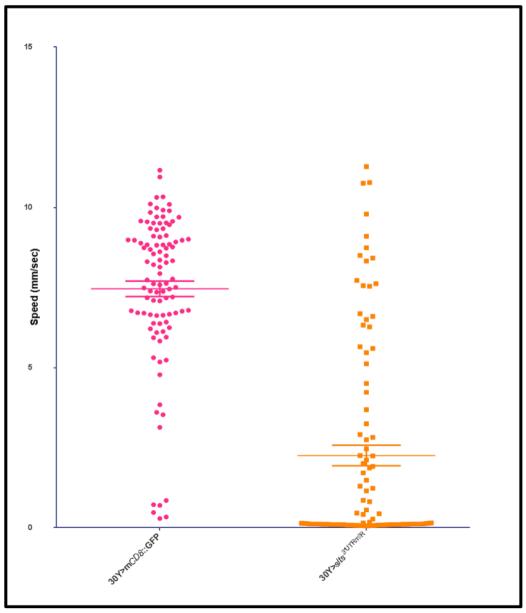

Figure B.1: *sits* knockdown at 25°C results in reduced locomotion. 30Y>mCD8::GFP & 30Y>*sits*3'UTRshmiR. N=100 for both genotypes. (Unpaired t test P value< 0.0001).

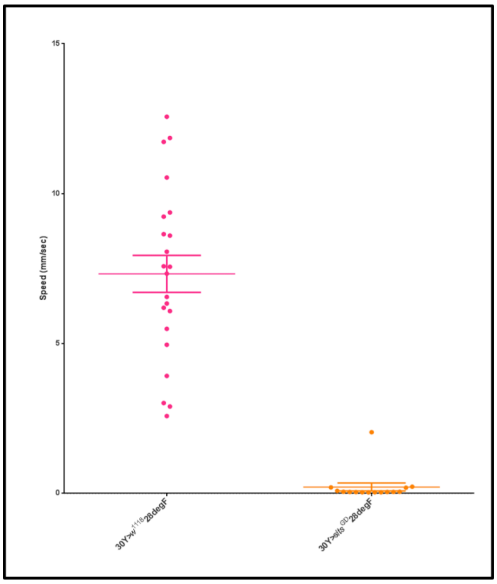

Figure B.2: Neuronal knockdown of *sits* in females at 28° C leads to the behavioral phenotype. The control flies (30Y>w^{1118}) and the mutants (30Y>sits^{GD}) have significantly different speeds (P<0.0001, unpaired t test). The speeds of individual flies are plotted for control (n=22) and mutant (n=15) females. The bars represent the mean and the SD.

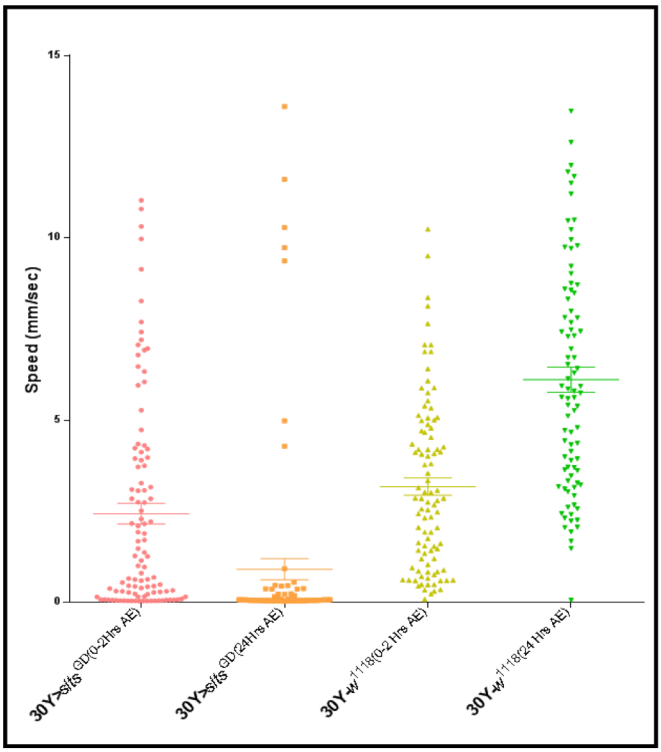

Figure B.3: Knockdown with *sits*^{GD} shows temporally dependent phenotype. N=104, 98, 96& 88respectively from LHS. P<0.0001, Kruskal Wallis test. Dunn test shows significant difference between the mutant groups(****). There is also significant difference between the two control groups (***) and the mutant (*sits*^{GD} 0-2 hrs) and control (0-2 hrs)(*).

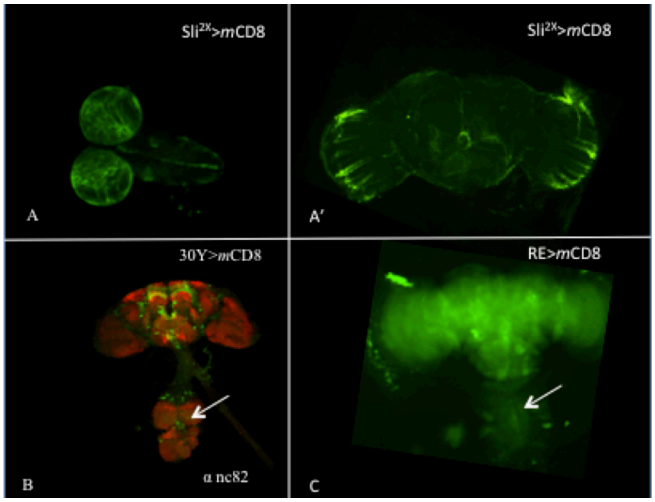

Figure B.4: GFP tagged expression of GAL4s in the CNS. All the GAL4s shown here exhibit locomotion defects for *sits* knockdown. A&A' are Sli^{2X}>mCD8 in larvae and adult brain respectively. B) 30Y>mCD8 in adult brain and the ventral nerve cord (VNC) (arrow). C) RE>mCD8 in pupal brain and VNC. α nc82 is used to stain the neuropils.

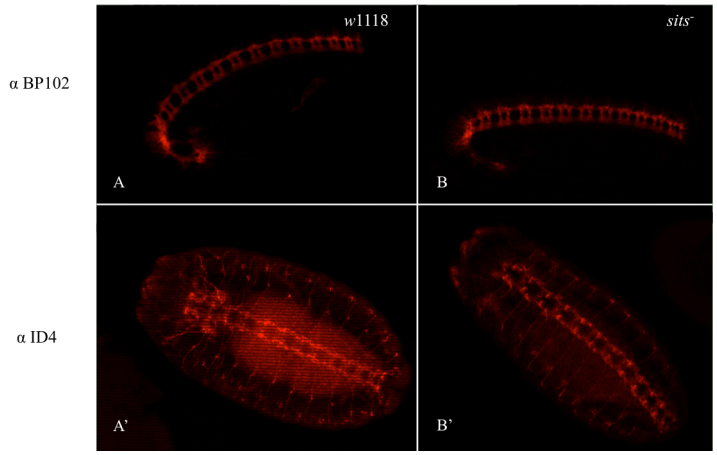

Figure B.5: *sits* mutant embryos do not exhibit overt morphological defects in the nervous system. A & A' are the w1118 embryos. B&B' are *sits* mutants (*sits*^{KG20194}). The top row shows the staining with α BP102, a CNS specific marker for axons. The bottom row shows α ID4 staining, a marker for Fascilin II.

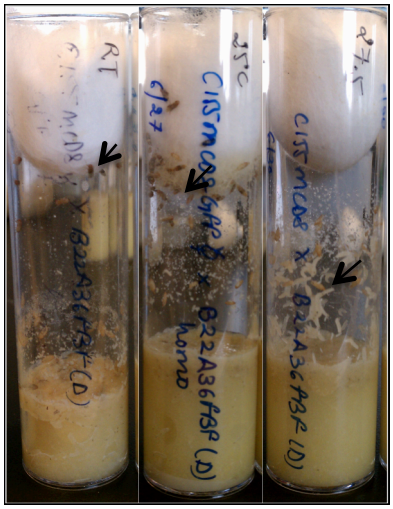

Figure B.6: Temperature dependence of *sits* misexpression effects on larval nervous system. C155>mCD8>*sits*^{MIS2X} crosses at Room Temperature (~ 23°C), 25°C and 27.5°C from LHS. The first vial (RT) has very few adults (arrow) and several larvae dead in the food. The second vial (25°C) has more number of adults and pupae and relatively lower number of dead larvae. The third vial at the highest temperature has a lot of larvae and pupae on the side of vial and almost no dead larvae in the food.

Table B.1: List of Bloomington stock center drivers tested for *sits* function. The highlighted drivers showed an effect with *sits* knockdown.

Driver	BS #	Description	Phenotype
P{GawB}elav [C155]	***458***	***Pan neural***	***Yes***
y[1] w[*]; P{w[+mC]=GAL4-Mef2.R}3	27390	Expresses GAL4 in muscle cells	No
w[*]; P{w[+mW.hs]=GawB}D42	8816	Expresses GAL4 in motor neurons	No
P{GAL4-sli.S}3	***9580***	***Expresses GAL4 in embryonic midline glial cells and MP1 neurons***	***Yes***
P{GAL4-sim.3.7}3	9150	Expresses GAL4 in CNS midline precursor cells.	No
Alarm GAL4		Astrocytes	No
GAL4}repo/TM3, Sb[1]	7415	Expresses GAL4 in glia	No
GAL4-ftz.ng	8767	Expresses GAL4 in a subset of neurons	No
EcR.GET-BD-GAL4	5910	Expresses GAL4 in larval EcR-A-expressing neurons destined for apoptosis at metamorphosis; also expressed in imaginal discs	No
Akh-gal4.L	25684	Expresses GAL4 in the Adipokinetic hormone-secreting cells of the corpora cardiaca	No
GawB}007Y	30812	Expresses GAL4 in the ellipsoid body, nodulus, small field neurons, pb-eb-no neurons & protocerebral bridge(mushroom bodies, fan shaped body)	No
GawB}129Y	***30816***	***Expresses GAL4 in the antennal nerve & subesophageal ganglion***	***Yes***
GawB}lilli[189Y]	30817	Expresses GAL4 in ellipsoid & mushroom bodies, pars intercerebralis, antennal lobe & labral, chemosensory, large field, GABa-expressing & segmental nerves	No
GawB}30y	***30818***	***Expresses GAL4 in mushroom, ellipsoid and fan shaped bodies, subesophageal ganglion, antennal & optic lobes, protocerebrum & median bundle***	***Yes***
GawB}50y	30820	Expresses GAL4 in sensory nerves of chordotonal organs & thoracic neuromeres	No
GawB}078Y	30821	Expresses GAL4 in the ellipsoid body, nodulus, protocerebral bridge, pb-eb-no neurons, pars intercerebralis & small field neurons	Repeat
GawB}c205	30826	Expresses GAL4 in the fan shaped body &	Repeat

		subesophageal ganglion	
GawB}Aph-4[c232]	30828	Expresses GAL4 in ring neurons, Malpighian tubules, large field neurons & ellipsoid body	No
GawB}C5[C5]	30839	Expresses GAL4 in large field neurons, wing disc, protocerebrum & mushroom & fan shaped bodies	No
GawB}Aph-4[c507]	30840	Expresses GAL4 in ring neurons, large field neurons, ellipsoid body & Malpighian tubule	No
GawB}c767	30848	Expresses GAL4 in the ellipsoid body & PI neurons	No
GawB}c819	30849	Expresses GAL4 in Bolwig's nerve, ring neurons, ellipsoid body, pars intercerebralis & large field neurons	No
GawB}neur[GAL4-A101]	6393	Assumed to express GAL4 in all sensory organs and their precursors	No
npf-GAL4.1}2	25681	Expresses GAL4 in the neuropeptide F-secreting neurons of the larval protocerebral lobe and subesophageal ganglion and in the midgut endocrine cells	No
npf-GAL4.1}1	25682	Expresses GAL4 in the neuropeptide F-secreting neurons of the larval protocerebral lobe and subesophageal ganglion and in the midgut endocrine cells	No
GawB}167Y	3741	GAL4 pattern in third instar larva: brain - neuroblasts in central brain and ventral ganglion, Bolwig's nerve, discs - spot in leg disc only	No
GawB}Tab2[201Y]	4440	GAL4 expressed primarily in mushroom body	No
GawB}OK107	854	GAL4 expressed in mushroom bodies	No
GawB}c747	6494	GAL4 expressed in mushroom body, thoracic ganglion and wing and leg discs (antennal lobe interneurons, cc)	Repeat
Cha-GAL4.7.4}19B P{w[+mC]=UAS-GFP.S65T}T2	6793	Expresses GFP specifically in cholinergic neurons	No
GawB}c309	6906	GAL4 expressed in mushroom body, thoracic ganglion and eye-antennal disc, optic lobe neurons, lobe neurons, a subset of central complex neurons	No
GawB}c739	7362	Expressed in brain, ventral ganglion and wing and haltere discs. Expressed in the alpha and beta lobes of the mushroom body	No
GAL4-Eh.2.4}C21	6301	Expresses GAL4 in eclosion hormone-expressing neurons	No
Sgs3-GAL4.PD}TP1	6870	Expresses GAL4 in the salivary gland	No
Ddc-GAL4.L}4.36	7009	Expresses GAL4 in dopaminergic and serotonergic neurons	No
GawB}43	7148	Expresses GAL4 in longitudinal glial cells and a subset of peripheral neurons starting at	No

		embryonic stage 12	
P{da-GAL4.w[-]}3	8641	Expresses GAL4 in the pattern of the da gene	No
GawB}1407	8751	Expresses GAL4 in all nerves	No
Eaat1-GAL4.R}2	8849	Expresses GAL4 in the glial cells that produce the glutamate transporter EAAT1	No
GAL4-da.G32}UH1	5460	GAL4 expression is ubiquitous in embryos	No
GawB}SG18.1	***6405***	***GAL4 expressed in antennal olfactory receptors, neurons and processing centers in CNS, also imaginal precursors***	***Yes***
GawB}OK376	6487	GAL4 expressed in oenocytes	Yes
Pdf-GAL4.P2.4}2; P{w[+mC]=UAS-PV-Myc}3a P{UAS-PV-Myc}3b	25031	Expresses parvalbumin, a vertebrate Ca[2+] buffer protein, in PDF-expressing ventrolateral brain neurons	No
hs-GAL4.ER}ER156	25038	Expresses estrogen-activated GAL4 in the CNS	No
GawB}386Y	25410	Expresses GAL4 in peptidergic neurons. Reflects expression of amon gene	No
GawB}VGlut[OK371]	26160	Expresses GAL4 in glutamatergic neurons from embryonic stage 15 to adult	No
TrpA1-GAL4.R}3/TM3, Sb[1]	27593	Expresses GAL4 in the central brain in the pattern of the TrpA1 gene	No
GawB}pain[GAL4]	27894	Expresses GAL4 in multidendritic neurons, chordotonal neurons, a subset of cells in the CNS and a subset of sensory neurons in the antennal-maxillary complex	No
Gr66a-GAL4.D}2; Gr93a[3]	28801	Expresses GAL4 in Gr66a-expressing gustatory neurons of the leg, labral and cibarial sense organs and labial palps	No
GawB}Pdfr[EY11181-GAL4] w[67c23]	33070	Expresses GAL4 in Pdfr-expressing neurons including circadian pacemaker neurons	No
P{GawB}C68a	30847	Expresses GAL4 in the central complex, Kenyon cells & genital disc.	No
w[*]; P{w[+mW.hs]=GawB}V55	2683	Embryonic tissue(s) showing GAL4 expression: PNS	No
w[*]; P{w[+mW.hs]=GawB}4G	6927	GAL4 expression pan-neural in late embryos, in a subset of motor neurons in 3rd instar larvae, and enriched in mushroom bodies in adults	No
w[*]; P{w[+mW.hs]=GawB}43	7148	Expresses GAL4 in longitudinal glial cells and a subset of peripheral neurons starting at embryonic stage 12,	No
w[*]; P{w[+mW.hs]=GawB}A51/TM6	8764	Expresses GAL4 in muscles and motor neurons in segment-specific patterns	No
w[*]; P{w[+mW.hs]=GawB}OK72	6486	GAL4 expressed in oenocytes	Repeat
P{J21.17-GAL4}JO15	6753	GAL4 expressed in Johnston's organ	No
P{GawB}Hr39[c739]	7362	Expressed in brain, alpha and beta lobes of the mushroom body, ventral ganglion, wing and	No

		haltere discs	
P{GawB}DJ646	8169	Adult expression increases at mid-age. Expressed in adult sensory neurons, oenocytes & testis	No
P{Orco-GAL4.W}11.17	26818	Expresses GAL4 in the pattern of the Or83b gene.	No
P{Gr66a-GAL4.D}2	28801	Expresses GAL4 in Gr66a-expressing gustatory neurons of the leg, labral and cibarial sense organs and labial palps	No
P{GawB}c316	30830	Expresses GAL4 in dorsal paired medial neurons	No
P{GawB}c584	30842	Expresses GAL4 in haltere & wing discs, antennal lobe, pars intercerebralis & mushroom, ellipsoid & fan shaped bodies	No
P{GawB}GH298	37294	Expresses GAL4 in antennal lobe local interneurons.	No
w[1118]; P{w[+mW.hs]=GawB}drl[PGAL8]	***4669***	***GAL4 in brain, primarily mushroom body and central body complexes***	***Lethal***
w[*]; P{w[+mC]=ple-GAL4.F}3	8848	Expresses GAL4 in dopaminergic cells	No
y[1] w[*]; P{w[+mC]=so7-GAL4}A	26810	Expresses GAL4 in the pattern of the sine oculis gene in the eye-antennal disc	No
w[*]; P{w[+mW.hs]=GawB}smid[C161]/TM6B, Tb[1]	27893	Expresses GAL4 in Bolwig's nerve, chordotonal organs, nodulus, ellipsoid & fan shaped bodies, protocerebral bridge & imaginal discs	No
w[*]; P{w[+mW.hs]=GawB}c305a	30829	Expresses GAL4 in mushroom body alpha' and beta' lobes, ellipsoid body & antennal lobes	No
w[*]; P{w[+mW.hs]=GawB}c061	30845	Expresses GAL4 in the fan shaped body, dorsal protocerebrum, mushroom body & dopaminergic neurons regulating appetite	No
P{w[+mW.hs]=GawB}C164	33807	Expresses GAL4 in the central body complex and in the posterior tip of the thoracic ganglion	No
y[1] w[*]; P{w[+mW.hs]=GawB}gcm[rA87.C]/CyO	35541	Expresses GAL4 in glia, glial precursor cells, lamina precursor cells and lamina neurons	No
w[*]; P{w[+mW.hs]=GawB}MT14	***37293***	***Expresses GAL4 in olfactory, gustatory and mechanosensory neurons, as well as photoreceptor cells R2, R5 and R8***	***Yes (mild)***
w[*]; P{w[+mW.hs]=GawB}GH298	37294	Expresses GAL4 in antennal lobe local interneurons	No
w[*]; P{w[+mW.hs]=GawB}c105	30822	Expresses GAL4 in the ellipsoid body, ring neurons & large field neurons	No
w[*];	30823	Expresses GAL4 in small field neurons, fb-eb	No

P{w[+mW.hs]=GawB}c 107		neurons fan shaped & ellipsoid bodies &optic tract	
w[*]; P{w[+mW.hs]=GawB}c 119	30824	Expresses GAL4 in the ellipsoid body	No

APPENDIX C

This section contains the sequences and the primers used in the study.

Elongases Protein sequences

>CG5278
MAAVNATQVDYWNFLFTDLADPRTNDWFLIKSPLPLLGILAFYLFFVLSWGPKFMKDRK
PFKLERTLLVYNFFQVALSVWMVYEGVVIWQYYSWRCQPVDWSRTPKAYREARVVYV
YYLAKITELLDTIFFVLRKNDRQVTFLHVYHHTVMPMISWGTSKYYPGGHGTFIGWINSF
VHIIMYSYYFLSAFGPQMQKYLWWKKYITNLQMIQFCCAFIHQTQLLYTDCGYPRWSVC
FTLPNAVFFYFLFNDFYQKSYKKKQAAAKEKALSADNNNDGCAKDLNKAIQLQQEKQK
AL

>CG8534
MADLLNGTLIISEDPVRLPLIGSPWPSLTIVSLYLLFVLKLGRKFMENRKPYDLRRVIRAY
NIMQIVYNGVILIAGLHFLFVLKAYDLRCITKLPLDHELKSRERWLTYSYFFNKFMDLLET
VFFVLRKKDRQISFLHVFHHLVMSFGGYLHITFNGYGGTLFPLCLLNVAVHVIMYAYYY
LSSVSKDVQTSRWKKYITIVQLVQFILVLANFSYTLMQPDCNASRTVIYTGMFISTTFILM
FANFYIHNYILNGSKQKSALKSD

>CG2781
MDYLTMFYDGWRDLMDNKSDPRTRDYPLMSSPFPTIAISLTYAYIVKVLGPKLMENRKP
FELRKVLIVYNAAQVIFSAWLFYESCIGGWLNGYNLRCEPVNYSYSPKAIRTAEGCWWY
YFSKFTEFFDTFFFVMRKRYDQVSTLHVIHHGIMPVSVWWGVKFTPGGHSTFFGFLNTFV
HIFMYAYYMLAAMGPKVQKYLWWKKYLTVMQMIQFVLVMVHSFQLFFKNDCNYPIGF
AYFIGAHAVMFYFLFSNFYKRAYVKRDGKDKASVKANGHANGHVKALKDGDVAPTSN
GQANGFHNTFSKFTTDMCNPALNSSTRQRVLVNAGNK

>CG5326
MSVRLNETTTIVDRMVNFFVEHEDLRTKQWFLSNAPGPLFMILGAYLYFCLYAGPRYMR
DRKPFELKNTLLVYNAVQVLLSWVLFYEGYKGGWGGHYNFKCQPVTYESDPISMRMA
RAVWLYYIAKITELLDTVFFVLRKKQRQISFLHLYHHTLMPVCAFIGVKYFAGGHGTLLG
FINSFIHIIMYAYYLLSAMGPKVQKYLWWKKYITILQIVQFLIIFVHTLQIQFQPNCNFPKSI
AALLTFNAGLFTYMFSAFYVANYKKEAAAQAKLAAKKE

>CG6660
MVAYLYCLVRDLYAEHGDPRVAHLPLLGNLWIVLAIVALYVAFVLHYGPRWMANRAP
FELKRVMQVYNVVQVLANATIFVIGLSNTYLQPGYSWTCQPVDHTDRSPAMMKTLYAS
YAYYMLKYLDLLDTVFIVLRKKNSQVSFLHVYHHGGMVFGVSIFMTFLGGSHCSMLGII
NLLVHTVMYAYYYAASLGAVKNLLWWKQRITQLQLMQFGYLTFHFLLVIVRNPCQFPV
FIAFIGFIQNIFMFSMFFDFYCKTYIRKQRKSAEHKLKAS

>CG6921
MTNYIKIVEERISGLSKGVDETVDSWFLMSSPMPVVAVVLVYLAFVLKIGPEYMKNRKP
MDLKRIMVFYNAFQVLYSIWMCRTSIQESNVMASIFSKKCEINRTREQNLTLYSGAWFYF
FSKIIDLLDTTFFVLRKKDNQVSFLHVYHHTITVLFSWGYLKYAPGEQGVIIGILNSGVHII

MYFYYMVAAMGPQYQKYLWWKKYMTSIQLIQFVLILGYMLTVGAKGCNMPKTLTFFF
VGNTVIFLYLFGNFYRKTYKKAKSVDGGSRTTGSSLAQSALRAAGGMGCMPQTMNAG
KHLLQNGQVGKAYIDLNNNSVKPMKLE
>CG9458
MLGDLVDFLGKSPPDPVRLPLLASHKPVLMVLATYLFFVKIAGPKIMRNRKPFDLRGLIK
AYNIMQIVYNVIMCFFAVHFMLGPGDYNFKCIKNLPPDHEYKTWERWLTYSYFFNKLLD
LLETVFFVLRKKDRQISFLHVFHHMYMLYFSFMYLYYYGYGGHGFFMCFFNVVVHIMM
YSYYYQSSLNRDSKGDLWWKKYITIVQLIQFGIVLGHSIYTLKQPDCPSARFSATCAGSIS
VVFIILFSNFYFHAYIRPKKRKQKNI

>CG9459
MFAHMLDFLNRSPPDPVRLPLTSSHWPVLTILGIYLVFIKIVGPWFMQNQKPYNLDRAIKI
YNIVQIAYNVILLIFSVHFMLGPGNYNFSCISNLPLDHEYKNWERWLSYSYFFNKLMDLL
ETVFFIFRKKYRQISFLHVFHHVYMVYIGFLYMYYYGYGGHGFFLITFNVVVHTMMYTY
YYQSSLNRNSGGDLWWKKYITVVQLVQFVIIFSHSVYILRQTDCQTSRLSATWGSLISVV
FIILFSNFYVRTYILPKKTKSAVGR

>CG11801
MTSSMGNDTKTESYSYPFADLADERTQDWPLVKSPWNIIALLALYLLMVRYAPKWTAR
CKPLQLRVPLFCHSLAMIFLNGYICLEFLTASLSLGYNFACQECRVSHDPHEIRIAAAMW
WFYISKILEFVDTAFFILRHKWNQLSFLHVYHHSTMFLFCWTYVKWLPTGSTFFPSMINS
FVHVIMYSYYALSVLGPRVQRFLWWKRYLTGLQLVQFTIIFFWASQLVFRGCEYGKWLT
PIGAAYMVPFLFMFGRFYAQKYCVSAVVKKAK

>CG30008
MEASASINLQPVVNVPTIYKDPWYMITVLVLYLYFVTKAGPHFMEWRKPYELKRLILLH
NFIQVVSCIYAIKEVLYITDNTIYIFWKCRDIGSSPELVRRYYNLAYFLFWLKISELIETVIF
VLRKKQNQVSKLHIFHHFSTVTLVYALINFNENGSAAYFCVFLNSIVHVIMYSYYFVAAV
ADKTLVQALTPVKKCITVIQMTQFVLILTQVAFQLVLCGMPPLVLLYFTTVILGMFYGFY
DFYNSAYQASQRRKSQTPQSDSKK

>BalsCG3971
MINMDISVTPNYSYIFDFENDFIHQRTRKWMLENWTWVFYYCGIYMLVIFGGQHFMQN
RPRFQLRGPLIIWNTLLAMFSIMGAARTAPELIHVLRHYGLFHSVCVPSYIEQDRVCGFW
TWLFVLSKLPELGDTIFIVLRKQPLIFLHWYHHITVLIYSWFSYTEYTSSARWFIVMNYCV
HSVMYSYYALKAARFNPPRFISMIITSLQLAQMIIGCAINVWANGFLKTHGTSSCHISQRN
INLSIAMYSSYFVLFARFFYKAYLAPGGHKSRRMAASLAAQNVVKQSSSPQQASESSKFI
GAGEDQAAYLRKAKAQ

>CG16905
MFAPIDPVKIPVVSNPWITMGTLIGYLLFVLKLGPKIMEHRKPFHLNGVIRIYNIFQILYNG
LILVLGVHFLFVLKAYQISCIVSLPMDHKYKDRERLICTLYLVNKFVDLVETIFFVLRKKD
RQISFLHVFHHFAMAFFGYLYYCFHGYGGVAFPQCLLNTAVHVIMYAYYYLSSISKEVQ
RSLWWKKYITIAQLVQFAIILLHCTITLAQPNCAVNRPLTYGCGSLSAFFAVIFSQFYYHN
YIKPGKKSAKQNKN

>CG17821
MNFTLLDLFRGLPADPVHLPMFGTPLPAIVIVLGYLLLIFKVGPDFMRSRKPYNMRKAML
IYNFCQVLMNSGIFLMGTYYLFIKKLYDFRCMTMLSSDHPDKDVDRLLTYFYFINKVIDL
IDTIFFVLRKSNKQITVLHVYHHVFMVLGVPLTYYFYGPGGQYNLMGYLNSFVHVVMY

AYYFASAWYPNVKSTFWWKEYITKLQFLQFMILFAQSVLTLWLNPGCRFPKVLQYVQL
GGSVSMMTMFGNFYYQTYVKAKSKEQ

>CG18609
MLRYLRIPQADPNPIPLAGSPWPITLILIAYLLFVLKLGKIFMRNRKPYDLKTVLKVYNLF
QVLYNGLYFGMVFYYLFIVGICNLHCIESFPEGHERKQLERVLHAAYLLNKVLDLMDTV
FFVLRKSYKQITFLHIYHHVFMSFGSYALTRYYGTGGHVNAVGLLNSLVHTVMYFYYFL
SSEYPGVRANIWWKKYITLTQLCQFFMLLSYAIYVRFFSPNCGVPRGLLYLNMVQGVVFI
YLFGKFYIDNYLRPPKAKINAKQS
>CG31141
MLEIFRTPYADSKQLPLATGPGPIIIILIGYLLVVFKAGRKFMEHREPYNLRKVLKYYNMF
QIFYNIMMLLPGYYFMLVFQPYNFRCMTVLQQDHPLKNWERCISYAYYINKIVDLLDTV
FCVLRKKYSQITFLHVFHHVLMPSAGYLIIRFYGYGGQLFFLCSFNVFVHIFMYAYYYSAI
KGNTVRWKRYLTLMQMLQFLLMFGHCALTAMQRQCTASQGTLFLVSCSATIMFIMFAN
FYFQCYLRPKHKEN

>SitsCG31522
MALIMKYIDSISRYMDSHSDSRTKGWPMMSSPFPTLAVCLTYVYLVKVLGPRLMENRKP
LNLQNTLVMYNAIQVVFSAWLFYECLMGGWWGSYSFRCQPVDYTDSPTSRRMVHACW
WYYFSKFTEFMDTIFFVLRKKSSQVTTLHVIHHGCMPMSVWFGVKFTPGGHSTFFGLLN
TFVHIVMYTYYMFSAMGPQYQKYLWWKKYLTTLQMVQFILIMVHAFQLLFIDCNYPKA
FVWWIGMHAVMFFFLFNEFYKAAYRSRMMKKNGALANGHAKPNGYCKSINAHDDLA
MPQTTEATATATPASKANGSSTPPSNGHANGVENVYKQVANGSAHKGSNGGLSNGYAT
KLLDDASQELKQRKTPK

>CG31523
MAIILQEAQKWYRDLMDNKSDPRVNDFFLLSSPLPTLCMCIFYAYFSKSLGPRLMAKRK
PMELRSVLVVYNAIQTIFSAWIFYEYLMSGWWGHYSLKCQPVDYSTTGLAMRMVNICW
WYYISKFTEFFDTLFFILRKKNEHVSTLHVIHHGCMPFSVWMGLKFAPGGHSTFFALLNS
FVHIVMYFYYMIAAMGPKYQKYIWWKKYLTTFQMVQFVAIFTHQFQLLFRECDYPKGF
MVWIGLHGVMFLFLFSDFYKAKYLNAARRRRQAVKANGYANGSASNGHSKHLGEGDA
LIANGCNTGACMPVMEDEYVKSKGQSNGAYKEGFFKEGVLSNNDAIFNPDSSSSSLHQR
KVK

>CG32072
MASLGISFHPFPDQPDERTRNWPLVDSFWTVPVLLSIYLLMVRYAPKWTTRHKPLQLRA
PLFCHSLAMVFLNGYICLELYAATRDLDYNFGCQPCRVSFDPHEMRLTKAFWWFYISKIL
EFADTAFFILRQKWSQLSFLHVYHHSTMFVFCWILIKWMPTGSTYVPAMINSFVHIIMYG
YYALSVLGPRVQRFLWWKRYLTGLQLVQFTIIFFWASQMLVRGCEYGTWITLSMAIYSL
PFLFMFGKFYMQKYTVSAVGKKPI

>CG33110
MSMNYHNYNSSSRFEMVVEIANIALDEFKTHHITRNYTGLVQRYYQLVEEDYGDPRAK
RFPLMEHPMFTFGMVAVYLSWVLVIGPLFMRDRKPFQLRRTLVVYNAFQVALSGYMFY
EHLMAGWLNYYNLKCQPVDYSDSPSSKRMLNLCYLYYLSKLTEFADTMFFVLRKKSSQ
ITWLHVYHHSVTPLETWVLVKFLAGGNATFPNLLNNFVHVCMYFYYMMAAMGPEYAK
FLWWKKYMTELQIAQFVLCIFHTLRALFSNQCQFSKFISALLLLNASIFFCLFMNFYMQS
YRKTKAAQQLQQQQQQQKQQQQLDATPCKADSNNNTAMLAQKLKAN

>CG16904

MFEVFDKPFADPVQLPLAGSIRTSVIIITVYLLFVLKLGRKLMDKHEALQLRGVLKFYNIG
QVLFNSVIFVWGIHLLFVQKPYNLSCMQVLPQDHELKSTERTLSYMYHLNKVLDLMDTI
FFVLRKKQRQITFLHVFHHVFMVFTSHMLIRFYGFGGHVFLICMFNVLVHIVMYGYYYA
SSQSQNVQESLWWKKYLTLGQLVQFLLMFLHCMYTYFQPNCSASRGVIYVISSASAFMF
LMFTKFYIKTYIRPKEVKSKGKVN

>MmElovl1
MEAVVNLYHELMKHADPRIQSYPLMGSPLLITSILLTYVYFILSLGPRIMANRKPFQLRGF
MIVYNFSLVILSLYIVYEFLMSGWLSTYTWRCDPIDFSNSPEALRMVRVAWLFMLSKVIE
LMDTVIFILRKKDGQVTFLHVFHHSVLPWSWWWGIKIAPGGMGSFHAMINSSVHVVMY
LYYGLSALGPVAQPYLWWKKHMTAIQLIQFVLVSLHISQYYFMPSCNYQYPIIIHLIWMY
GTIFFILFSNFWYHSYTKGKRLPRAVQQNGAPATTKVKAN

>MmElovl2
MEQLKAFDNEVNAFLDNMFGPRDSRVRGWFLLDSYLPTFILTITYLLSIWLGNKYMKNR
PALSLRGILTLYNLAITLLSAYMLVELILSSWEGGYNLQCQNLDSAGEGDVRVAKVLWW
YYFSKLVEFLDTIFFVLRKKTNQITFLHVYHHASMFNIWWCVLNWIPCGQSFFGPTLNSFI
HILMYSYYGLSVFPSMHKYLWWKKYLTQAQLVQFVLTITHTLSAVVKPCGFPFGCLIFQ
SSYMMTLVILFLNFYIQTYRKKPVKKELQEKEVKNGFPKAHLIVANGMTDKKAQ

>MmElovl3
MDTSMNFSRGLKMDLMQPYDFETFQDLRPFLEEYWVSSFLIVVVYLLLIVVGQTYMRTR
KSFSLQRPLILWSFFLAIFSILGTLRMWKFMATVMFTVGLKQTVCFAIYTDDAVVRFWSF
LFLLSKVVELGDTAFIILRKRPLIFVHWYHHSTVLLFTSFGYKNKVPSGGWFMTMNFGVH
SVMYTYYTMKAAKLKHPNLLPMVITSLQILQMVLGTIFGILNYIWRQEKGCHTTTEHFF
WSFMLYGTYFILFAHFFHRAYLRPKGKVASKSQ

>MmElovl4
MGLLDSEPGSVLNAMSTAFNDTVEFYRWTWTIADKRVADWPLMQSPWPTISISTLYLLF
VWLGPKWMKDREPFQMRLVLIIYNFGMVLLNLFIFRELFMGSYNAGYSYICQSVDYSND
VNEVRIAAALWWYFVSKGVEYLDTVFFILRKKNNQVSFLHVYHHCTMFTLWWIGIKWV
AGGQAFFGAQMNSFIHVIMYSYYGLTAFGPWIQKYLWWKRYLTMLQLVQFHVTIGHTA
LSLYTDCPFPKWMHWALIAYAISFIFLFLNFYTRTYNEPKQSKTGKTATNGISSNGVNKSE
KALENGKPQKNGKPKGE

>MmElovl5
MEHFDASLSTYFKAFLGPRDTRVKGWFLLDNYIPTFVCSVIYLLIVWLGPKYMKNRQPFS
CRGILQLYNLGLTLLSLYMFYELVTGVWEGKYNFFCQGTRSAGESDMKIIRVLWWYYFS
KLIEFMDTFFFILRKNNHQITVLHVYHHATMLNIWWFVMNWVPCGHSYFGATLNSFIHV
LMYSYYGLSSIPSMRPYLWWKKYITQGQLVQFVLTIIQTTCGVFWPCSFPLGWLFFQIGY
MISLIALFTNFYIQTYNKKGASRRKEHLKGHQNGSVAAVNGHTNSFPSLENSVKPRKQR
KD

>MmElovl6
MNMSVLTLQEYEFEKQFNENEAIQWMQENWKKSFLFSALYAAFIFGGRHLMNKRAKFE
LRKPLVLWSLTLAVFSIFGALRTGAYMLYILMTKGLKQSVCDQSFYNGPVSKFWAYAFV
LSKAPELGDTIFIILRKQKLIFLHWYHHITVLLYSWYSYKDMVAGGGWFMTMNYGVHA
VMYSYYALRAAGFRVSRKFAMFITLSQITQMLMGCVINYLVFNWMQHDNDQCYSHFQ
NIFWSSLMYLSYLVLFCHFFFEAYIGKVKKATKAE

>MmElovl7
MAFSDLTSRTVRFYDNWIKDADPRFEDYLLMSSPLPQTIILGLYVYFVTSLGPKLMENRK
PFELKKAMITYNFFIVLFSVYMCYEFVMSGWGTGYSFRCDIVDYSQSPRAMRMVHTCW
LYYFSKFIELLDTIFFVLRKKNSQVTFLHVFHHTIMPWTWWFGVKFAAGGLGTFHAFLNT
AVHVVMYSYYGLCAMGPAYQKYLWWKKHLTSLQLVQFVLVTIHIGQIFFMEDCNYQY
PVFLYIIMSYGCIFLLLFLHFWYRAYTKGQRLPKTLENGNCKSKRH

>HsELOVL1
MEAVVNLYQEVMKHADPRIQGYPLMGSPLLMTSILLTYVYFVLSLGPRIMANRKPFQLR
GFMIVYNFSLVALSLYIVYEFLMSGWLSTYTWRCDPVDYSNSPEALRMVRVAWLFLFSK
FIELMDTVIFILRKKDGQVTFLHVFHHSVLPWSWWWGVKIAPGGMGSFHAMINSSVHVI
MYLYYGLSAFGPVAQPYLWWKKHMTAIQLIQFVLVSLHISQYYFMSSCNYQYPVIIHLI
WMYGTIFFMLFSNFWYHSYTKGKRLPRALQQNGAPGIAKVKAN

>HsELOVL2
MEHLKAFDDEINAFLDNMFGPRDSRVRGWFMLDSYLPTFFLTVMYLLSIWLGNKYMKN
RPALSLRGILTLYNLGITLLSAYMLAELILSTWEGGYNLQCQDLTSAGEADIRVAKVLW
WYYFSKSVEFLDTIFFVLRKKTSQITFLHVYHHASMFNIWWCVLNWIPCGQSFFGPTLNS
FIHILMYSYYGLSVFPSMHKYLWWKKYLTQAQLVQFVLAITHTMSAVVKPCGFPFGCLI
FQSSYMLTLVILFLNFYVQTYRKKPMKKDMQEPPAGKEVKNGFSKAYFTAANGVMNK
KAQ

>HsELOVL3
MVTAMNVSHEVNQLFQPYNFELSKDMRPFFEEYWATSFPIALIYLVLIAVGQNYMKERK
GFNLQGPLILWSFCLAIFSILGAVRMWGIMGTVLLTGGLKQTVCFINFIDNSTVKFWSWV
FLLSKVIELGDTAFIILRKRPLIFIHWYHHSTVLVYTSFGYKNKVPAGGWFVTMNFGVHAI
MYTYYTLKAANVKPPKMLPMLITSLQILQMFVGAIVSILTYIWRQDQGCHTTMEHLFWS
FILYMTYFILFAHFFCQTYIRPKVKAKTKSQ

>HsELOVL4
MGLLDSEPGSVLNVVSTALNDTVEFYRWTWSIADKRVENWPLMQSPWPTLSISTLYLLF
VWLGPKWMKDREPFQMRLVLIIYNFGMVLLNLFIFRELFMGSYNAGYSYICQSVDYSNN
VHEVRIAAALWWYFVSKGVEYLDTVFFILRKKNNQVSFLHVYHHCTMFTLWWIGIKWV
AGGQAFFGAQLNSFIHVIMYSYYGLTAFGPWIQKYLWWKRYLTMLQLIQFHVTIGHTAL
SLYTDCPFPKWMHWALIAYAISFIFLFLNFYIRTYKEPKKPKAGKTAMNGISANGVSKSE
KQLMIENGKKQKNGKAKGD

>HsELOVL5
MEHFDASLSTYFKALLGPRDTRVKGWFLLDNYIPTFICSVIYLLIVWLGPKYMRNKQPFS
CRGILVVYNLGLTLLSLYMFCELVTGVWEGKYNFFCQGTRTAGESDMKIIRVLWWYYF
SKLIEFMDTFFFILRKNNHQITVLHVYHHASMLNIWWFVMNWVPCGHSYFGATLNSFIH
VLMYSYYGLSSVPSMRPYLWWKKYITQGQLLQFVLTIIQTSCGVIWPCTFPLGWLYFQIG
YMISLIALFTNFYIQTYNKKGASRRKDHLKDHQNGSMAAVNGHTNSFSPLENNVKPRKL
RKD

>HsELOVL6
MNMSVLTLQEYEFEKQFNENEAIQWMQENWKKSFLFSALYAAFIFGGRHLMNKRAKFE
LRKPLVLWSLTLAVFSIFGALRTGAYMVYILMTKGLKQSVCDQGFYNGPVSKFWAYAF
VLSKAPELGDTIFIILRKQKLIFLHWYHHITVLLYSWYSYKDMVAGGGWFMTMNYGVH

AVMYSYYALRAAGFRVSRKFAMFITLSQITQMLMGCVVNYLVFCWMQHDQCHSHFQN
IFWSSLMYLSYLVLFCHFFFEAYIGKMRKTTKAE

>HsELOVL7
MAFSDLTSRTVHLYDNWIKDADPRVEDWLLMSSPLPQTILLGFYVYFVTSLGPKLMENR
KPFELKKAMITYNFFIVLFSVYMCYEFVMSGWGIGYSFRCDIVDYSRSPTALRMARTCW
LYYFSKFIELLDTIFFVLRKKNSQVTFLHVFHHTIMPWTWWFGVKFAAGGLGTFHALLN
TAVHVVMYSYYGLSALGPAYQKYLWWKKYLTSLQLVQFVIVAIHISQFFFMEDCKYQF
PVFACIIMSYSFMFPLLFLHFWYRAYTKGQRLPKTVKNGTCKNKDN

>Scelo1
MVSDWKNFCLEKASRFRPTIDRPFFNIYLWDYFNRAVGWATAGRFQPKDFEFTVGKQPL
SEPRPVLLFIAMYYVVIFGGRSLVKSCKPLKLRFISQVHNLMLTSVSFLWLILMVEQMLPI
VYRHGLYFAVCNVESWTQPMETLYYLNYMTKFVEFADTVLMVLKHRKLTFLHTYHHG
ATALLCYNQLVGYTAVTWVPVTLNLAVHVLMYWYYFLSASGIRVWWKAWVTRLQIV
QFMLDLIVVYYVLYQKIVAAYFKNACTPQCEDCLGSMTAIAAGAAILTSYLFLFISFYIEV
YKRGSASGKKKINKNN

>Scelo2
MNSLVTQYAAPLFERYPQLHDYLPTLERPFFNISLWEHFDDVVTRVTNGRFVPSEFQFIA
GELPLSTLPPVLYAITAYYVIIFGGRFLLSKSKPFKLNGLFQLHNLVLTSLSLTLLLLMVEQ
LVPIIVQHGLYFAICNIGAWTQPLVTLYYMNYIVKFIEFIDTFFLVLKHKKLTFLHTYHHG
ATALLCYTQLMGTTSISWVPISLNLGVHVVMYWYYFLAARGIRVWWKEWVTRFQIIQF
VLDIGFIYFAVYQKAVHLYFPILPHCGDCVGSTTATFAGCAIISSYLVLFISFYINVYKRKG
TKTSRVVKRAHGGVAAKVNEYVNVDLKNVPTPSPSPKPQHRRKR

>Scelo3
MNTTTSTVIAAVADQFQSLNSSSSCFLKVHVPSIENPFGIELWPIFSKVFEYFSGYPAEQFE
FIHNKTFLANGYHAVSIIIVYYIIIFGGQAILRALNASPLKFKLLFEIHNLFLTSISLVLWLLM
LEQLVPMVYHNGLFWSICSKEAFAPKLVTLYYLNYLTKFVELIDTVFLVLRRKKLLFLHT
YHHGATALLCYTQLIGRTSVEWVVILLNLGVHVIMYWYYFLSSCGIRVWWKQWVTRFQ
IIQFLIDLVFVYFATYTFYAHKYLDGILPNKGTCYGTQAAAAYGYLILTSYLLLFISFYIQS
YKKGGKKTVKKESEVSGSVASGSSTGVKTSNTKVSSRKA

>/AteloB/
MASIYSSLTYWLVNHPYISNFTWIEGETLGSTVFFVSVVVSVYLSATFLLRSAIDSLPSLSP
RILKPITAVHSLILCLLSLVMAVGCTLSITSSHASSDPMARFLHAICFPVDVKPNGPLFFWA
QVFYLSKILEFGDTILIILGKSIQRLSFLHVYHHATVVVMCYLWLRTRQSMFPIALVTNST
VHVIMYGYYFLCAVGSRPKWKRLVTDCQIVQFVFSFGLSGWMLREHLFGSGCTGIWGW
CFNAAFNASLLALFSNFHSKNYVKKPTREDGKKSD

>/AteloA/
MASVYSTLTYWLVHHPYIANFTWTEGETLGSTVFFVFVVVSLYLSATFLLRYTVDSLPTL
GPRILKPITAVHSLILFLLSLTMAVGCTLSLISSSDPKARLFDAVCFPLDVKPKGPLFFWAQ
VFYLSKILEFVDTLLIILNKSIQRLSFLHVYHHATVVILCYLWLRTRQSMFPVGLVLNSTV
HVIMYGYYFLCAIGSRPKWKKLVTNFQMVQFAFGMGLGAAWMLPEHYFGSGCAGIWT
VYFNGVFTASLLALFYNFHSKNYEKTTTSPLYKIESFIFIHGERWANKAITLFSKKND

Protein sequences of the other enzymes of the biosynthetic pathway

>Sc FAT1p
MSPIQVVVFALSRIFLLLFRLIKLIITPIQKSLGYLFGNYFDELDRKYRYKEDWYIIPYFLKS
VFCYIIDVRRHRFQNWYLFIKQVQQNGDHLAISYTRPMAEKGEFQLETFTYIETYNIVLRL
SHILHFDYNVQAGDYVAIDCTNKPLFVFLWLSLWNIEQDLMHELLNSQSPEFLQQDNVR
TPLGLTDFKPSMLIYTSGTTGLPKSAIMSWRKSSVGCQVFGHVLHMTNESTVFTAMPLFH
STAALLGACAILSHGGCLALSHKFSASTFWKQVYLTGATHIQYVGEVCRYLLHTPISKYE
KMHKVKVAYGNGLRPDIWQDFRKRFNIEVIGEFYAATEAPFATTTFQKGDFGIGACRNY
GTIIQWFLSFQQTLVRMDPNDDSVIYRNSKGFCEVAPVGEPGEMLMRIFFPKKPETSFQG
YLGNAKETKSKVVRDVFRRGDAWYRCGDLLKADEYGLWYFLDRMGDTFRWKSENVS
TTEVEDQLTASNKEQYAQVLVVGIKVPKYEGRAGFAVIKLTDNSLDITAKTKLLNDSLSR
LNLPSYAMPLFVKFVDEIKMTDNHKILKKVYREQKLPKGLDGNDTIFWLKNYKRYEVLT
AADWEAIDAQTIKL

>HsFATp
MLLGASLVGVLLFSKLVLKLPWTQVGFSLLFLYLGSGGWRFIRVFIKTIRRDIFGGLVLLK
VKAKVRQCLQERRTVPILFASTVRRHPDKTALIFEGTDTHWTFRQLDEYSSSVANFLQAR
GLASGDVAAIFMENRNEFVGLWLGMAKLGVEAALINTNLRRDALLHCLTTSRARALVF
GSEMASAICEVHASPDPSLSLFCSGSWEPGAVPPSTEHLDPLLKDAPKHLPSCPDKGFTDK
LFYIYTSGTTGLPKAAIVVHSRYYRMAALVYYGFRMRPNDIVYDCLPLYHSAGNIVGIGQ
CLLHGMTVVIRKKFSASRFWDDCIKYNCTIVQYIGELCRYLLNQPPREAENQHQVRMAL
GNASGSPSGPTFPAASTYPRWLSSTGPECNCSLGNFDSQVGACGFNSRILSFVYPIRLVRV
NEDTMELIRGPDGVCIPCQPGEPGQLVGRIIQKDPLRRFDGYLNQGANNKKIAKDVFKKG
DQAYLTGDVLVMDELGYLYFRDRTGDTFRWKGENVSTTEVEGTLSRLLDMADVAVYG
VEVPGTEGRAGMAAVASPTGNCDLERFAQVLEKELPLYARPIFLRLLPELHKTGTYKFQ
KTELRKEAFDPAIVKTRCSIYIEKGRYVPLDQEAYSRIQAGEEKL

>MmFATp-4
MLLGASLVGALLFSKLVLKLPWTQVGFSLLLLYLGSGGWRFIRVFIKTVRRDIFGGMVLL
KVKTKVRRYLQERKTVPLLFASMVQRHPDKTALIFEGTDTHWTFRQLDEYSSSVANFLQ
ARGLASGNVVALFMENRNEFVGLWLGMAKLGVEAALINTNLRRDALRHCLDTSKARA
LIFGSEMASAICEIHASLEPTLSLFCSGSWEPSTVPVSTEHLDPLLEDAPKHLPSHPDKGFT
DKLFYIYTSGTTGLPKAAIVVHSRYYRMASLVYYGFRMRPDDIVYDCLPLYHSAGNIVGI
GQCLLHGMTVVIRKKFSASRFWDDCIKYNCTIVQYIGELCRYLLNQPPREAESRHKVRM
ALGNGLRQSIWTDFSSRFHIPQVAEFYGATECNCSLGNFDSRVGACGFNSRILSFVYPIRL
VRVNEDTMELIRGPDGVCIPCQPGQPGQLVGRIIQQDPLRRFDGYLNQGANNKKIANDVF
KKGDQAYLTGDVLVMDELGYLYFRDRTGDTFRWKGENVSTTEVEGTLSRLLHMADVA
VYGVEVPGTEGRAGMAAVASPISNCDLESFAQTLKKELPLYARPIFLRFLPELHKTGTFK
FQKTELRKEGFDPSVVKDPLFYLDARKGCYVALDQEAYTRIQAGEEKL

>DmCG7400 FATp
MFLQHNSLLDNYANSNVIINIDNCALYSTNRPADRKSITDGSHDRQRRRRQRFLVIFRFFC
ATVAFGLAIACVIYTLHTMGWIFAVLVALVALLLTKPGWRWFYIAGATASRDLTALWA
YIKLLRYTKRHERLNYTVADVFERNVQAHPDKVAVVSETQRWTFRQVNEHANKVANV
LQAQGYKKGDVVALLLENRAEYVATWLGLSKIGVITPLINTNLRGPSLLHSITVAHCSAL
IYGEDFLEAVTDVAKDLPANLTLFQFNNENNNSETEKNIPQAKNLNALLTTASYEKPNKT
QVNHHDKLVYIYTSGTTGLPKAAVISHSRYLFIAAGIHYTMGFQEEDIFYTPLPLYHTAG
GIMCMGQSVLFGSTVSIRKKFSASNYFADCAKYNATIGQYIGEMARYILATKPSEYDQKH
RVRLVFGNGLRPQIWPQFVQRFNIAKVGEFYGATEGNANIMNHDNTVGAIGFVSRILPKI
YPISIIRADPDTGEPIRDRNGLCQLCAPNEPGVFIGKIVKGNPSREFLGYVDEKASAKKIVK

DVFKHGDMAFISGDLLVADEKGYLYFKDRTGDTFRWKGENVSTSEVEAQVSNVAGYK
DTVVYGVTIPHTEGRAGMAAIYDPERELDLDVFAASLAKVLPAYARPQIIRLLTKVDLTG
TFKLRKVDLQKEGYDPNAIKDALYYQTSKGRYELLTPQVYDQVQRNEIRF

>DmCG30194 FATp
MCTAGVVDGGAGATTGGADAADNSGAAPAPSSTALNPPQVSISMNEPENLKPPAKSNFR
RYLQWILAPVLTAISGLILYYQGPWYGVATLYAALISILLVRPGWRWFYIAAVTTPRDTV
ALFAYIRVLLFIKRQERKNLNIGDIFESNVARQPDKLAIVSESQQWTFRQVNEHSNRVAN
VFHSHGYKKGDVVGLLLENRAEFVATWLGLSKIGVITPLINTNLRGASLQHSITVGQCTA
LIYGASFRSAVMDIAKDLPAHVGLYQFNDESNQEVVASEGLSQGLAQQLNGLLETAAKD
KVAAGASRADHHDKLVYIYTSGTTGLPKAAVITHSRYFFIAAGIHYTLGFKDQDVFYTPL
PLYHTAGGVMSMGQALLFGSTVVIRKKFSASGYFSDCARFQCTVGQYIGEMARYILATP
SAPHDRNHQVRMVFGNGLRPQIWPQFVERFGIRKVGEFYGATEGNANIMNNDSTVGAIG
FISRILPQIYPISIIKADPHTGEPLRNSQGLCERCEADEPGVFVGKIVRGNPCREFLGYVDQK
ASSKKVVHDVFSKGDMAFISGDLLVADERGYLYFKDRTGDTFRWKGENVSTSEVEAQL
SNLAGYKDVIVYGVSIPNTEGRAGMAAIYDPTREVNVSQLGVELAKSLPNYARPQFLRFL
RKIDLTGTFKLRKVELQQQGFNPEIIDDELFYAQPDGVYAPLTPSVYERIVRNELRF

>ScTsc13p
MPITIKSRSKGLRDTEIDLSKKPTLDDVLKKISANNHNISKYRIRLTYKKESKQVPVISESFF
QEEADDSMEFFIKDLGPQISWRLVFFCEYLGPVLVHSLFYYLSTIPTVVDRWHSASSDYN
PFLNRVAYFLILGHYGKRLFETLFVHQFSLATMPIFNLFKNCFHYWVLSGLISFGYFGYGF
PFGNAKLFKYYSYLKLDDLSTLIGLFVLSELWNFYCHIKLRLWGDYQKKHGNAKIRVPL
NQGIFNLFVAPNYTFEVWSWIWFTFVFKFNLFAVLFLTVSTAQMYAWAQKKNKKYHTR
RAFLIPFVF

>MmTER1
MKHYEVEIRDAKTREKLCFLDKVEPQATISEIKTLFTKTHPQWYPARQSLRLDPKGKSLK
DEDVLQKLPVGTTATLYFRDLGAQISWVTVFLTEYAGPLFIYLLFYFRVPFIYGRKYDFTS
SRHTVVHLACMCHSFHYIKRLLETLFVHRFSHGTMPLRNIFKNCTYYWGFAAWMAYYI
NHPLYTPPTYGVQQVKLALAVFVICQLGNFSIHMALRDLRPAGSKTRKIPYPTKNPFTWL
FLLVSCPNYTYEVGSWIGFAILTQCVPVALFSLVGFTQMTIWAKGKHRSYLKEFRDYPPL
RMPIIPFLL

>HsTER1
MKHYEVEILDAKTREKLCFLDKVEPHATIAEIKNLFTKTHPQWYPARQSLRLDPKGKSLK
DEDVLQKLPVGTTATLYFRDLGAQISWVTVFLTEYAGPLFIYLLFYFRVPFIYGHKYDFTS
SRHTVVHLACICHSFHYIKRLLETLFVHRFSHGTMPLRNIFKNCTYYWGFAAWMAYYIN
HPLYTPPTYGAQQVKLALAIFVICQLGNFSIHMALRDLRPAGSKTRKIPYPTKNPFTWLFL
LVSCPNYTYEVGSWIGFAIMTQCLPVALFSLVGFTQMTIWAKGKHRSYLKEFRDYPPLR
MPIIPFLL

>DmCG10849-Sc2
MELEILNAKNSKPYGKVKVPSGATPIGDLRALIHKTLKQTPHANRQSLRLELKGKSLKDT
DTLESLSLRSGDKIYVKDLGPQIGWKTVFLAEYAGPLIVYLIFYFRPELVYGKAASLPISLT
THIAAGCYTVHYVKRLLETIFVHRFSHATMPLRNLFKNCTYYWGFTAYVSYHVNHPQFT
SPCMCTVWGALGAFALCELGNFSVHIALRNLRPPGTKVRKIPVADGNPLTKLFDLVSCPN
YTYEIGAWVSFSVLTSCLAAYLFAFAGAFQMTIWALAKHRNYKKEFKDYPRQRRSIFPF
VL

>DmCG7840
MAPPENGILEVLENLLDRYKINLLQMMFGTFIATIVFFGGLMTFVEKYLPNSIRQSFRYGK
HSFKGETDPLVAWLEVPKSWFKHFYTFALFWSWLAFYVLVSTVREQKEAPEYVLQFLDI
MGGGRSHRKVEIDSTTACVGAFMLTLQCTRRFYETNFVQIFSKKSKINLSHYAVGYVHY
FGAVIALLSNTSGFVRGSKPMEFSLDKLTSQQILYLGVFFLAWQQQYASNMILVNLRKDP
RTGSVKTEKHLLPKGGLFNLLSSPHMFLEVVMYFCIADLYMPVRIWRLIFLWVASNQTIN
ALLTHKWYQETFREYPKNRRAIIPFLL

>ScYbr159wpKAR
MTFMQQLQEAGERFRCINGLLWVVFGLGVLKCTTLSLRFLALIFDLFLLPAVNFDKYGA
KSGKYCVITGASDGIGKEFARQMAKRGFNLVLISRTQSKLEALQKELEDQHHVVVKILAI
DIAEDKESNYESIKELCAQLPITVLVNNVGQSHSIPVPFLETEEKELRDIITINNTATLLITQI
IAPKIVETVKAENKKSGTRGLILTMGSFGGLIPTPLLATYSGSKSFLQSWSNSLAGELSKD
AIDVELIISYLVTSSMSKIRRSSLMIPNPQQFVKSTLRSVGRRCGSQERYATMTPYWAHAV
YQFVITETFGVYSKIVNSINYSFHKSIRIRALKKAARQVKKE

>Hs 3-KAR
MTFMQQLQEAGERFRCINGLLWVVFGLGVLKCTTLSLRFLALIFDLFLLPAVNFDKYGA
KSGKYCVITGASDGIGKEFARQMAKRGFNLVLISRTQSKLEALQKELEDQHHVVVKILAI
DIAEDKESNYESIKELCAQLPITVLVNNVGQSHSIPVPFLETEEKELRDIITINNTATLLITQI
IAPKIVETVKAENKKSGTRGLILTMGSFGGLIPTPLLATYSGSKSFLQSWSNSLAGELSKAI
DVELIISYLVTSSMSKIRRSSLMIPNPQQFVKSTLRSVGRRCGSQERYATMTPYWAHAVY
QFVITETFGVYSKIVNSINYSFHKSIRIRALKKAARQVKKE

>DmCG1444
MEENNSQVLSLLGGLAIGIVGFQVFRKVLPWIYANVVGPKVFGSSVDLSKMGEWAVVT
GSTDGIGKAYAKELARRGLKLVLISRSLEKLNVVAKEIGDKYGVEVRVIDVDFTGGDEIY
DKIREKTTGLNVGVLVNNVGISYGHPEYFLDCYKADPPFLRNIVAANIHSVTHMTALFLP
GMISQRRGVIINVSSTAGVIPNPLLSVYSSTKAFVNKFSDDLQTEYKEHGILIQSVQPGFVA
TNMSKIRKASVFAPSPETYVRSALSTLGIATQTAGYLPHALLQLVIHFTEAVFGEQFARNI
VMKNILGTRKRALRRLAKEQ

>DmCG13284
MQPVLEVSIYTLLKMAFIWQLISAAIYLVGLLTIGVFLYDNLKSLVSIIKAVLEPYFQPHLP
RTLVDKFGQWAVVTGATDGIGKEYARELARQGINLVLISRTKEKLIAVTNEIESQYKVKT
KWIAADFAKGREVYDQIEKELAGIDVGILVNNVGMMYEHPESLDLVSEDLLWNLLTVN
MGSVTMLTRKILPQMIGRRKGAIVNLGSSSELQPLPNMTVYAASKKFVTYFSKALELEV
AEHNIHVQLVMPNFVVTKMNAYTDRVMQGGLFFPNAYTFARSAVFTLGKTSETNGFWT
HGIQYAIMKLAPLPIRTYLGHQLFKRLRIEALEQKQKKLKLT

>DmCG31809
MGLIYIVGSLSIAAFLYENLKSLFSIIKSVVEPFFRPNLPKTLAEKFGNWAVVTGATDGIGK
EYARELARQGLNLVLVSRKEEKLIAVTNEIGSQYNVKIKWIVADFAKGREVYAHIEKELN
GIEVGILVNNVGTIHDPESLDKVSEDMLWDLLTVNVGSVTMLTRKILPQMISRRKGAIVN
LGSSSELQPHPNLTAYAATKKFVTHFTKGLEYEVAEHNIHVQLVMPAFVATNMNSYSDK
VRQGGLLFPNAYSYARSAVFTLGKTSETNGFWVHGLQYALMKLFPMEIRTYFVYQLFK
RMRIEAMEHRLKNQKLS

>DmCG31810
MALILQVISTGIYIVGSLSIVAYLYENLKSLFSIIKSVVEPFFRPNLPKTLAEKFGNWAVVT
GATDGIGKEYARELARQGLNLVLVSRKEEKLIAVTNEIGSQYNVKIKWIVADFAKGREV
YAHIEKELNGIEVGILVNNVGTIHDPESLDKVSEDMLWDLLTVNVGSVTMLTRKILPQMI
SRRKGAIVNLGSSSELQPHPNLTAYAATKKFVTHFTKGLEYEVAEHNIHVQLVMPAFVA
TNMNSYSDKVRQGGLLFPNAYSYARSAVFTLGKTSETNGFWVHGLQYAFMKLAPMDIR
TYFGYQLFKRMRIEAMEHRLKNQKLS

>DmCG6012
MFCALSAFLTFVGVYALSSYLYEQLRTPYKLIKIRYFSGTRPTLKERFGDWAAVTGASDG
IGKEYAKELARQNINVVLIARTEEKLQAVAKEIADCGAGVQTKIVIADFTKGSQVYEHIE
KETANIPISILVNNVGIATPKSLLKYNQEETQNIIDTNVVAVSQLSRIFFQRMKASKLKGAI
VNVGSGTELQPLPNGAYYAASKAYTRSLTLALYHEAKPYGIHVQMLSPNFVVTKINSYS
RQIMKGGLLIPSASAYAKSAVNQLRDEVDETPGYLWHHVQNAVATAFTWRVRTYVAC
KLFNKISDNI

>ScPhs1p-dehydratase
MSKKLASPLSFLPLYNLLSAVGWSYLLYLVISLYPKVGQPAFFYQTKNVATLVQCGAIIEI
INSFLGVVRSPLLTTVAQVSSRLLVVLGIFQLLPNTSGVQSVVYISLLLAWSITEIVRYLYY
FFMLVFKNGAPKILILLRYNLFWILYPTGVASELRIIYCALNAAESQYSLLYKRILIAAMLA
YIPGFPMLFLHMVAQRKKVMKSLRSSFGKKLI

>Mm 3-HADC2
MAAAAATAATKGNGGGSGRVGAGDSSGARKKKGPGPVATAYLVIYNVVMTAGWLVI
AVGLVRAYLAKGSYHSLYYSIERPLKFFQTGALLEILHCAIGIVPSSVVLTSFQVMSRVFLI
WAVTHSVKEVQSEDSVLLFVIAWTITEIIRYSFYTFSLLNHLPYIIKWARYTLFIVLYPMG
VTGELLTIYAALPFVRQAGLYSISLPNKYNFSFDYHAFLILIMISYIPLFPQLYFHMIHQRR
KVLSHTEEHKKFE

>Hs 3-HADC2
MAAVAATAAAKGNGGGGGRAGAGDASGTRKKKGPGPLATAYLVIYNVVMTAGWLVI
AVGLVRAYLAKGSYHSLYYSIEKPLKFFQTGALLEILHCAIGIVPSSVVLTSFQVMSRVFLI
WAVTHSVKEVQSEDSVLLFVIAWTITEIIRYSFYTFSLLNHLPYLIKWARYTLFIVLYPMG
VSGELLTIYAALPFVRQAGLYSISLPNKYNFSFDYYAFLILIMISYIPIFPQLYFHMIHQRRK
ILSHTEEHKKFE

>DmCG6746
MSAKAVSKSSKPGASKEPSAVTKLYLFAYNAGQVVGWSYILWQLVNYYILQGPEFRAQ
VTLWEYTRLAVIIFQNAAFVEILNASFGLVKSNPVVTGFQVFSRMMVVVGVVMATPTGK
VSPGLPIALLAWAITEIIRYGYYALNIVKVVPHFVVFLRYTTFIVLYPIGVTGELLCFWWA
QSYARENSVWSVVMPNKWNATFSYFGFLWIVMLGYIPIFPQLYLHMFAQRRKILGGGSS
GSPQKKAN

>DmCG9267
MANLSPFVYWSQTKQTLLLKVDLKDAKGAIADFSPVSVNFSANGHGARGVNAYKFELH
FYALIDDENATFVVSDNKIELQIRKLEPEWWPRLVATPQKPHWLKIDFDRWRTEDDVEV
EEKPRDVRQDYEKEYADLQKRELGYIKEKTKKVYMIFYNLAMFVGYLYIMVVMGVLY
YRDGVDSIGKTYANVGNAFKFIQLLQYLEVMHPMFGYTKGSPVVPFFQVSGRNFILFLMI
DMEPRMYAKPVVFYVFIIWSLVELVRYPYYLAQLLGREVGLLTWLRYTIWIPLYPMGIL
CEGIIVLRNIPYIEETKRFTVEMPNPWNITFDMVLFLKIYLMLLIIPGSYLVMSHMAKLRSK

KLGKGRAKRQQHLHAD

>HsFASN
MEEVVIAGMSGKLPESENLQEFWDNLIGGVDMVTDDDRRWKAGLYGLPRRSGKLKDLS
RFDASFFGVHPKQAHTMDPQLRLLLEVTYEAIVDGGINPDSLRGTHTGVWVGVSGSETS
EALSRDPETLVGYSMVGCQRAMMANRLSFFFDFRGPSIALDTACSSSLMALQNAYQAIH
SGQCPAAIVGGINVLLKPNTSVQFLRLGMLSPEGTCKAFDTAGNGYCRSEGVVAVLLTK
KSLARRVYATILNAGTNTDGFKEQGVTFPSGDIQEQLIRSLYQSAGVAPESFEYIEAHGTG
TKVGDPQELNGITRALCATRQEPLLIGSTKSNMGHPEPASGLAALAKVLLSLEHGLWAP
NLHFHSPNPEIPALLDGRLQVVDQPLPVRGGNVGINSFGFGGSNVHIILRPNTQPPPAPAP
HATLPRLLRASGRTPEAVQKLLEQGLRHSQDLAFLSMLNDIAAVPATAMPFRGYAVLGG
ERGGPEVQQVPAGERPLWFICSGMGTQWRGMGLSLMRLDRFRDSILRSDEAVKPFGLK
VSQLLLSTDESTFDDIVHSFVSLTAIQIGLIDLLSCMGLRPDGIVGHSLGEVACGYADGCL
SQEEAVLAAYWRGQCIKEAHLPPGAMAAVGLSWEECKQRCPPGVVPACHNSKDTVTIS
GPQAPVFEFVEQLRKEGVFAKEVRTGGMAFHSYFMEAIAPPLLQELKKVIREPKPRSAR
WLSTSIPEAQWHSSLARTSSAEYNVNNLVSPVLFQEALWHVPEHAVVLEIAPHALLQAV
LKRGLKPSCTIIPLMKKDHRDNLEFFLAGIGRLHLSGIDANPNALFPPVEFPAPRGTPLISPL
IKWDHSLAWDVPAAEDFPNGSGSPSAAIYNIDTSSESPDHYLVDHTLDGRVLFPATGYLS
IVWKTLARALGLGVEQLPVVFEDVVLHQATILPKTGTVSLEVRLLEASRAFEVSENGNLV
VSGKVYQWDDPDPRLFDHPESPTPNPTEPLFLAQAEVYKELRLRGYDYGPHFQGILEASL
EGDSGRLLWKDNWVSFMDTMLQMSILGSAKHGLYLPTRVTAIHIDPATHRQKLYTLQD
KAQVADVVVSRWLRVTVAGGVHISGLHTESAPRRQQEQQVPILEKFCFTPHTEEGCLSE
RAALQEELQLCKGLVQALQTKVTQQGLKMVVPGLDGAQIPRDPSQQELPRLLSAACRL
QLNGNLQLELAQVLAQERPKLPEDPLLSGLLDSPALKACLDTAVENMPSLKMKVVEVL
AGHGHLYSRIPGLLSPHPLLQLSYTATDRHPQALEAAQAELQQHDVAQGQWDPADPAPS
ALGSADLLVCNCAVAALGDPASALSNMVAALREGGFLLLHTLLRGHPLGDIVAFLTSTE
PQYGQGILSQDAWESLFSRVSLRLVGLKKSFYGSTLFLCRRPTPQDSPIFLPVDDTSFRWV
ESLKGILADEDSSRPVWLKAINCATSGVVGLVNCLRREPGGNRLRCVLLSNLSSTSHVPE
VDPGSAELQKVLQGDLVMNVYRDGAWGAFRHFLLEEDKPEEPTAHAFVSTLTRGDLSSI
RWVCSSLRHAQPTCPGAQLCTVYYASLNFRDIMLATGKLSPDAIPGKWTSQDSLLGMEF
SGRDASGKRVMGLVPAKGLATSVLLSPDFLWDVPSNWTLEEAASVPVVYSTAYYALVV
RGRVRPGETLLIHSGSGGVGQAAIAIALSLGCRVFTTVGSAEKRAYLQARFPQLDSTSFA
NSRDTSFEQHVLWHTGGKGVDLVLNSLAEEKLQASVRCLATHGRFLEIGKFDLSQNHPL
GMAIFLKNVTFHGVLLDAFFNESSADWREVWALVQAGIRDGVVRPLKCTVFHGAQVED
AFRYMAQGKHIGKVVVQVLAEEPEAVLKGAKPKLMSAISKTFCPAHKSYIIAGGLGGFG
LELAQWLIQRGVQKLVLTSRSGIRTGYQAKQVRRWRRQGVQVQVSTSNISSLEGARGLI
AEAAQLGPVGGVFNLAVVLRDGLLENQTPEFFQDVCKPKYSGTLNLDRVTREACPELDY
FVVFSSVSCGRGNAGQSNYGFANSAMERICEKRRHEGLPGLAVQWGAIGDVGILVETMS
TNDTIVSGTLPQRMASCLEVLDLFLNQPHMVLSSFVLAEKAAAYRDRDSQRDLVEAVAH
ILGIRDLAAVNLDSSLADLGLDSLMSVEVRQTLERELNLVLSVREVRQLTLRKLQELSSK
ADEASELACPTPKEDGLAQQQTQLNLRSLLVNPEGPTLMRLNSVQSSERPLFLVHPIEGST
TVFHSLASRLSIPTYGLQCTRAAPLDSIHSLAAYYIDCIRQVQPEGPYRVAGYSYGACVAF
EMCSQLQAQQSPAPTHNSLFLFDGSPTYVLAYTQSYRAKLTPGCEAEAETEAICFFVQQF
TDMEHNRVLEALLPLKGLEERVAAAVDLIIKSHQGLDRQELSFAARSFYYKLRAAEQYT
PKAKYHGNVMLLRAKTGGAYGEDLGADYNLSQVCDGKVSVHVIEGDHRTLLEGSGLES
IISIIHSSLAEPRVSVREG

>MmFASN
MEEVVIAGMSGKLPESENLQEFWANLIGGVDMVTDDDRRWKAGLYGLPKRSGKLKDL
SKFDASFFGVHPKQAHTMDPQLRLLLEVSYEAIVDGGINPASLRGTNTGVWVGVSGSEA
SEALSRDPETLLGYSMVGCQRAMMANRLSFFFDFKGPSIALDTACSSSLLALQNAYQAIR

SGECPAALVGGINLLLKPNTSVQFMKLGMLSPDGTCRSFDDSGSGYCRSEAVVAVLLTK
KSLARRVYATILNAGTNTDGSKEQGVTFPSGEVQEQLICSLYQPAGLAPESLEYIEAHGT
GTKVGDPQELNGITRSLCAFRQAPLLIGSTKSNMGHPEPASGLAALTKVLLSLEHGVWAP
NLHFHNPNPEIPALLDGRLQVVDRPLPVRGGNVGINSFGFGGSNVHVILQPNTQAPAPTA
HAALPHLLHASGRTLEAVQDLLEQGRQHSQDLAFVSMLNDIAATPTAAMPFRGYTVLG
VEGRVQEVQQVSTNKRPLWFICSGMGTQWRGMGLSLMRLDSFRESILRSDEAVKPLGV
KVSDLLLSTDERTFDDIVHAFVSLTAIQIALIDLLTSVGLKPDGIIGHSLGEVACGYADGCL
SQREAVLAAYWRGQCIKDAHLPPGSMAAVGLSWEECKQRCPAGVVPACHNSEDTVTIS
GPQAAVNEFVEQLKQEGVFAKEVRTGGLAFHSYFMEGIAPTLLQALKKVIREPRPRSAR
WLSTSIPEAQWQSSLARTSSAEYNVNNLVSPVLFQEALWHIPEHAVVLEIAPHALLQAVL
KRGVKSSCTIIPLMKRDHKDNLEFFLTNLGKVHLTGINVNPNALFPPVEFPAPRGTPLISPH
IKWDHSQTWDVPVAEDFPNGSSSSSATVYSIDASPESPDHYLVDHCIDGRVIFPGTGYLCL
VWKTLARSLGLSLEETPVVFENVSFHQATILPKTGTVALEVRLLEASHAFEVSDTGNLIVS
GKVYLWEDPNSKLFDHPEVPTPPESASVSRLTQGEVYKELRLRGYDYGPQFQGICEATLE
GEQGKLLWKDNWVTFMDTMLQVSILGSSQQSLQLPTRVTAIYIDPATHRQKVYRLKEDT
QVADVTTSRCLGITVSGGIHISRLQTTATSRRQQEQLVPTLEKFVFTPHMEAECLSESTAL
QKELQLCKGLARALQTKATQQGLKAAMLGQEDPPQHGLPRLLAAACQLQLNGNLQLEL
GEALAQERLLLPEDPLISGLLNSQALKACVDTALENLSTLKMKVAEVLAGEGHLYSRIPA
LLNTQPMLQLEYTATDRHPQALKDVQTKLQQHDVAQGQWNPSDPAPSSLGALDLLVCN
CALATLGDPALALDNMVAALKEGGFLLVHTVLKGHALGETLACLPSEVQPAPSLLSQEE
WESLFSRKALHLVGLKRSFYGTALFLCRRAIPQEKPIFLSVEDTSFQWVDSLKSTLATSSS
QPVWLTAMDCPTSGVVGLVNCLRKEPGGHRIRCILLSNLSNTSHAPKLDPGSPELQQVLK
HDLVMNVYRDGAWGAFRHFQLEQDKPKEQTAHAFVNVLTRGDLASIRWVSSPLKHTQ
PSSSGAQLCTVYYASLNFRDIMLATGKLSPDAIPGKWASRDCMLGMEFSGRDRCGRRV
MGLVPAEGLATSVLLSSDFLWDVPSSWTLEEAASVPVVYTTAYYSLVVRGRIQRGETVL
IHSGSGGVGQAAISIALSLGCRVFTTVGSAEKRAYLQARFPQLDDTSFANSRDTSFEQHVL
LHTGGKGVDLVLNSLAEEKLQASVRCLAQHGRFLEIGKFDLSNNHPLGMAIFLKNVTFH
GILLDALFEEANDSWREVAALLKAGIRDGVVKPLKCTVFPKAQVEDAFRYMAQGKHIG
KVLVQVREEEPEAVLPGAQPTLISAISKTFCPAHKSYIITGGLGGFGLELARWLVLRGAQR
LVLTSRSGIRTGYQAKHIREWRRQGIQVLVSTSNVSSLEGARALIAEATKLGPVGGVFNL
AMVLRDAMLENQTPELFQDVNKPKYNGTLNLDRATREACPELDYFVAFSSVSCGRGNA
GQTNYGFANSTMERICEQRRHDGLPGLAVQWGAIGDVGIVLEAMGTNDTVIGGTLPQRI
SSCMEVLDLFLNQPHAVLSSFVLAEKKAVAHGDGDTQRDLVKAVAHILGIRDLAGINLD
STLADLGLDSLMGVEVRQILEREHDLVLPMREVRQLTLRKLQEMSSKTDSATDTTAPKS
RSDTSLKQNQLNLSTLLVNPEGPTLTQLNSVQSSERPLFLVHPIEGSTTVFHSLAAKLSVP
TYGLQCTQAAPLDSIPNLAAYYIDCIKQVQPEGPYRIAGYSFGACVAFEMCSQLQAQQGP
APTHNNLFLFDGSHTYVLAYTQSYRAKMTPGCEAEAEAEALCFFIKQFLDVEHSKVLEA
LLPLKSLEDRVAASVDLITKSHHSLDRRELSFAAVSFYHKRAADQYKPKAKYHGNVTLL
RAKTGGTYGEDLGADYNLSQVCDGKVSVHIIEGDHRTLLEGSGLESIINIIHSSLAEPRVS
VREG

>DmCG3523
MPARFAEEVITAEPAQRAAPQLDLGGGHYVPRQQHLNDEIAITGFSGRLPESSTIEEFKQN
LFDGVDMVNDDPRRWERGLYGLPDRIGKLKDSDLENFDQQFFGVHQKQAECMDPLLR
MLLELTHEAIIDAGLNPSDLRGSRTGVYIGVSNSETEQHWCSDADRVNGYGLTGCARAM
FANRISFTFDFKGPSYSIDTACSSSLYALEQAFSDMREGKVDNALVAGAGLILKPTMSLQF
KRLNMLSPDGSCKAFDESGNGYVRSDGCVVLLLQRTSAARRVYASILNVRTNTDGFKEQ
GITYPIGKMQNRLIRETYEEIGLNPADVVYVEAHGTGTKVGDPQEVNSITDFFCKDRTTPL
LIGSVKSNMGHSEPASGVCSVAKILIAMEEGVIPGNLHYNKPNPDLYGLVDGRLKVVDR
NLPWNGGIIGLNSFGFGGANAHVILKSNPKPKALTPKDGALKVVLASGRTFEAVEQLLES
ASTNADDDEYLQLINEIHSKAIPNHFFRGYGVVSSKGTHQREVIESNDDKRPIWYIYSGM

GSQWASMAKDLMKIEAFAKTIQRCADVLKPEGVDLIDVLTRSTDKSFENILNSFISIAAM
QVALTDLLSSLGIHPDGIVGHSVGELGCAYADGCFTPEQTVLAAYWRGKSILDTQLAKG
KMAAVGLSWEDAHSRVPSDCFPVCHNSEDNCTISGPEASIEALVAKLNAEGVFAKAVNS
SGYAFHSKYIAEAGPKLRKSLEKIIPNAKNRTARWISTSIPESAWNTPVAKQSSAAYHVN
NLLSPVLFHEALQHVPKNAISVEIAPHGLLQAILKRALGPDATNLSLVKRGHENNVEFFLT
NVGKLFAAGAQPQVLTLVRPISYPVGRGTPMLNSKVGWDHTQKWLVAKFGKETSSGET
IVEVDLSKEDDAFLAGHTIDGRILFPATGYMTLAWQTFAKMQGSEFHKTPVVMENLVFH
RATILNKNAVVKFGINFFDGTGAFEICESGSLAVSGKITIPESIDNEELPLEEQTPSAVAKEL
GTNDVYKELRLRGYDYGGIFRGIVRSDTVASTGKLQWVDNWISFMDTMLQFSILSKNLR
ELYLPTRIERAVINPAKHFELLSALTKEEQVETGLPVQWYSDINVIKSAGVELRGLKANL
AQRRPGTQAPPTLERYQFVPNINTTDLNENSEKARLHALDVAIQVIIENSSGAVKLKGVE
LANGRNPDVLVANRLLQIIEGEPVLTGDVAVVTSNNNEETITAALGDSGVRVVSKDVLK
EPVEQNCHFVFGIDVLSRPDTKTLENSIASIRENGFLILEETLPTYTKTGRALLTKFGFVAV
QEQSLGATRVLVLARKAVDLKTRKSVVVVATEQNFNWVDDLKAALATAATEEQYVYV
VCQGEELFGAVGLMTCIKNENGGKLARLVFVQDAKAEKFSLTSTLYRQQLEKDLISNVL
KNGAWGTFRHLKLETQQATLQVEHAYVNALVKGDLASLKWIEAAQADTAATVDKNLE
TCTVYYAPINFRDVMLTSGKLAADALPGDLAEQDCVLGLEFAGRDTQGRRVMAMVPA
KSLATTCVASKRMMWQIPEKWTMEEASTVPCVYSTVYYALVVRGQMKKGEKILIHAGS
GGVGQAAISVALAHGLTVFTTVGSKEKREFLLKRFPKLQERNIGNSRDTSFEQLVLRETK
GRGVDLVLNSLSEEKLQASIRCLGLNGRFLEIGKFDLSNNSPLGMSVFLKNTSFHGILLDS
VMEGEEEMQNQVVSLVAEGIKTGAVVPLPTSVFNDQQVEQAFRFMASGKHIGKVVIKV
RDEEAGKKALQPKPRLINAIPRTYMHPEKSYILVGGLGGFGLELTNWLVTRGARYIVLTS
RSGVKTGYQGLMIRRWQERGVKVVIDTSDVTTAAGAKKLLENSNKLALVGGIFNLAAV
LRDALIEDQTAKDFKTVADPKVTATKYLDQFSRDICTELDYFICFSSVSCGRGNIGQTNY
GLANSAMERICEQRQVSGFPGTAIQWGAIGDTGLVLENLGDNDTVIGGTLPQRMPSCLQ
TIDLFLQQPHPVVASMVVAEKRKSDQSAGVSLIATIANILGLRDTKNIQDGASLADLGMD
SLMSAEIKQTLERNFDIVLSAQEIRQLTFGALKAMDGGADVKPAAAAPAAAAGVPEANI
TSGGSSRTASPMGDGTQVVFTTSLIPTEAIVQLDTKAPANSKQSPIFFISPIEGFASALEPLA
KRLEVPAYGLQYTEAVPSDSLESAAKFFIKQLRTVQPKGPYKLAGYSFGCLLTYVMAGIL
EETNEVANVIMLDGAPSYVNWYTSSFKQRYTDGTNADNDNQSYGLAYFGIVLANIDYK
ALVRLLIVIPTWEEKLERFAELMSNEITQPVETIKKSATLFYKKLELADGYQPTLKLKTNV
TLVKPTDNSAKLDEDYRLK EVCTKPVEVHTVEGNHRTFLIEDQSLKTIQSILKRLFN

Table C.1: Primers used for *sits* miRNA synthesis and *sits* excision mapping.

Primer name	*Primer sequence*	*WPI primer No.*
5' sits 3 'UTR	CTA GCA GTC CAG CGG ATT GTA TAA TAC AAT AGT TAT ATT CAA GCA TAT TGT ATT ATA CAA TCC GCT GGG CG	W347
3' sits 3'UTR	AATTCGCCCAGCGGATTGTATAATACAATATGCTTGAATATAACTATTGTATTATACAATCCG CTGGACTG	W348'
5' sits ORF	CTA GCA GTC ACA TAG TGA CTC GAG GAC AAT AGT TAT ATT CAA GCA TAT TGT CCT CGA GTC ACT ATG TGG CG	W345
3' sits ORF	AATTCGCCACATAGTGACTCGAGGACAATATGCTTGAATATAACTATTGTCCTCGAGTCACT ATGTGACTG	W346'
5' sits 5'UTR	CTA GCA GTC AGC AAG GAA CAC GAA CTA CAT AGT TAT ATT CAA GCA TAT GTA GTT CGT GTT CCT TGC TGG CG	W349
3' sits 5'UTR	AATTCGCCAGCAAGGAACACGAACTACATATGCTTGAATATAACTATGTAGTTCGTGTTCCTT GCTGACTG	W350'
5' sits excision	GAATTTTCCTATTTTCCACCTCCAACAAG	W180
3' sits excision	GAC ATA ATG CCG TCA CCT ACA CAC GTA C	W181

APPENDIX D

This section contains the information about the movies listed in Chapter 4. The crosses to generate the flies were carried out at 26°C unless mentioned otherwise.

Movie 4.1: Neuronal knockdown of *sits* exhibits locomotion defects in adult flies. A) C155>mCD8::GFP (control) and B) C155>*sits*^{GD} (mutant) flies. *sits* mutants do not fly away like their control counterparts on being released in open and exhibit lack of coordination and immobility. It can be seen that the mutant flies are alive as they seem to have some degree of limb movements.

Movie 4.2: Vortexing assay for assessing *sits* mutants. A) C155>mCD8::GFP (control) and B) C155>*sits*^{GD} (mutant) are vortexed for ten seconds and observed for fifteen seconds. The flies that could climb up the wall are considered as movers. The cross was carried out at 27.5°C.

Movie 4.3: Flip over Assay for assessing *sits* mutants. A) Sli^{2X}>mCD8::GFP (control) and B) Sli^{2X}>*sits*^{GD} (mutant) are flipped over and the movement is assessed based on ability of fly to move in a particular direction. The cross was carried out at 27.5°C.

Movie 4.4: Ctrax annotated movie with fly tracks. Annotated one minute clips of A) C155>mCD8::GFP (control) and B) C155>*sits*^{GD} (mutant) allowed to move freely in the chamber. The tracks are displayed in different colors and are erased continuously as the fly moves forward.

Movie 4.5: Ctrax annotated movie with fly tracks for 30Y. Annotated one minute clips of A) 30Y>mCD8::GFP (control) and B) 30Y>*sits*^{GD} (mutant) allowed to move freely in the chamber. The tracks are displayed in different colors and are erased continuously as the fly moves forward.

Movie 4.6: *sits* mutants exhibit twitching. Twitching can be seen in the front leg of the fly in middle.
The fly on the LHS of the screen also exhibits abnormal shaking of the wings.

Movie 4.7: Absence of *sits* in the brain leads to circling behavior in some flies. A) A short clip of 30Y>*sits*$^{5'UTR}$ female going in circles in one direction. B) Annotated video of 30Y>*sits*$^{5'UTR}$ flies in the chamber. A fly with green trajectory can be seen going in circles in clockwise direction, whereas the other fly with the magenta trajectory starts moving in the counter clockwise direction.

Movie 4.8: *sits* mutant flies exhibit poor balance. The video depicts *sits* mutants (30Y>*sits*$^{5'UTR}$) in the chamber. Two flies seem to have trouble maintaining the upright posture and getting back on their feet.

Movie 4.9: *sits* mutants have uncoordinated erratic movements. Mutant (30Y>*sits*^{GD}) flies in the chamber. A fly on the LHS of the chamber displays erratic, uncontrolled movement.

Movie 4.10: *sits* mutants exhibit grooming. A video clip showing *sits* mutant (30Y>*sits*^{GD}) grooming its wings with its back legs.

Movie 4.11: Hopping: *sits* mutants hop when provided with a stimuli. The clip shows that the mutants (C155>*sits*^{GD}) hop when poked with a paint brush.

Movie 4.12: Temporal dependence of *sits* affect on locomotion. A) 0-2 hrs post eclosion control (30Y>w^{1118}) and mutant (30Y>w^{1118}) males. B) 24 hrs post eclosion control (30Y>w^{1118}) and mutant (30Y>w^{1118}) males.

Movie 4.13: No overt locomotion defects are observed for neuronal knockdown of *sits* in the larvae. A short clip depicting the control (w^{1118}, green abdomen and the mutant (C155>$sits^{GD}$, red abdomen) larvae moving one behind the other. The *sits* mutant larvae seem to have similar movement as the control larvae.

REFERENCES

Akalal, D.B., Yu, D., and Davis, R.L. (2010). A late-phase, long-term memory trace forms in the gamma neurons of Drosophila mushroom bodies after olfactory classical conditioning. The Journal of neuroscience : the official journal of the Society for Neuroscience *30*, 16699-16708.

Aldahmesh, M.A., Mohamed, J.Y., Alkuraya, H.S., Verma, I.C., Puri, R.D., Alaiya, A.A., Rizzo, W.B., and Alkuraya, F.S. (2011). Recessive mutations in ELOVL4 cause ichthyosis, intellectual disability, and spastic quadriplegia. American journal of human genetics *89*, 745-750.

Apostolopoulou, A.A., Widmann, A., Rohwedder, A., Pfitzenmaier, J.E., and Thum, A.S. (2013). Appetitive associative olfactory learning in Drosophila larvae. Journal of visualized experiments : JoVE.

Ayyagari, R., Zhang, K., Hutchinson, A., Yu, Z., Swaroop, A., Kakuk, L.E., Seddon, J.M., Bernstein, P.S., Lewis, R.A., Tammur, J.*, et al.* (2001). Evaluation of the ELOVL4 gene in patients with age-related macular degeneration. Ophthalmic genetics *22*, 233-239.

Beaudoin, F., Gable, K., Sayanova, O., Dunn, T., and Napier, J.A. (2002). A Saccharomyces cerevisiae gene required for heterologous fatty acid elongase activity encodes a microsomal beta-keto-reductase. The Journal of biological chemistry *277*, 11481-11488.

Beaudoin, F., Michaelson, L.V., Hey, S.J., Lewis, M.J., Shewry, P.R., Sayanova, O., and Napier, J.A. (2000a). Heterologous reconstitution in yeast of the polyunsaturated fatty acid biosynthetic pathway. Proceedings of the National Academy of Sciences of the United States of America *97*, 6421-6426.

Beaudoin, F., Michaelson, L.V., Lewis, M.J., Shewry, P.R., Sayanova, O., and Napier, J.A. (2000b). Production of C20 polyunsaturated fatty acids (PUFAs) by pathway engineering: identification of a PUFA elongase component from Caenorhabditis elegans. Biochemical Society transactions *28*, 661-663.

Beaver, L.M., Klichko, V.I., Chow, E.S., Kotwica-Rolinska, J., Williamson, M., Orr, W.C., Radyuk, S.N., and Giebultowicz, J.M. (2012). Circadian regulation of glutathione levels and biosynthesis in Drosophila melanogaster. PloS one *7*, e50454.

Berns, K., Hijmans, E.M., Mullenders, J., Brummelkamp, T.R., Velds, A., Heimerikx, M., Kerkhoven, R.M., Madiredjo, M., Nijkamp, W., Weigelt, B.*, et al.* (2004). A large-scale RNAi screen in human cells identifies new components of the p53 pathway. Nature *428*, 431-437.

Birmingham, A., Anderson, E., Sullivan, K., Reynolds, A., Boese, Q., Leake, D., Karpilow, J., and Khvorova, A. (2007). A protocol for designing siRNAs with high functionality and specificity. Nature protocols *2*, 2068-2078.

Blacklock, B.J., and Jaworski, J.G. (2006). Substrate specificity of Arabidopsis 3-ketoacyl-CoA synthases. Biochemical and biophysical research communications *346*, 583-590.

Booth, G.E., Kinrade, E.F., and Hidalgo, A. (2000). Glia maintain follower neuron survival during Drosophila CNS development. Development *127*, 237-244.

Branson, K., Robie, A.A., Bender, J., Perona, P., and Dickinson, M.H. (2009). High-throughput ethomics in large groups of Drosophila. Nature methods *6*, 451-457.

Cameron, D.J., Tong, Z., Yang, Z., Kaminoh, J., Kamiyah, S., Chen, H., Zeng, J., Chen, Y., Luo, L., and Zhang, K. (2007). Essential role of Elovl4 in very long chain fatty acid synthesis, skin permeability barrier function, and neonatal survival. International journal of biological sciences *3*, 111-119.

Castel, S.E., and Martienssen, R.A. (2013). RNA interference in the nucleus: roles for small RNAs in transcription, epigenetics and beyond. Nature reviews Genetics *14*, 100-112.

Certel, S.J., Leung, A., Lin, C.Y., Perez, P., Chiang, A.S., and Kravitz, E.A. (2010). Octopamine neuromodulatory effects on a social behavior decision-making network in Drosophila males. PloS one *5*, e13248.

Chakravarty, B., Gu, Z., Chirala, S.S., Wakil, S.J., and Quiocho, F.A. (2004). Human fatty acid synthase: structure and substrate selectivity of the thioesterase domain. Proceedings of the National Academy of Sciences of the United States of America *101*, 15567-15572.

Chertemps, T., Duportets, L., Labeur, C., Ueda, R., Takahashi, K., Saigo, K., and Wicker-Thomas, C. (2007). A female-biased expressed elongase involved in long-chain hydrocarbon biosynthesis and courtship behavior in Drosophila melanogaster. Proceedings of the National Academy of Sciences of the United States of America *104*, 4273-4278.

Chertemps, T., Duportets, L., Labeur, C., and Wicker-Thomas, C. (2005). A new elongase selectively expressed in Drosophila male reproductive system. Biochemical and biophysical research communications *333*, 1066-1072.

Chirala, S.S., Chang, H., Matzuk, M., Abu-Elheiga, L., Mao, J., Mahon, K., Finegold, M., and Wakil, S.J. (2003). Fatty acid synthesis is essential in embryonic development: fatty acid synthase null mutants and most of the heterozygotes die

in utero. Proceedings of the National Academy of Sciences of the United States of America *100*, 6358-6363.

Chyb, S., Raghu, P., and Hardie, R.C. (1999). Polyunsaturated fatty acids activate the Drosophila light-sensitive channels TRP and TRPL. Nature *397*, 255-259.

Cinti, D.L., Cook, L., Nagi, M.N., and Suneja, S.K. (1992). The fatty acid chain elongation system of mammalian endoplasmic reticulum. Progress in lipid research *31*, 1-51.

Clarke, P.G. (1990). Developmental cell death: morphological diversity and multiple mechanisms. Anatomy and embryology *181*, 195-213.

Cork, M.J., Danby, S.G., Vasilopoulos, Y., Hadgraft, J., Lane, M.E., Moustafa, M., Guy, R.H., Macgowan, A.L., Tazi-Ahnini, R., and Ward, S.J. (2009). Epidermal barrier dysfunction in atopic dermatitis. The Journal of investigative dermatology *129*, 1892-1908.

Costaglioli, P., Joubes, J., Garcia, C., Stef, M., Arveiler, B., Lessire, R., and Garbay, B. (2005). Profiling candidate genes involved in wax biosynthesis in Arabidopsis thaliana by microarray analysis. Biochimica et biophysica acta *1734*, 247-258.

David, D., Sundararabu, S., and Gerst, J.E. (1998). Involvement of long chain fatty acid elongation in the trafficking of secretory vesicles in yeast. The Journal of cell biology *143*, 1167-1182.

Denic, V., and Weissman, J.S. (2007). A molecular caliper mechanism for determining very long-chain fatty acid length. Cell *130*, 663-677.

Desplats, P.A., Denny, C.A., Kass, K.E., Gilmartin, T., Head, S.R., Sutcliffe, J.G., Seyfried, T.N., and Thomas, E.A. (2007). Glycolipid and ganglioside metabolism imbalances in Huntington's disease. Neurobiology of disease *27*, 265-277.

Dietzl, G., Chen, D., Schnorrer, F., Su, K.C., Barinova, Y., Fellner, M., Gasser, B., Kinsey, K., Oppel, S., Scheiblauer, S.*, et al.* (2007). A genome-wide transgenic RNAi library for conditional gene inactivation in Drosophila. Nature *448*, 151-156.

Dittrich, F., Zajonc, D., Huhne, K., Hoja, U., Ekici, A., Greiner, E., Klein, H., Hofmann, J., Bessoule, J.J., Sperling, P.*, et al.* (1998). Fatty acid elongation in yeast--biochemical characteristics of the enzyme system and isolation of elongation-defective mutants. European journal of biochemistry / FEBS *252*, 477-485.

Doestch, A.R (2004). Characterization of two targets of epidermal growth factor receptor activity, kekkon1 and baldspot. Doctoral dissertation. Indiana University.

Dourlen, P., Bertin, B., Chatelain, G., Robin, M., Napoletano, F., Roux, M.J., and Mollereau, B. (2012). Drosophila fatty acid transport protein regulates rhodopsin-1 metabolism and is required for photoreceptor neuron survival. PLoS genetics *8*, e1002833.

Dubnau, J., and Chiang, A.S. (2013). Systems memory consolidation in Drosophila. Current opinion in neurobiology *23*, 84-91.

Duffy, J.B., and Gergen, J.P. (1991). The Drosophila segmentation gene runt acts as a position-specific numerator element necessary for the uniform expression of the sex-determining gene Sex-lethal. Genes & development *5*, 2176-2187.

Featherstone, D.E., Yanoga, F., and Grosjean, Y. (2008). Accelerated bang recovery in Drosophila genderblind mutants. Communicative & integrative biology *1*, 14-17.

Fehling, E., and Mukherjee, K.D. (1991). Acyl-CoA elongase from a higher plant (Lunaria annua): metabolic intermediates of very-long-chain acyl-CoA products and substrate specificity. Biochimica et biophysica acta *1082*, 239-246.

Feingold, K.R. (2007). Thematic review series: skin lipids. The role of epidermal lipids in cutaneous permeability barrier homeostasis. Journal of lipid research *48*, 2531-2546.

Ferrer, I., Aubourg, P., and Pujol, A. (2010). General aspects and neuropathology of X-linked adrenoleukodystrophy. Brain Pathol *20*, 817-830.

Fortier, E., and Belote, J.M. (2000). Temperature-dependent gene silencing by an expressed inverted repeat in Drosophila. Genesis *26*, 240-244.

Friedman, B. (1971). Tay-Sachs and other lipid storage diseases. HSMHA health reports *86*, 769-774.

Fuchs, Y., and Steller, H. (2011). Programmed cell death in animal development and disease. Cell *147*, 742-758.

Gaffori, O., Le Moal, M., and Stinus, L. (1980). Locomotor hyperactivity and hypoexploration after lesion of the dopaminergic-A10 area in the ventral mesencephalic tegmentum (VMT) of rats. Behavioural brain research *1*, 313-329.
Galko, M.J., and Krasnow, M.A. (2004). Cellular and genetic analysis of wound healing in Drosophila larvae. PLoS biology *2*, E239.

Gangishetti, U., Veerkamp, J., Bezdan, D., Schwarz, H., Lohmann, I., and Moussian, B. (2012). The transcription factor Grainy head and the steroid hormone

ecdysone cooperate during differentiation of the skin of Drosophila melanogaster. Insect molecular biology *21*, 283-295.

Gargano, J.W., Martin, I., Bhandari, P., and Grotewiel, M.S. (2005). Rapid iterative negative geotaxis (RING): a new method for assessing age-related locomotor decline in Drosophila. Experimental gerontology *40*, 386-395.

Ghez, C., Hening, W., and Gordon, J. (1991). Organization of voluntary movement. Current opinion in neurobiology *1*, 664-671.

Gimeno, R.E. (2007). Fatty acid transport proteins. Curr Opin Lipidol *18*, 271-276.
Gottrand, F. (2008). Long-chain polyunsaturated fatty acids influence the immune system of infants. The Journal of nutrition *138*, 1807S-1812S.

Grasl-Kraupp, B., Ruttkay-Nedecky, B., Koudelka, H., Bukowska, K., Bursch, W., and Schulte-Hermann, R. (1995). In situ detection of fragmented DNA (TUNEL assay) fails to discriminate among apoptosis, necrosis, and autolytic cell death: a cautionary note. Hepatology *21*, 1465-1468.

Grayson, C., and Molday, R.S. (2005). Dominant negative mechanism underlies autosomal dominant Stargardt-like macular dystrophy linked to mutations in ELOVL4. The Journal of biological chemistry *280*, 32521-32530.

Gregory, M.K., Gibson, R.A., Cook-Johnson, R.J., Cleland, L.G., and James, M.J. (2011). Elongase reactions as control points in long-chain polyunsaturated fatty acid synthesis. PloS one *6*, e29662.

Griffiths-Jones, S. (2004). The microRNA Registry. Nucleic acids research *32*, D109-111.

Grishok, A., and Mello, C.C. (2002). RNAi (Nematodes: Caenorhabditis elegans). Advances in genetics *46*, 339-360.

Guignard, T.J., Jin, M., Pequignot, M.O., Li, S., Chassigneux, Y., Chekroud, K., Guillou, L., Richard, E., Hamel, C.P., and Brabet, P. (2010). FATP1 inhibits 11-cis retinol formation via interaction with the visual cycle retinoid isomerase RPE65 and lecithin:retinol acyltransferase. The Journal of biological chemistry *285*, 18759-18768.

Guillou, H., Zadravec, D., Martin, P.G., and Jacobsson, A. (2010). The key roles of elongases and desaturases in mammalian fatty acid metabolism: Insights from transgenic mice. Progress in lipid research *49*, 186-199.

Gul, S., Smith, A.D., Thompson, R.H., Wright, H.P., and Zilkha, K.J. (1970). Fatty acid composition of phospholipids from platelets and erythrocytes in multiple sclerosis. Journal of neurology, neurosurgery, and psychiatry *33*, 506-510.

Han, G., Gable, K., Kohlwein, S.D., Beaudoin, F., Napier, J.A., and Dunn, T.M. (2002). The Saccharomyces cerevisiae YBR159w gene encodes the 3-ketoreductase of the microsomal fatty acid elongase. The Journal of biological chemistry *277*, 35440-35449.

Hashimoto, K., Yoshizawa, A.C., Okuda, S., Kuma, K., Goto, S., and Kanehisa, M. (2008). The repertoire of desaturases and elongases reveals fatty acid variations in 56 eukaryotic genomes. Journal of lipid research *49*, 183-191.

Helfrich-Forster, C., Wulf, J., and de Belle, J.S. (2002). Mushroom body influence on locomotor activity and circadian rhythms in Drosophila melanogaster. Journal of neurogenetics *16*, 73-109.

Herrmann, T., Buchkremer, F., Gosch, I., Hall, A.M., Bernlohr, D.A., and Stremmel, W. (2001). Mouse fatty acid transport protein 4 (FATP4): characterization of the gene and functional assessment as a very long chain acyl-CoA synthetase. Gene *270*, 31-40.

Herrmann, T., van der Hoeven, F., Grone, H.J., Stewart, A.F., Langbein, L., Kaiser, I., Liebisch, G., Gosch, I., Buchkremer, F., Drobnik, W.*, et al.* (2003). Mice with targeted disruption of the fatty acid transport protein 4 (Fatp 4, Slc27a4) gene show features of lethal restrictive dermopathy. The Journal of cell biology *161*, 1105-1115.

Hidalgo, A., and Booth, G.E. (2000). Glia dictate pioneer axon trajectories in the Drosophila embryonic CNS. Development *127*, 393-402.

Hirsch, D., Stahl, A., and Lodish, H.F. (1998). A family of fatty acid transporters conserved from mycobacterium to man. Proceedings of the National Academy of Sciences of the United States of America *95*, 8625-8629.

Homyk, T. (1977). Behavioral Mutants of DROSOPHILA MELANOGASTER. II. Behavioral Analysis and Focus Mapping. Genetics *87*, 105-128.

Huang, C., Zheng, X., Zhao, H., Li, M., Wang, P., Xie, Z., Wang, L., and Zhong, Y. (2012). A permissive role of mushroom body alpha/beta core neurons in long-term memory consolidation in Drosophila. Current biology : CB *22*, 1981-1989.

Huang, X., Suyama, K., Buchanan, J., Zhu, A.J., and Scott, M.P. (2005). A Drosophila model of the Niemann-Pick type C lysosome storage disease: dnpc1a is required for molting and sterol homeostasis. Development *132*, 5115-5124.

Ikeda, M., Kanao, Y., Yamanaka, M., Sakuraba, H., Mizutani, Y., Igarashi, Y., and Kihara, A. (2008). Characterization of four mammalian 3-hydroxyacyl-CoA dehydratases involved in very long-chain fatty acid synthesis. FEBS letters *582*, 2435-2440.

Ilius, M., Wolf, R., and Heisenberg, M. (2007). The central complex of Drosophila melanogaster is involved in flight control: studies on mutants and mosaics of the gene ellipsoid body open. Journal of neurogenetics *21*, 321-338.

Jakobsson, A., Westerberg, R., and Jacobsson, A. (2006). Fatty acid elongases in mammals: their regulation and roles in metabolism. Progress in lipid research *45*, 237-249.

James, D.W., Jr., Lim, E., Keller, J., Plooy, I., Ralston, E., and Dooner, H.K. (1995). Directed tagging of the Arabidopsis FATTY ACID ELONGATION1 (FAE1) gene with the maize transposon activator. The Plant cell *7*, 309-319.

Jenett, A., Rubin, G.M., Ngo, T.T., Shepherd, D., Murphy, C., Dionne, H., Pfeiffer, B.D., Cavallaro, A., Hall, D., Jeter, J.*, et al.* (2012). A GAL4-driver line resource for Drosophila neurobiology. Cell reports *2*, 991-1001.

Jenks, M.A., Tuttle, H.A., Eigenbrode, S.D., and Feldmann, K.A. (1995). Leaf Epicuticular Waxes of the Eceriferum Mutants in Arabidopsis. Plant physiology *108*, 369-377.

Jenni, S., Leibundgut, M., Boehringer, D., Frick, C., Mikolasek, B., and Ban, N. (2007). Structure of fungal fatty acid synthase and implications for iterative substrate shuttling. Science *316*, 254-261.

Jordan, K.W., Craver, K.L., Magwire, M.M., Cubilla, C.E., Mackay, T.F., and Anholt, R.R. (2012). Genome-wide association for sensitivity to chronic oxidative stress in Drosophila melanogaster. PloS one *7*, e38722.

Jors, S., Kazanski, V., Foik, A., Krautwurst, D., and Harteneck, C. (2006). Receptor-induced activation of Drosophila TRP gamma by polyunsaturated fatty acids. The Journal of biological chemistry *281*, 29693-29702.

Joubes, J., Raffaele, S., Bourdenx, B., Garcia, C., Laroche-Traineau, J., Moreau, P., Domergue, F., and Lessire, R. (2008). The VLCFA elongase gene family in Arabidopsis thaliana: phylogenetic analysis, 3D modelling and expression profiling. Plant molecular biology *67*, 547-566.

Jump, D.B. (2009). Mammalian fatty acid elongases. Methods Mol Biol *579*, 375-389.

Jung, A., Hollmann, M., and Schafer, M.A. (2007). The fatty acid elongase NOA is necessary for viability and has a somatic role in Drosophila sperm development. Journal of cell science *120*, 2924-2934.

Kalish, B.T., Fallon, E.M., and Puder, M. (2012). A tutorial on fatty acid biology. JPEN Journal of parenteral and enteral nutrition *36*, 380-388.

Karan, G., Lillo, C., Yang, Z., Cameron, D.J., Locke, K.G., Zhao, Y., Thirumalaichary, S., Li, C., Birch, D.G., Vollmer-Snarr, H.R.*, et al.* (2005a). Lipofuscin accumulation, abnormal electrophysiology, and photoreceptor degeneration in mutant ELOVL4 transgenic mice: a model for macular degeneration. Proceedings of the National Academy of Sciences of the United States of America *102*, 4164-4169.

Karan, G., Yang, Z., Howes, K., Zhao, Y., Chen, Y., Cameron, D.J., Lin, Y., Pearson, E., and Zhang, K. (2005b). Loss of ER retention and sequestration of the wild-type ELOVL4 by Stargardt disease dominant negative mutants. Molecular vision *11*, 657-664.

Karan, G., Yang, Z., and Zhang, K. (2004). Expression of wild type and mutant ELOVL4 in cell culture: subcellular localization and cell viability. Molecular vision *10*, 248-253.

Keaney, J., Campbell, M., and Humphries, P. (2011). From RNA interference technology to effective therapy: how far have we come and how far to go? Therapeutic delivery *2*, 1395-1406.

Khan, M., Singh, J., Gilg, A.G., Uto, T., and Singh, I. (2010). Very long-chain fatty acid accumulation causes lipotoxic response via 5-lipoxygenase in cerebral adrenoleukodystrophy. Journal of lipid research *51*, 1685-1695.

Kihara, A., Sakuraba, H., Ikeda, M., Denpoh, A., and Igarashi, Y. (2008). Membrane topology and essential amino acid residues of Phs1, a 3-hydroxyacyl-CoA dehydratase involved in very long-chain fatty acid elongation. The Journal of biological chemistry *283*, 11199-11209.

Kim, J., Jung, J.H., Lee, S.B., Go, Y.S., Kim, H.J., Cahoon, R., Markham, J.E., Cahoon, E.B., and Suh, M.C. (2013). Arabidopsis 3-ketoacyl-coenzyme a synthase9 is involved in the synthesis of tetracosanoic acids as precursors of cuticular waxes, suberins, sphingolipids, and phospholipids. Plant physiology *162*, 567-580.

Klar, J., Schweiger, M., Zimmerman, R., Zechner, R., Li, H., Torma, H., Vahlquist, A., Bouadjar, B., Dahl, N., and Fischer, J. (2009). Mutations in the fatty acid transport protein 4 gene cause the ichthyosis prematurity syndrome. American journal of human genetics *85*, 248-253.

Kniazeva, M., Sieber, M., McCauley, S., Zhang, K., Watts, J.L., and Han, M. (2003). Suppression of the ELO-2 FA elongation activity results in alterations of the fatty acid composition and multiple physiological defects, including abnormal ultradian rhythms, in Caenorhabditis elegans. Genetics *163*, 159-169.

Kobayashi, T., Zadravec, D., and Jacobsson, A. (2007). ELOVL2 overexpression enhances triacylglycerol synthesis in 3T3-L1 and F442A cells. FEBS letters *581*, 3157-3163.

Kohlwein, S.D., Eder, S., Oh, C.S., Martin, C.E., Gable, K., Bacikova, D., and Dunn, T. (2001). Tsc13p is required for fatty acid elongation and localizes to a novel structure at the nuclear-vacuolar interface in Saccharomyces cerevisiae. Molecular and cellular biology *21*, 109-125.

Kopytova, T.V., Abalikhina, E.P., and Shchelchkova, N.A. (2007). [Significance of determination of lipids in biological substrates for evaluation of metabolic processes in psoriasis]. Klinicheskaia laboratornaia diagnostika, 20-23.

Le, H.D., Fallon, E.M., Kalish, B.T., de Meijer, V.E., Meisel, J.A., Gura, K.M., Nose, V., Pan, A.H., Bistrian, B.R., and Puder, M. (2012). The effect of varying ratios of docosahexaenoic acid and arachidonic acid in the prevention and reversal of biochemical essential fatty acid deficiency in a murine model. Metabolism: clinical and experimental.

Lee, C.Y., and Baehrecke, E.H. (2000). Genetic regulation of programmed cell death in Drosophila. Cell research *10*, 193-204.

Lee, P.T., Lin, H.W., Chang, Y.H., Fu, T.F., Dubnau, J., Hirsh, J., Lee, T., and Chiang, A.S. (2011). Serotonin-mushroom body circuit modulating the formation of anesthesia-resistant memory in Drosophila. Proceedings of the National Academy of Sciences of the United States of America *108*, 13794-13799.

Lee, S.H., Stephens, J.L., Paul, K.S., and Englund, P.T. (2006). Fatty acid synthesis by elongases in trypanosomes. Cell *126*, 691-699.

Leiserson, W.M., Harkins, E.W., and Keshishian, H. (2000). Fray, a Drosophila serine/threonine kinase homologous to mammalian PASK, is required for axonal ensheathment. Neuron *28*, 793-806.

LeMosy, E.K., and Hashimoto, C. (2000). The nudel protease of Drosophila is required for eggshell biogenesis in addition to embryonic patterning. Developmental biology *217*, 352-361.

Leonard, A.E., Bobik, E.G., Dorado, J., Kroeger, P.E., Chuang, L.T., Thurmond, J.M., Parker-Barnes, J.M., Das, T., Huang, Y.S., and Mukerji, P. (2000). Cloning of a human cDNA encoding a novel enzyme involved in the elongation of long-chain polyunsaturated fatty acids. The Biochemical journal *350 Pt 3*, 765-770.

Levine, R.B., Morton, D.B., and Restifo, L.L. (1995). Remodeling of the insect nervous system. Current opinion in neurobiology *5*, 28-35.

Li, F., Wu, X., Lam, P., Bird, D., Zheng, H., Samuels, L., Jetter, R., and Kunst, L. (2008). Identification of the wax ester synthase/acyl-coenzyme A: diacylglycerol acyltransferase WSD1 required for stem wax ester biosynthesis in Arabidopsis. Plant physiology *148*, 97-107.

Li, W., Sandhoff, R., Kono, M., Zerfas, P., Hoffmann, V., Ding, B.C., Proia, R.L., and Deng, C.X. (2007). Depletion of ceramides with very long chain fatty acids causes defective skin permeability barrier function, and neonatal lethality in ELOVL4 deficient mice. International journal of biological sciences *3*, 120-128.

Li, Y., Beisson, F., Pollard, M., and Ohlrogge, J. (2006a). Oil content of Arabidopsis seeds: the influence of seed anatomy, light and plant-to-plant variation. Phytochemistry *67*, 904-915.

Li, Y.C., Park, M.J., Ye, S.K., Kim, C.W., and Kim, Y.N. (2006b). Elevated levels of cholesterol-rich lipid rafts in cancer cells are correlated with apoptosis sensitivity induced by cholesterol-depleting agents. The American journal of pathology *168*, 1107-1118; quiz 1404-1105.

Locke, M. (2001). The Wigglesworth Lecture: Insects for studying fundamental problems in biology. Journal of insect physiology *47*, 495-507.

Lomakin, I.B., Xiong, Y., and Steitz, T.A. (2007). The crystal structure of yeast fatty acid synthase, a cellular machine with eight active sites working together. Cell *129*, 319-332.

Lopez, S., Bermudez, B., Abia, R., and Muriana, F.J. (2009). The influence of major dietary fatty acids on insulin secretion and action. Curr Opin Lipidol.

Lu, S., and Archer, M.C. (2005). Fatty acid synthase is a potential molecular target for the chemoprevention of breast cancer. Carcinogenesis *26*, 153-157.

Mandal, S and Duffy, J.B. (2009). Identification of the sit still gene – shaky suspicions about flies, fats, and multiple sclerosis. Major Qualifying Project. Worcester Polytechnic Institute.

Margaritis, L.H., Kafatos, F.C., and Petri, W.H. (1980). The eggshell of Drosophila melanogaster. I. Fine structure of the layers and regions of the wild-type eggshell. Journal of cell science *43*, 1-35.

Matsuzaka, T., Shimano, H., Yahagi, N., Kato, T., Atsumi, A., Yamamoto, T., Inoue, N., Ishikawa, M., Okada, S., Ishigaki, N.*, et al.* (2007). Crucial role of a long-chain fatty acid elongase, Elovl6, in obesity-induced insulin resistance. Nature medicine *13*, 1193-1202.

Maugeri, A., Meire, F., Hoyng, C.B., Vink, C., Van Regemorter, N., Karan, G., Yang, Z., Cremers, F.P., and Zhang, K. (2004). A novel mutation in the ELOVL4 gene causes autosomal dominant Stargardt-like macular dystrophy. Investigative ophthalmology & visual science *45*, 4263-4267.

McMahon, A., Jackson, S.N., Woods, A.S., and Kedzierski, W. (2007). A Stargardt disease-3 mutation in the mouse Elovl4 gene causes retinal deficiency of C32-C36 acyl phosphatidylcholines. FEBS letters *581*, 5459-5463.

Millar, A.A., Clemens, S., Zachgo, S., Giblin, E.M., Taylor, D.C., and Kunst, L. (1999). CUT1, an Arabidopsis gene required for cuticular wax biosynthesis and pollen fertility, encodes a very-long-chain fatty acid condensing enzyme. The Plant cell *11*, 825-838.

Millar, A.A., Wrischer, M., and Kunst, L. (1998). Accumulation of very-long-chain fatty acids in membrane glycerolipids is associated with dramatic alterations in plant morphology. The Plant cell *10*, 1889-1902.

Miller, J.P., Yates, B.E., Al-Ramahi, I., Berman, A.E., Sanhueza, M., Kim, E., de Haro, M., DeGiacomo, F., Torcassi, C., Holcomb, J.*, et al.* (2012). A genome-scale RNA-interference screen identifies RRAS signaling as a pathologic feature of Huntington's disease. PLoS genetics *8*, e1003042.

Milte, C.M., Sinn, N., and Howe, P.R. (2009). Polyunsaturated fatty acid status in attention deficit hyperactivity disorder, depression, and Alzheimer's disease: towards an omega-3 index for mental health? Nutrition reviews *67*, 573-590.

Moon, Y.A., Hammer, R.E., and Horton, J.D. (2009). Deletion of ELOVL5 leads to fatty liver through activation of SREBP-1c in mice. Journal of lipid research *50*, 412-423.

Moon, Y.A., and Horton, J.D. (2003). Identification of two mammalian reductases involved in the two-carbon fatty acyl elongation cascade. The Journal of biological chemistry *278*, 7335-7343.

Moon, Y.A., Shah, N.A., Mohapatra, S., Warrington, J.A., and Horton, J.D. (2001). Identification of a mammalian long chain fatty acyl elongase regulated by sterol regulatory element-binding proteins. The Journal of biological chemistry *276*, 45358-45366.

Moussian, B., Schwarz, H., Bartoszewski, S., and Nusslein-Volhard, C. (2005). Involvement of chitin in exoskeleton morphogenesis in Drosophila melanogaster. Journal of morphology *264*, 117-130.

Naganuma, T., Sato, Y., Sassa, T., Ohno, Y., and Kihara, A. (2011). Biochemical characterization of the very long-chain fatty acid elongase ELOVL7. FEBS letters *585*, 3337-3341.

Nelson, D.R., and Lee, R.E., Jr. (2004). Cuticular lipids and desiccation resistance in overwintering larvae of the goldenrod gall fly, Eurosta solidaginis (Diptera:

Tephritidae). Comparative biochemistry and physiology Part B, Biochemistry & molecular biology *138*, 313-320.

Ni, J.Q., Zhou, R., Czech, B., Liu, L.P., Holderbaum, L., Yang-Zhou, D., Shim, H.S., Tao, R., Handler, D., Karpowicz, P.*, et al.* (2011). A genome-scale shRNA resource for transgenic RNAi in Drosophila. Nature methods *8*, 405-407.

Nugteren, D.H. (1965). The enzymic chain elongation of fatty acids by rat-liver microsomes. Biochimica et biophysica acta *106*, 280-290.

Ofman, R., Dijkstra, I.M., van Roermund, C.W., Burger, N., Turkenburg, M., van Cruchten, A., van Engen, C.E., Wanders, R.J., and Kemp, S. (2010). The role of ELOVL1 in very long-chain fatty acid homeostasis and X-linked adrenoleukodystrophy. EMBO molecular medicine *2*, 90-97.

Oh, C.S., Toke, D.A., Mandala, S., and Martin, C.E. (1997). ELO2 and ELO3, homologues of the Saccharomyces cerevisiae ELO1 gene, function in fatty acid elongation and are required for sphingolipid formation. The Journal of biological chemistry *272*, 17376-17384.

Ohno, Y., Suto, S., Yamanaka, M., Mizutani, Y., Mitsutake, S., Igarashi, Y., Sassa, T., and Kihara, A. (2010). ELOVL1 production of C24 acyl-CoAs is linked to C24 sphingolipid synthesis. Proceedings of the National Academy of Sciences of the United States of America *107*, 18439-18444.

Okuda, A., Naganuma, T., Ohno, Y., Abe, K., Yamagata, M., Igarashi, Y., and Kihara, A. (2010). Hetero-oligomeric interactions of an ELOVL4 mutant protein: implications in the molecular mechanism of Stargardt-3 macular dystrophy. Molecular vision *16*, 2438-2445.

Papassideri, I.S., and Margaritis, L.H. (1996). The eggshell of Drosophila melanogaster: IX. Synthesis and morphogenesis of the innermost chorionic layer. Tissue & cell *28*, 401-409.

Papassideri, I.S., Margaritis, L.H., and Gulik-Krzywicki, T. (1993). The eggshell of Drosophila melanogaster. VIII. Morphogenesis of the wax layer during oogenesis. Tissue & cell *25*, 929-936.

Parisi, M., Li, R., and Oliver, B. (2011). Lipid profiles of female and male Drosophila. BMC research notes *4*, 198.

Patel, N.H. (1994). Imaging neuronal subsets and other cell types in whole-mount Drosophila embryos and larvae using antibody probes. Methods in cell biology *44*, 445-487.

Paul, S., Gable, K., Beaudoin, F., Cahoon, E., Jaworski, J., Napier, J.A., and Dunn, T.M. (2006). Members of the Arabidopsis FAE1-like 3-ketoacyl-CoA synthase gene family substitute for the Elop proteins of Saccharomyces cerevisiae. The Journal of biological chemistry *281*, 9018-9029.

Pfeiffer, B.D., Jenett, A., Hammonds, A.S., Ngo, T.T., Misra, S., Murphy, C., Scully, A., Carlson, J.W., Wan, K.H., Laverty, T.R.*, et al.* (2008). Tools for neuroanatomy and neurogenetics in Drosophila. Proceedings of the National Academy of Sciences of the United States of America *105*, 9715-9720.

Poeck, B., Triphan, T., Neuser, K., and Strauss, R. (2008). Locomotor control by the central complex in Drosophila-An analysis of the tay bridge mutant. Developmental neurobiology *68*, 1046-1058.

Proksch, E., Jensen, J.M., and Elias, P.M. (2003). Skin lipids and epidermal differentiation in atopic dermatitis. Clin Dermatol *21*, 134-144.

Qi, B., Fraser, T., Mugford, S., Dobson, G., Sayanova, O., Butler, J., Napier, J.A., Stobart, A.K., and Lazarus, C.M. (2004). Production of very long chain polyunsaturated omega-3 and omega-6 fatty acids in plants. Nature biotechnology *22*, 739-745.

Qin, Y., Dalen, K.T., Gustafsson, J.A., and Nebb, H.I. (2009). Regulation of hepatic fatty acid elongase 5 by LXRalpha-SREBP-1c. Biochimica et biophysica acta *1791*, 140-147.

Reina-Pinto, J.J., Voisin, D., Kurdyukov, S., Faust, A., Haslam, R.P., Michaelson, L.V., Efremova, N., Franke, B., Schreiber, L., Napier, J.A.*, et al.* (2009). Misexpression of FATTY ACID ELONGATION1 in the Arabidopsis epidermis induces cell death and suggests a critical role for phospholipase A2 in this process. The Plant cell *21*, 1252-1272.

Ren, Q., Li, H., Wu, Y., Ren, J., and Guo, A. (2012). A GABAergic inhibitory neural circuit regulates visual reversal learning in Drosophila. The Journal of neuroscience : the official journal of the Society for Neuroscience *32*, 11524-11538.

Riederer, M., and Schreiber, L. (2001). Protecting against water loss: analysis of the barrier properties of plant cuticles. Journal of experimental botany *52*, 2023-2032.

Riemensperger, T., Isabel, G., Coulom, H., Neuser, K., Seugnet, L., Kume, K., Iche-Torres, M., Cassar, M., Strauss, R., Preat, T.*, et al.* (2011). Behavioral consequences of dopamine deficiency in the Drosophila central nervous system. Proceedings of the National Academy of Sciences of the United States of America *108*, 834-839.

Riezman, H. (2007). The long and short of fatty acid synthesis. Cell *130*, 587-588.
Ruan, X.Z., Varghese, Z., and Moorhead, J.F. (2009). An update on the lipid nephrotoxicity hypothesis. Nat Rev Nephrol.

Ruiperez, V., Darios, F., and Davletov, B. (2010). Alpha-synuclein, lipids and Parkinson's disease. Progress in lipid research *49*, 420-428.

Sansores-Garcia, L., Atkins, M., Moya, I.M., Shahmoradgoli, M., Tao, C., Mills, G.B., and Halder, G. (2013). Mask Is Required for the Activity of the Hippo Pathway Effector Yki/YAP. Current biology : CB *23*, 229-235.

Sassa, T., Ohno, Y., Suzuki, S., Nomura, T., Nishioka, C., Kashiwagi, T., Hirayama, T., Akiyama, M., Taguchi, R., Shimizu, H.*, et al.* (2013). Impaired epidermal permeability barrier in mice lacking elovl1, the gene responsible for very-long-chain fatty acid production. Molecular and cellular biology *33*, 2787-2796.

Savant, S.S., and Waring, G.L. (1989). Molecular analysis and rescue of a vitelline membrane mutant in Drosophila. Developmental biology *135*, 43-52.

Schaffer, J.E., and Lodish, H.F. (1994). Expression cloning and characterization of a novel adipocyte long chain fatty acid transport protein. Cell *79*, 427-436.

Schneiter, R., Tatzer, V., Gogg, G., Leitner, E., and Kohlwein, S.D. (2000). Elo1p-dependent carboxy-terminal elongation of C14:1Delta(9) to C16:1Delta(11) fatty acids in Saccharomyces cerevisiae. Journal of bacteriology *182*, 3655-3660.

Serway, C.N., Kaufman, R.R., Strauss, R., and de Belle, J.S. (2009). Mushroom bodies enhance initial motor activity in Drosophila. Journal of neurogenetics *23*, 173-184.

Shaik, K.S., Meyer, F., Vazquez, A.V., Flotenmeyer, M., Cerdan, M.E., and Moussian, B. (2012). delta-Aminolevulinate synthase is required for apical transcellular barrier formation in the skin of the Drosophila larva. European journal of cell biology *91*, 204-215.

Shanklin, J., Whittle, E., and Fox, B.G. (1994). Eight histidine residues are catalytically essential in a membrane-associated iron enzyme, stearoyl-CoA desaturase, and are conserved in alkane hydroxylase and xylene monooxygenase. Biochemistry *33*, 12787-12794.

Simon, J.C., and Dickinson, M.H. (2010). A new chamber for studying the behavior of Drosophila. PloS one *5*, e8793.

Slawson, J.B., Kuklin, E.A., Ejima, A., Mukherjee, K., Ostrovsky, L., and Griffith, L.C. (2011). Central regulation of locomotor behavior of Drosophila melanogaster

depends on a CASK isoform containing CaMK-like and L27 domains. Genetics *187*, 171-184.

Smith, S., Witkowski, A., and Joshi, A.K. (2003). Structural and functional organization of the animal fatty acid synthase. Progress in lipid research *42*, 289-317.

Spindler, S.R., Ortiz, I., Fung, S., Takashima, S., and Hartenstein, V. (2009). Drosophila cortex and neuropile glia influence secondary axon tract growth, pathfinding, and fasciculation in the developing larval brain. Developmental biology *334*, 355-368.

Sporl, F., Wunderskirchner, M., Ullrich, O., Bomke, G., Breitenbach, U., Blatt, T., Wenck, H., Wittern, K.P., and Schrader, A. Real-time monitoring of membrane cholesterol reveals new insights into epidermal differentiation. The Journal of investigative dermatology *130*, 1268-1278.

Stefanis, L. (2005). Caspase-dependent and -independent neuronal death: two distinct pathways to neuronal injury. The Neuroscientist : a review journal bringing neurobiology, neurology and psychiatry *11*, 50-62.

Strauss, R., and Heisenberg, M. (1993). A higher control center of locomotor behavior in the Drosophila brain. The Journal of neuroscience : the official journal of the Society for Neuroscience *13*, 1852-1861.

Sujkowski, A., Saunders, S., Tinkerhess, M., Piazza, N., Jennens, J., Healy, L., Zheng, L., and Wessells, R. (2012). dFatp regulates nutrient distribution and long-term physiology in Drosophila. Aging cell *11*, 921-932.

Szafer-Glusman, E., Giansanti, M.G., Nishihama, R., Bolival, B., Pringle, J., Gatti, M., and Fuller, M.T. (2008). A role for very-long-chain fatty acids in furrow ingression during cytokinesis in Drosophila spermatocytes. Current biology : CB *18*, 1426-1431.

Tamura, K., Makino, A., Hullin-Matsuda, F., Kobayashi, T., Furihata, M., Chung, S., Ashida, S., Miki, T., Fujioka, T., Shuin, T*., et al.* (2009). Novel lipogenic enzyme ELOVL7 is involved in prostate cancer growth through saturated long-chain fatty acid metabolism. Cancer research *69*, 8133-8140.

Tautz, D., and Pfeifle, C. (1989). A non-radioactive in situ hybridization method for the localization of specific RNAs in Drosophila embryos reveals translational control of the segmentation gene hunchback. Chromosoma *98*, 81-85.

Taylor, R.C., Cullen, S.P., and Martin, S.J. (2008). Apoptosis: controlled demolition at the cellular level. Nature reviews Molecular cell biology *9*, 231-241.

Tehlivets, O., Scheuringer, K., and Kohlwein, S.D. (2007). Fatty acid synthesis and elongation in yeast. Biochimica et Biophysica Acta (BBA) - Molecular and Cell Biology of Lipids *1771*, 255-270.

Thon, L., Mohlig, H., Mathieu, S., Lange, A., Bulanova, E., Winoto-Morbach, S., Schutze, S., Bulfone-Paus, S., and Adam, D. (2005). Ceramide mediates caspase-independent programmed cell death. The FASEB journal : official publication of the Federation of American Societies for Experimental Biology *19*, 1945-1956.

Todd, J., Post-Beittenmiller, D., and Jaworski, J.G. (1999). KCS1 encodes a fatty acid elongase 3-ketoacyl-CoA synthase affecting wax biosynthesis in Arabidopsis thaliana. The Plant journal : for cell and molecular biology *17*, 119-130.

Toke, D.A., and Martin, C.E. (1996). Isolation and characterization of a gene affecting fatty acid elongation in Saccharomyces cerevisiae. The Journal of biological chemistry *271*, 18413-18422.

Tomancak, P., Beaton, A., Weiszmann, R., Kwan, E., Shu, S., Lewis, S.E., Richards, S., Ashburner, M., Hartenstein, V., Celniker, S.E.*, et al.* (2002). Systematic determination of patterns of gene expression during Drosophila embryogenesis. Genome biology *3*, RESEARCH0088.

Tomancak, P., Berman, B.P., Beaton, A., Weiszmann, R., Kwan, E., Hartenstein, V., Celniker, S.E., and Rubin, G.M. (2007). Global analysis of patterns of gene expression during Drosophila embryogenesis. Genome biology *8*, R145.

Tootle, T.L., Williams, D., Hubb, A., Frederick, R., and Spradling, A. (2011). Drosophila eggshell production: identification of new genes and coordination by Pxt. PloS one *6*, e19943.

Trenkamp, S., Martin, W., and Tietjen, K. (2004). Specific and differential inhibition of very-long-chain fatty acid elongases from Arabidopsis thaliana by different herbicides. Proceedings of the National Academy of Sciences of the United States of America *101*, 11903-11908.

Tripathy, S., and Jump, D.B. (2013). Elovl5 regulates the mTORC2-Akt-FOXO1 pathway by controlling hepatic cis-vaccenic acid synthesis in diet-induced obese mice. Journal of lipid research *54*, 71-84.

Tripathy, S., Torres-Gonzalez, M., and Jump, D.B. (2010). Elevated hepatic fatty acid elongase-5 activity corrects dietary fat-induced hyperglycemia in obese C57BL/6J mice. Journal of lipid research *51*, 2642-2654.

Truman, J.W. (1990). Metamorphosis of the central nervous system of Drosophila. Journal of neurobiology *21*, 1072-1084.

Tusnady, G.E., and Simon, I. (2001). The HMMTOP transmembrane topology prediction server. Bioinformatics *17*, 849-850.

Tvrdik, P., Westerberg, R., Silve, S., Asadi, A., Jakobsson, A., Cannon, B., Loison, G., and Jacobsson, A. (2000). Role of a new mammalian gene family in the biosynthesis of very long chain fatty acids and sphingolipids. The Journal of cell biology *149*, 707-718.

Tweedie, S., Ashburner, M., Falls, K., Leyland, P., McQuilton, P., Marygold, S., Millburn, G., Osumi-Sutherland, D., Schroeder, A., Seal, R.*, et al.* (2009). FlyBase: enhancing Drosophila Gene Ontology annotations. Nucleic acids research *37*, D555-559.

Ueyama, M., Chertemps, T., Labeur, C., and Wicker-Thomas, C. (2005). Mutations in the desat1 gene reduces the production of courtship stimulatory pheromones through a marked effect on fatty acids in Drosophila melanogaster. Insect biochemistry and molecular biology *35*, 911-920.

Ullio, C., Casas, J., Brunk, U.T., Sala, G., Fabrias, G., Ghidoni, R., Bonelli, G., Baccino, F.M., and Autelli, R. (2012). Sphingosine mediates TNFalpha-induced lysosomal membrane permeabilization and ensuing programmed cell death in hepatoma cells. Journal of lipid research *53*, 1134-1143.

Ulloth, J.E., Casiano, C.A., and De Leon, M. (2003). Palmitic and stearic fatty acids induce caspase-dependent and -independent cell death in nerve growth factor differentiated PC12 cells. Journal of neurochemistry *84*, 655-668.

Vasireddy, V., Jablonski, M.M., Khan, N.W., Wang, X.F., Sahu, P., Sparrow, J.R., and Ayyagari, R. (2009). Elovl4 5-bp deletion knock-in mouse model for Stargardt-like macular degeneration demonstrates accumulation of ELOVL4 and lipofuscin. Experimental eye research *89*, 905-912.

Vasireddy, V., Jablonski, M.M., Mandal, M.N., Raz-Prag, D., Wang, X.F., Nizol, L., Iannaccone, A., Musch, D.C., Bush, R.A., Salem, N., Jr.*, et al.* (2006). Elovl4 5-bp-deletion knock-in mice develop progressive photoreceptor degeneration. Investigative ophthalmology & visual science *47*, 4558-4568.

Vasireddy, V., Uchida, Y., Salem, N., Jr., Kim, S.Y., Mandal, M.N., Reddy, G.B., Bodepudi, R., Alderson, N.L., Brown, J.C., Hama, H.*, et al.* (2007). Loss of functional ELOVL4 depletes very long-chain fatty acids (> or =C28) and the unique omega-O-acylceramides in skin leading to neonatal death. Human molecular genetics *16*, 471-482.

Vasireddy, V., Vijayasarathy, C., Huang, J., Wang, X.F., Jablonski, M.M., Petty, H.R., Sieving, P.A., and Ayyagari, R. (2005). Stargardt-like macular dystrophy protein

ELOVL4 exerts a dominant negative effect by recruiting wild-type protein into aggresomes. Molecular vision *11*, 665-676.

Vaux, D.L., and Korsmeyer, S.J. (1999). Cell death in development. Cell *96*, 245-254.

Vert, J.P., Foveau, N., Lajaunie, C., and Vandenbrouck, Y. (2006). An accurate and interpretable model for siRNA efficacy prediction. BMC bioinformatics *7*, 520.

Wallis, J.G., Watts, J.L., and Browse, J. (2002). Polyunsaturated fatty acid synthesis: what will they think of next? Trends in biochemical sciences *27*, 467.

Wang, Y., Botolin, D., Christian, B., Busik, J., Xu, J., and Jump, D.B. (2005). Tissue-specific, nutritional, and developmental regulation of rat fatty acid elongases. Journal of lipid research *46*, 706-715.

Wang, Y., Torres-Gonzalez, M., Tripathy, S., Botolin, D., Christian, B., and Jump, D.B. (2008). Elevated hepatic fatty acid elongase-5 activity affects multiple pathways controlling hepatic lipid and carbohydrate composition. Journal of lipid research *49*, 1538-1552.

Waring, G.L. (2000). Morphogenesis of the eggshell in Drosophila. International review of cytology *198*, 67-108.

Watts, J.L., and Browse, J. (2002). Genetic dissection of polyunsaturated fatty acid synthesis in Caenorhabditis elegans. Proceedings of the National Academy of Sciences of the United States of America *99*, 5854-5859.

Watts, J.L., Phillips, E., Griffing, K.R., and Browse, J. (2003). Deficiencies in C20 polyunsaturated fatty acids cause behavioral and developmental defects in Caenorhabditis elegans fat-3 mutants. Genetics *163*, 581-589.

Westerberg, R., Mansson, J.E., Golozoubova, V., Shabalina, I.G., Backlund, E.C., Tvrdik, P., Retterstol, K., Capecchi, M.R., and Jacobsson, A. (2006). ELOVL3 is an important component for early onset of lipid recruitment in brown adipose tissue. The Journal of biological chemistry *281*, 4958-4968.

Westerberg, R., Tvrdik, P., Unden, A.B., Mansson, J.E., Norlen, L., Jakobsson, A., Holleran, W.H., Elias, P.M., Asadi, A., Flodby, P.*, et al.* (2004). Role for ELOVL3 and fatty acid chain length in development of hair and skin function. The Journal of biological chemistry *279*, 5621-5629.

White, S.W., Zheng, J., Zhang, Y.M., and Rock (2005). The structural biology of type II fatty acid biosynthesis. Annual review of biochemistry *74*, 791-831.

Wigglesworth, V.B. (1985). Sclerotin and lipid in the waterproofing of the insect cuticle. Tissue & cell *17*, 227-248.

Xu, S.Y., Cang, C.L., Liu, X.F., Peng, Y.Q., Ye, Y.Z., Zhao, Z.Q., and Guo, A.K. (2006). Thermal nociception in adult Drosophila: behavioral characterization and the role of the painless gene. Genes, brain, and behavior *5*, 602-613.

Yephremov, A., Wisman, E., Huijser, P., Huijser, C., Wellesen, K., and Saedler, H. (1999). Characterization of the FIDDLEHEAD gene of Arabidopsis reveals a link between adhesion response and cell differentiation in the epidermis. The Plant cell *11*, 2187-2201.

Youdim, K.A., Martin, A., and Joseph, J.A. (2000). Essential fatty acids and the brain: possible health implications. International journal of developmental neuroscience : the official journal of the International Society for Developmental Neuroscience *18*, 383-399.

Yu, H.H., Awasaki, T., Schroeder, M.D., Long, F., Yang, J.S., He, Y., Ding, P., Kao, J.C., Wu, G.Y., Peng, H.*, et al.* (2013). Clonal Development and Organization of the Adult Drosophila Central Brain. Current biology : CB.

Yu, M., Benham, A., Logan, S., Brush, R.S., Mandal, M.N., Anderson, R.E., and Agbaga, M.P. (2012). ELOVL4 protein preferentially elongates 20:5n3 to very long chain PUFAs over 20:4n6 and 22:6n3. Journal of lipid research *53*, 494-504.

Zadravec, D., Tvrdik, P., Guillou, H., Haslam, R., Kobayashi, T., Napier, J.A., Capecchi, M.R., and Jacobsson, A. (2011). ELOVL2 controls the level of n-6 28:5 and 30:5 fatty acids in testis, a prerequisite for male fertility and sperm maturation in mice. Journal of lipid research *52*, 245-255.

Zhang, K., Kniazeva, M., Han, M., Li, W., Yu, Z., Yang, Z., Li, Y., Metzker, M.L., Allikmets, R., Zack, D.J.*, et al.* (2001). A 5-bp deletion in ELOVL4 is associated with two related forms of autosomal dominant macular dystrophy. Nature genetics *27*, 89-93.

Zhang, W., Li, P., Hu, X., Zhang, F., Chen, J., and Gao, Y. (2011). Omega-3 polyunsaturated fatty acids in the brain: metabolism and neuroprotection. Frontiers in bioscience : a journal and virtual library *16*, 2653-2670.

Zwarts, L., Magwire, M.M., Carbone, M.A., Versteven, M., Herteleer, L., Anholt, R.R., Callaerts, P., and Mackay, T.F. (2011). Complex genetic architecture of Drosophila aggressive behavior. Proceedings of the National Academy of Sciences of the United States of America *108*, 17070-17075.